

CZECH UNIVERSITY OF LIFE SCIENCES  
PRAGUE  
FACULTY OF ENVIRONMENTAL  
SCIENCES



**Numerical simulation of herbicide transport and  
biogeochemical fate in the unsaturated zone of  
a lysimeter**

**DIPLOMA THESIS**

**2023**

**Amr Abouamer**

# CZECH UNIVERSITY OF LIFE SCIENCES PRAGUE

Faculty of Environmental Sciences

## DIPLOMA THESIS ASSIGNMENT

B.Sc. Amr Abouamer, BSc

Environmental Geosciences

Thesis title

**Numerical simulation of herbicide transport and biogeochemical fate in the unsaturated zone of a lysimeter**

---

### Objectives of thesis

Numerical simulation of unsaturated flow and reactive transport using HYDRUS-1D: including the investigation of transformation processes (herbicides into metabolites). Describing the transport and fate of herbicides and metabolites within the lysimeter. Comparison between the simulation results and measured concentrations of herbicides and metabolites in lysimeter outflow.

### Methodology

The intensive use of agrochemicals like fertilizers and pesticides often leads to considerable contamination of the subsurface. This results in impacts on biodiversity and fundamental ecological services and often does

also threaten human health. This Master's thesis is embedded within ongoing research on lysimeter experiments on subsurface water flow and the fate of herbicides within the soil, groundwater, and maize plants.

Numerical simulations are done using HYDRUS-1D in order to investigate herbicide transport within the lysimeters and chemical transformation of herbicides into metabolites, i.e. microbe-induced biodegradation processes. Simulation studies also involve the transport of these herbicides within the lysimeters. Simulation results are compared to measured concentrations of herbicides and metabolites in lysimeter outflow.

**The proposed extent of the thesis**

50 – 60 pages

**Keywords**

Agrochemical Pollution, Groundwater, HYDRUS-1D, Modelling, PEST, Pesticides, Metabolites, Unsaturated Zone, Maize, Vegetation, Numerical Simulation, Lysimeter

---

**Recommended information sources**

- F. Shajari, F. Einsiedl, and A. Rein, "Characterizing Water Flow in Vegetated Lysimeters with Stable Water Isotopes and Modeling," *Groundwater*, vol. 58, no. 5, pp. 759–770, 2020, doi: 10.1111/gwat.12970.
- Imig, A., Augustin, L., Groh, J., Pütz, T., Elsner, M. E. M., Einsiedl, F. E. F., & Rein, A. (in preparation). Fate of herbicides in cropped lysimeters: 2. Leaching of four maize herbicides considering different model setups.
- Maloszewski, P., Maciejewski, S., Stumpp, C., Stichler, W., Trimborn, P., & Klotz, D. (2006). Modelling of water flow through typical Bavarian soils: 2. Environmental deuterium transport. *Hydrological Sciences Journal*, 51(2), 298–313. <https://doi.org/10.1623/hysj.51.2.29>
- Strauß, C., Bayer, A., & Obernolte, M. (2017). Lysimeteruntersuchungen zum Austragsverhalten von im Maisanbau eingesetzten Herbiziden unter Freilandbedingungen (Standort Wielenbach). 17. Gumpensteiner Lysimetertagung 2017, 27–32.
- Šimůnek, J., Šejna, M., & van Genuchten, M. T. (2018). Hydrus-1d. code for simulating the one-dimensional movement of water, heat, and multiple solutes in variably saturated porous media.
- 

**Expected date of thesis defence**

2022/23 WS – FES

**The Diploma Thesis Supervisor**

doc. Mgr. Lukáš Trakal, Ph.D.

**Supervising department**

Department of Environmental Geosciences

**Advisor of thesis**

Dr. Arno Rein and M.Sc. Anne Imig (Technical University of Munich, TUM School of Engineering and Design, Chair of Hydrogeology)

Electronic approval: 22. 2. 2023

**prof. RNDr. Michael Komárek, Ph.D.**

Head of department

Electronic approval: 23. 2. 2023

**prof. RNDr. Vladimír Bejček, CSc.**

Dean

Prague on 27. 03. 2023

---

## **Declaration**

I hereby declare that I have independently elaborated the diploma/final thesis with the topic of: Numerical simulation of herbicide transport and biogeochemical fate in the unsaturated zone of a lysimeter, and that I have cited all the information sources that I used in the thesis and that are also listed at the end of the thesis in the list of used information sources. I am aware that my diploma/final thesis is subject to Act No. 121/2000 Coll., on copyright, on rights related to copyright and on amendment of some acts, as amended by later regulations, particularly the provisions of Section 35(3) of the act on the use of the thesis. I am aware that by submitting the diploma/final thesis I agree with its publication under Act No. 111/1998 Coll., on universities and on the change and amendments of some acts, as amended, regardless of the result of its defence. With my own signature, I also declare that the electronic version is identical to the printed version, and the data stated in the thesis have been processed in relation to the GDPR. The student adds the date and place of the statement and signs it (Appendix No. 1).

Date: 27/03/2022

Signature: Amr Abouamer

## **Acknowledgement**

At first, I would like to thank Allah who helped me throughout my life. I give my warmest thanks to my supervisors from the Technical University of Munich PD Dr. rer. nat. habil. Arno Rein and M.Sc. Anne Imig, for their support, guidance, patience and considering me one of their team to make this work possible, as well as my supervisor and teacher from Czech University of Life Sciences Prague Doc. Mgr. Lukáš Trakal, Ph.D., for his support, aid, and advice that helped me to move forward. The deepest appreciation is to M.Sc. Lea Augustin for her continuous support and paving the way and exerting time and effort to help me to know more about modeling and PEST software. The cordial and special thanks to my parents, my brother, and my friends for their backing me up and rooting for me to continue.

## Abstract

This study discusses the contamination potential for groundwater of four herbicides and their metabolites, which was evaluated by numerical modeling of unsaturated flow and reactive transport using HYDRUS-1D. The herbicides were applied to a lysimeter vegetated with maize located in Wielenbach, Germany. The core of the soil of the weighable lysimeter contained a sandy gravel soil. Four models (the two models of the terbuthylazine and metolachlor branches with and without root water uptake) were set up to study the fate of the herbicides, simulating transport as well as biodegradation, metabolite production, sorption, and the influence of root water uptake. The considered herbicides were metolachlor, terbuthylazine, nicosulfuron and prosulfuron. The formation of two metabolites was simulated for (metolachlor ethanesulfonic acid, MESA, and metolachlor oxanilic acid, MOXA), and four metabolites of terbuthylazine (desethyl-terbuthylazine, MT1, 2-hydroxy-terbuthylazine, MT13, terbuthylazine 2 CGA 324007, LM5, and terbuthylazine 1 SYN 545666, LM6). Concentrations of these compounds were monitored in lysimeter discharge. Reactive transport models have been set up on available soil hydraulic parameters. The results of the modelling were correlated with the measured data and calibration of biodegradation and sorption parameters was performed using PEST. Calibrated parameters of sorption, biodegradation, and percentages of produced metabolites 'daughters' agree well with literature findings. Consideration root water uptake did not show high differences compared to the approach without root water uptake. Observations could be described overall well by modelling; however, concentration peaks partly under- or overestimated sometimes three to fivefold so that improvements are recommended in future studies.

**Keywords:** Agrochemical Pollution, Groundwater, HYDRUS-1D, Lysimeter, Maize, Metabolites, Modelling, Numerical Simulation, PEST, Pesticides, Unsaturated Zone, Vegetation

## Český Abstraktní

Tato studie pojednává o kontaminačním potenciálu podzemních vod obsahující čtyři herbicidy a jejich metabolity, kdy tento potenciál kontaminace byl hodnocen numerickým modelováním nenasyceného proudění a reaktivního transportu pomocí HYDRUS-1D. Herbicidy byly aplikovány do lysimetru porostlého kukuřicí a tento experiment byl realizován ve Wielenbachu v Německu. Kontinuálně vážený lysimetr obsahoval písčitou štěrkovou půdu. Pro studium osudu vybraných herbicidů, simulujících transport biodegradaci, produkci metabolitů, sorpci a vliv příjmu kořenové vody, byly vytvořeny dva modely (s a bez příjmu kořenové vody). Uvažovanými herbicidy byly metolachlor, terbuthylazin, nicosulfuron a prosulfuron. Tvorba dvou metabolitů byla simulována pro metolachlor (kyselina ethansulfonová, MESA a kyselina metolachloroxanilová, MOXA) a čtyři metabolity terbuthylazinu (desethyl-terbuthylazin, MT1, 2-hydroxy-terbuthylazin, MT13, terbuthylazin 2 CGA 3254007, a terbuthylazin 1 SYN 545666, LM6). Koncentrace těchto látek byly sledovány ve výluhu z lysimetrů. Modely reaktivního transportu byly sestaveny na základě dostupných půdních hydraulických parametrů. Výsledky modelování byly korelovány s naměřenými daty a kalibrace degračních a sorpčních parametrů byla provedena pomocí PEST. Kalibrované parametry sorpce, biodegradace a

procenta produkovaných metabolitů dobře souhlasí s nálezy v literatuře. Zvažování příjmu kořenové vody neprokázalo velké rozdíly oproti přístupu bez příjmu. Pozorování lze celkově dobře popsat modelováním, avšak vrcholy koncentrací jsou částečně podhodnocené nebo nadhodnocené (někdy trojnásobně až pětinasobně), takže v budoucích studiích se doporučuje zlepšení.

**Klíčová slova:** Agrochemické znečištění, Podzemní voda, HYDRUS-1D, Lysimetr, Kukuřice, Metabolity, Modelování, Numerická simulace, PEST, Pesticidy, Nenasycená zóna, Vegetace

## Table of Contents

1. Introduction .....	1
2. Objectives and aims of this thesis.....	4
3. Literature review: background and state of the art .....	5
3.1 Study site description and data availability .....	6
3.1.1 Measurements.....	6
3.1.2 Soil characteristics .....	7
3.1.3 Herbicide application .....	7
3.1.4 Sampling at the Study site .....	8
3.2 Herbicides and their metabolites .....	8
3.2.1 Metolachlor .....	8
3.2.2 Terbutylazine .....	12
4. Methodology.....	18
4.1 Numerical model setup.....	18
4.1.1 Water flow in the unsaturated zone .....	18
4.1.2 Solute transport.....	19
4.2 boundary conditions .....	25
4.3 Plant uptake.....	26
4.3.1 Transpiration.....	26
4.3.2 Root uptake of dissolved compounds .....	26
4.3.3 Root uptake of dissolved compounds .....	30
4.3.4 Root growth.....	31
4.4 Model calibration .....	32
4.4.1 PEST .....	32
4.4.2 Model curve fit evaluation .....	33
5. Results and discussion .....	35
5.1 Hydrus-1D application issues .....	35
5.2 Results of running HYDRUS-1D models.....	35



5.2.1 Results of the first model with and without RWU .....	35
5.2.2 Results of the second model with and without RWU .....	48
5.3 Discussion of root water uptake.....	53
6. Summary and conclusion .....	54
7. References .....	56

## List of Figures

<b>Figure 1:</b> Biodegradation reactions of metolachlor herbicide and its major metabolite MESA and MOXA with a sum formula (Rose et al., 2012) .....	12
<b>Figure 2:</b> Schematic degradation reaction of terbuthylazine and its metabolites, metabolites marked in red are detected and measured in the leachate of the lysimeter and are compared with the modelled (ECPR, 2015).....	17
<b>Figure 3:</b> Biodegradation process of (solute A) and production of daughters (solute B, C ...) and the parameters governing the whole biodegradation process which are $\mu_w, 1$ , $\mu_s, 1$ , and $\mu_g, 1$ and production parameters are $\mu_w, 1'$ , $\mu_s, 1'$ and $\mu_g, 1'$ (Jacques et al., 2000; Šimůnek et al., 2013b; Šimůnek & van Genuchten, 1995) .....	21
<b>Figure 4:</b> Biodegradation paths and production reaction of the metabolites from their parent herbicides with the percentage of biodegradation $\mu_w$ and production $\mu_w'$ with percentages of degradation and production after (ECPR, 2015).....	23
<b>Figure 5:</b> The parameters of the water uptake stress response function and the relationship between water uptake and the soil pressure head as described by Feddes et al. (1978) (Šimůnek & Hopmans, 2009).....	28
<b>Figure 6:</b> Relationship between the ratio of actual to potential transpiration and stress index ( $\omega$ ) (Šimůnek & Hopmans, 2009).....	29
<b>Figure 7:</b> Metolachlor (MTLC) concentration in the first fitting model with and without root water uptake (in blue line) compared with the measured in the lysimeter drainage (in red dots), through the whole simulation period where right diagram with root water uptake and the left diagram without, with statistical parameters in the base .....	37
<b>Figure 8:</b> Measured concentrations of metolachlor, terbuthylazine, and their metabolites in the output leaching water and the amount of precipitation and irrigation water summed up in every season in lysimeter 1 by Imig et al. (submitted-a) .....	38
<b>Figure 9:</b> Measured concentrations of metolachlor, terbuthylazine, and their metabolites in the output leaching water as well as the concentration of applied "input" herbicides in lysimeter 1 by Imig et al. (submitted-a).....	39
<b>Figure 10:</b> Metolachlor ethanesulfonic acid (MESA) concentration in the first fitting model with and without root water uptake (in blue line) compared with the measured in the lysimeter drainage (in red dots), through the whole simulation period where right diagram with root water uptake and the left diagram without, with statistical parameters in the base.....	40
<b>Figure 11:</b> Terbuthylazine (TBA) concentration in the first fitting model with and without root water uptake (in blue line) compared with the measured in the lysimeter drainage (in	

red dots), through the whole simulation period where right diagram with root water uptake and the left diagram without, with statistical parameters in the base ..... 43

**Figure 12:** Desethyle-terbutylazine (MT1) concentration in the first fitting model with and without root water uptake (in blue line) compared with the measured in the lysimeter drainage (in red dots), through the whole simulation period where right diagram with root water uptake and the left diagram without, with statistical parameters in the base ..... 44

**Figure 13:** Terbutylazine 2 CGA 324007 (LM5) concentration in the first fitting model with and without root water uptake (in blue line) compared with the measured in the lysimeter drainage (in red dots), through the whole simulation period where right diagram with root water uptake and the left diagram without, with statistical parameters in the base ..... 46

**Figure 14:** Terbutylazine 1 SYN 545666 (LM6) concentration in the first fitting model with and without root water uptake (in blue line) compared with the measured in the lysimeter drainage (in red dots), through the whole simulation period where right diagram with root water uptake and the left diagram without, with statistical parameters in the base ..... 47

**Figure 15:** Metolachlor (MTLC) concentration in the second fitting model with and without root water uptake (in blue line) compared with the measured in the lysimeter drainage (in red dots), through the whole simulation period where right diagram with root water uptake and the left diagram without, with statistical parameters in the base ..... 49

**Figure 16:** Metolachlor oxanilic acid (MOXA) concentration in the second fitting model with and without root water uptake (in blue line) compared with the measured in the lysimeter drainage (in red dots), through the whole simulation period where right diagram with root water uptake and the left diagram without, with statistical parameters in the base ..... 50

**Figure 17:** Terbutylazine (TBA) concentration in the second fitting model with and without root water uptake (in blue line) compared with the measured in the lysimeter drainage (in red dots), through the whole simulation period where right diagram with root water uptake and the left diagram without, with statistical parameters in the base ..... 51

**Figure 18:** 2-hydroxy terbutylazine (MT13) concentration in the second fitting model with and without root water uptake (in blue line) compared with the measured in the lysimeter drainage (in red dots), through the whole simulation period where right diagram with root water uptake and the left diagram without, with statistical parameters in the base ..... 52

## List of Tables

<b>Table 1:</b> Soil characteristics of lysimeter 1 after Shajari et al., (2020).....	7
<b>Table 2:</b> Applied herbicides with their concentration between 2013 and 2017 after Strauß et al. (2017) .....	8
<b>Table 3:</b> Degradation properties of metolachlor and its metabolites (MESA and MOXA) (Rose et al., 2018) NA: means not available.....	11
<b>Table 4:</b> Names, chemical SMILES, chemical formula and CAS identifier for the herbicides metolachlor, terbuthylazine, and their metabolites .....	15
<b>Table 5:</b> Physical and chemical properties of the herbicides terbuthylazine and metolachlor and their metabolites .....	15
<b>Table 6:</b> Fitted parameters of biodegradation and production for model (1) before running PEST. ....	24
<b>Table 7:</b> Fitted parameters of degradation and production for model (2) before running PEST .....	24
<b>Table 8:</b> Manually fitted soil hydraulic parameters by Imig et al. (2022b) .....	25
<b>Table 9:</b> Fitted transport parameters for lysimeter 1 without consideration of RWU used in the model after Imig et al. (submitted-b) .....	25
<b>Table 10:</b> Fitted parameters of biodegradation and production for model (1) after running PEST. ....	36
<b>Table 11:</b> Fitted parameters of biodegradation and production for model (2) after running PEST .....	48

# 1. Introduction

Groundwater, as an important source of drinking water, is frequently contaminated with herbicides used for agricultural purposes and their degradation products. These may reach groundwater by surface runoff and leaching through the soil profile. It is a widespread problem affecting different aquifers in many countries (Fenoll et al., 2015; López-Piñeiro et al., 2014; Postigo & Barceló, 2015; C. P. Rice et al., 2016; Sidoli et al., 2020; Toccalino et al., 2014). The fate and transport of pesticides have been studied intensively in the last years to know their effect on the chemical, physical and hydrological conditions of the soil (Ulrich et al., 2021; Wołejko et al., 2020). As a part of sustainable development adopted by the European Union States, the production of biofuel, biogas, and biodiesel is one of the most important sources of renewable energy (European Union, 2009). Maize production is the second most cultivated crop in the EU where the grain maize area is estimated at 8.7 million ha while the green maize (silage) is 6.2 million ha (Eurostat, 2022). Silage maize is one of the most important plants for biogas production (Andert, 2021; Herrmann, 2013). Maize silage (*Zea mays* L.) is preferred in biogas production because of its high yielding energy and it is also growing fast. It has been accounted for 73% of the mass substrate of the renewable materials in biogas plants in 2012, which explains why maize cultivation increased in Germany until it changed the landscape (Zeitbild Wissen, 2013). About 2300 biogas plants out of 7000 in Germany are in Bavaria, where the amount of cultivated biogas maize is the second in Germany after Lower Saxony. The percentage of biogas maize cultivated lands increased by 14.5 % between 2008 to 2013 (Deutsches Maiskomitee e.V. (DMK), 2022).

The extensive cultivation of *Zea mays* L. can severely affect the environment due to the application of herbicides that control weed such as terbuthylazine and metolachlor (MTLC) that can be leached to the groundwater or their metabolites and contaminate it (Schuhmann et al., 2019). Since around 70 percent of drinking water used in Germany is dependent on groundwater and springs, that was a critical topic extensively studied to prevent contamination against soil nitrate and pesticide applications. That is why the German Environmental Agency name groundwater as the water body type of the year 2022 (Umwelt Bundesamt, 2022).

The European directive on the water framework has set some rules to be followed to protect groundwater (Scuri et al., 2006). Many answers about the transport and fate of herbicides and their metabolites, the time required for those compounds to reach groundwater and their mobility in the vadose zone, especially after they have been discovered in groundwater many years after applications in some studies (Arias-Estévez et al., 2008; Dubus et al., 2003). Herbicides and their metabolites leached to the groundwater aquifer will not be widely adsorbed to the aquifer material because of the lack of organic carbon. Some studies show that they can react with the aquifer material (Baran & Gourcy, 2013; Papiernik et al., 2006; Sidoli et al., 2016). According to the European directive 98/83/EEC, the allowed limits of pesticides in water for human consumption are 0.1 µg /L for the single compound concentration and 0.5 µg /L for all concentrations of pesticides (EC, 1998).

Metolachlor is one of the chloroacetanilide groups used for controlling the annual grass and broad leaf weeds in crops like corn, sunflower, soybeans, and potatoes (EFSA, 2012). It has been found that metolachlor is a contaminant in agricultural areas in Mediterranean countries like Italy, Greece, and Spain (Konstantinou et al., 2006). Metolachlor ethane sulfonic acid (MESA) and metolachlor oxanilic acid (MOXA) are the degradation products of metolachlor, they have been detected, as well as their parent compound, in groundwater (Chen et al., 2017).

The frequency of detection of herbicide in the environment is dependent on some factors: the amount of herbicide applied, its mobility, degradation, adsorption, volatilization, precipitation, and persistence (Gilliom et al., 2006). The fate of the herbicide is determined by some processes like adsorption, degradation, and leaching. The amount of organic matter in the soil can affect the adsorption, and the amount of precipitation can affect the leaching and mobilization (Sánchez-Martín et al., 1995). The adsorption of metolachlor is moderate and improved by increasing the organic matter, while it decreases downward in the soil profile (Ghosh et al., 2016). MESA is found in groundwater after the application of metolachlor (Baran et al., 2004; Bayless et al., 2008; Domagalski et al., 2008; Krutz et al., 2006) and is even more mobile than metolachlor (Bayless et al., 2008; Rose et al., 2018). The concentration of MESA is reported to be five times the amount of MOXA (Eckhardt et al., 1999). Little information is known about the adsorption of metolachlor and almost no data are available on the adsorption of MESA and MOXA in the vadose zone (Sidoli et al., 2020). Both metabolites (MESA and MOXA) are considered nonrelevant with a threshold of 3 µg/L in groundwater (BMG, 2014; Umweltbundesamt, 2015).

The terbuthylazine (TBA) chemical family is s-triazine, which includes a large number of herbicides used in weed control (Guzzella et al., 2003). There are many degradation products of terbuthylazine (TBA), but the ones of interest to be modelled in this study and compared with measured data are four of them, which are desethyl-terbuthylazine (MT1), hydroxy terbuthylazine (MT13), 6- (tert-butylamino) -1,3,5-triazine-2,4-diol (LM5) and 4-(tert-butylamino)-6-hydroxy-1-methyl-1,3,5-triazin-2(1H)-one (LM6), as named in (EFSA, 2019). Terbuthylazine (TBA) is highly persistent on the surface of the soil where it degrades into MT1 which is one of the most abundant metabolites in groundwater aquifers of the EU (Loos et al., 2010). Terbuthylazine (TBA) is a toxic chemical that affects living organisms at low doses (Brumovský et al., 2017). Terbuthylazine (TBA) with its metabolite desethyl-terbuthylazine (MT1) has been found in surface and groundwater to raise environmental concerns when its levels are getting higher than 0.1 µg/L which is the limit of toxicity determined by the EU in drinking water (Guzzella et al., 2006). The European Food Safety Authority (EFSA) reported that terbuthylazine (TBA) poses a high risk to aquatic organisms, mammals, plants, and earthworms (EFSA, 2019; EFSA, 2011b).

HYDRUS-1D is a reliable software to simulate pesticide transport and fate in soil (Šimůnek et al., 2018). Numerous models have been established to simulate the fate and transport of agricultural chemicals (Jacques et al., 2000; Köhne et al., 2009; Ladu & Zhang, 2011; Šimůnek et al., 2013a). The HYDRUS-1D code applies to different models of flow and transport in both saturated and variably saturated conditions due to the

flexibility of the code to a large number of processes that helps to solve different environmental and agricultural problems (Šimůnek et al., 2013a). It is free software available that is used to describe different processes in soil columns, it can also be used for modelling the metal transport in soil columns and accumulation as in (Trakal et al., 2013). The HYDRUS-1D code considers the transport of multiple solutes and the degradation chain which can be a first-order degradation chain or diverge and become independent (Šimůnek et al., 2013a). But HYDRUS-1D does not consider the divergence and convergence in the degradation chains in the same model (Jacques et al., 2000; Schaerlaekens et al., 1999), that is why two models were established in this work to simulate the divergent metabolites.

This work aims to numerically model the transport and fate (the biodegradation and metabolite production pathways of metolachlor and terbuthylazine) using HYDRUS-1D software (Šimůnek et al., 2018). As well as comparing the modeled results with the measured data for better understanding the biodegradation, sorption, and root water uptake effect on the herbicides applied and metabolites of metolachlor (MESA and MOXA) and terbuthylazine (MT1, MT14, LM5, and LM6). Also, fitting parameters of first-order biodegradation ( $\mu$ ), first-order chain production ( $\mu'$ ) and linear sorption isotherm ( $K_d$ ) using parameter estimation (PEST) (Doherty, 2020b, 2020a) as a calibration tool. After many trials to get the best fit between the measured and modelled data with the assumption of physical equilibrium and chemical one-dimensional nonequilibrium transport where the herbicides are involved in first-order decay production chains to form their metabolites (Šimůnek & van Genuchten, 1995).

## 2. Objectives and aims of this thesis

The main idea of this study was to investigate the transport and fate of the previously mentioned four herbicides and their metabolites. Metabolites of metolachlor are, metolachlor ethanesulfonic acid (MESA) and metolachlor oxanilic acid (MOXA) and of terbuthylazine are desethyl-terbuthylazine (MT1), hydroxy terbuthylazine (MT13), desethyl-terbuthylazine-2-hydroxy (MT14), 6-(tert-butylamino)-1,3,5-triazine-2,4-diol (LM5) and 4-(tert-butylamino)-6-hydroxy-1-methyl-1,3,5-triazin-2(1H)-one (LM6). This was done using the HYDRUS-1D reactive solute transport model to track the biodegradation chains of the herbicides (Šimůnek et al., 2018). In a trial to combine the numerical model and the observed data from one lysimeter (Ly1), to determine the influence of biodegradation, sorption, and root water uptake. The study is interested to optimize and calibrate the first-order biodegradation parameter ( $\mu$ ) and first-order production parameter ( $\mu'$ ) which is the most important parameter responsible for showing the daughters of the herbicides as discussed in the methodology chapter (Jacques et al., 2000; Schaerlaekens et al., 1999; Šimůnek et al., 2018).

Four HYDRUS-1D models have been set up because the biodegradation of the herbicides metabolites takes two different pathways (branches) with and without root water uptake in each branch for both metolachlor and terbuthylazine. HYDRUS-1D cannot deal with branching in the biodegradation chains of degradants; therefore, there must be two different models to model the biodegradation chain in each branch independently (Jacques et al., 2000). It has been noticed that the leachate observed data from the measurements fit the modelled data from the modeled. Accordingly, the model calibration process using Parameter Estimation suit 17.2 (PEST) by Doherty, (2020a, 2020b) was the solution to reduce the gap between the measured and modeled data. The two herbicides terbuthylazine and metolachlor and their metabolites that have been detected in leachate are of interest in this work, as they have been degraded and their biodegradation products were tracked. Unlike the other two herbicides porosulfuron and nicosulfuron, which appeared in the leachates but their metabolites did not.



### 3. Literature review: background and state of the art

The vulnerability of groundwater to contamination is high to the extent that some herbicides applied to the soil can affect it, especially in areas with intensive agriculture (Sidoli et al., 2016). The characteristics of the compounds and the soil can define the leachability of the compounds (Fenoll et al., 2015; López-Piñeiro et al., 2014; Weber et al., 2003). The fate of the herbicide depends on many factors: adsorption of the soil particles, transfer in the soil, biotic and abiotic degradation, production of metabolites and volatilization (Crisanto et al., 1995; Köhne et al., 2004; Navarro et al., 2007; Weber et al., 2003). Some studies proposed that some herbicides can react in the unsaturated zone (Baran & Gourcy, 2013; Papiernik et al., 2006; Sidoli et al., 2016). The difference in physical and chemical properties between herbicides and the soil can determine how the reaction will be (Sidoli et al., 2020). The degradation process is highly affecting the transport and fate process in the soil by the production of metabolites (Caracciolo et al., 2005; Vischetti et al., 1998). The plant root can also uptake those herbicides or their metabolites with water from the soil which can affect their concentrations either with passive or active uptake (An et al., 2022; Brunetti et al., 2022; Rein et al., 2011; Sur et al., 2022). There is no doubt that numerical modelling has become a promising tool for studying the transport and fate in the soil (Groh et al., 2022; Imig et al., 2022a; Imig et al., submitted-a; Imig et al., submitted-b; Imig et al., 2022b; Ladu & Zhang, 2011; Stumpp et al., 2009b). There are some studies on the modeling of fate and transport of herbicides in the vadose zone (Anlauf et al., 2018; Boivin et al., 2006; Hou et al., 2016). Other studies investigated the modelling of pesticide degradation and adsorption in the vadose zone using HYDRUS-1D. Non-volatile pesticides were studied in three soils using the dual porosity and transient mobile immobile approaches to model the degradation and adsorption of pesticides (Cheviron & Coquet, 2009). Another study of transport modifying the hydraulic functions to account for preferential water flow and transport of pesticides in three cultivated fields using HYDRUS-2D (Boivin et al., 2006). Five pesticides were applied to the soil with a conservative tracer (bromide) in a field in northern New Zealand using the models of HYDRUS-1D, LEACHM, GLEAMS, and SPASMO in comparison to the measured data. Optimization of leaching parameters, degradation and partition coefficient of the pesticides using PEST optimization package have been carried out (Sarmah et al., 2005). In another study, the pesticide transport model was set up to study the degradation kinetics of reactive solute transport and the fate of atrazine in the soil using HYDRUS-1D (Cheyins et al., 2010). A pesticide model for leaching and accumulation fate was established using HYDRUS-1D with ArcGIS using a python code to realise both tools (Anlauf et al., 2018).

In previous work the water flow in the unsaturated zone was studied in two lysimeters with different soil textures. Using stable water isotopes ( $\delta^{18}\text{O}$ ,  $\delta^2\text{H}$ ) as tracers, water flow was tracked together with lumped-parameter model application which was originally for the steady state. After improving the model using input functions, flow conditions were modelled and environmental tracers were interpreted using the data of two lysimeters in an experimental site in Wielenbach, Germany (Shajari et al., 2020). Another study extended the lumped-parameter model and subdivided the simulation period into several small periods as a trial to simulate the transient flow in the two lysimeters. The study

implemented the dual permeability approach to allow consideration of preferential flow and considered the implementation of different input functions. The results of the study were compared to numerical simulations in unsaturated conditions and isotope transport in HYDRUS-1D (Imig et al., 2022b). HYDRUS-1D was used to simulate water flow and solute transport in the lysimeters. Also, to compare the simulation results to the observed values from the lysimeters, we consider a single porosity approach with one lysimeter and a dual porosity approach with the other. It was observed that the low isotopes amount that has been improved using the immobile portion in the dual porosity approach. It has been concluded that the different soil hydraulic parameters between the two soils affect the water flow (Imig et al., submitted-a; Imig, et al., submitted-b). The HYDRUS-1D model was used to study the contamination potential of four herbicides (terbuthylazine, metolachlor, nicosulfuron, and prosulfuron) in the soil of two lysimeters in Wielenbach, Germany. The study is interested in the determination of the reactive transport parameters, such as the sorption and biodegradation of herbicides. The percentage of the herbicides in the lysimeter drainage varies between 0.5 and 15.9 %. The rest was assumed to be adsorbed, taken through the roots of the cropped maize, or biodegraded, where the high carbon isotopes in the leachate indicate the biodegradation of the herbicides. The high number of leached herbicides after high precipitation seasons was assumed to indicate the preferential flow influence.

### **3.1 Study site description and data availability**

The lysimeter facility is located 48 km southeast of Munich near Wielenbach, Germany at an elevation of 549 meters above sea level. It is operated by the Bavarian Environmental Agency (Bayerisches Landesamt für Umwelt, LfU) since 2002 as described in detail by Shajari et al. (2020). The measured data are provided from lysimeter 1 (Ly1), which is one of eight lysimeters over the facility in a time from 2013 to 2017. The lysimeter has a surface area of 1 m<sup>2</sup> and a length of 2 m, and is made of a cylinder of High-Density Polyethylene (HDPE). The lysimeter was grown with biogas maize in a pattern of 12 plants per m<sup>2</sup> during a period from 2013 to 2017 except in 2014 it was 9 plants per m<sup>2</sup>. The seeds was at the end of April/ beginning of May, and harvesting was at the end of September/ October. The lysimeter is automatically weighed every half hour. The lysimeter was lower-boundary controlled to permit seepage in case of water saturation of the soil but no inflow upward.

#### **3.1.1 Measurements**

The lysimeter system automatically measures and monitors the volume of seepage water, the volume of precipitation, the seepage water volume, precipitation volume, outflow, and the weight of the lysimeter with a precision of 0.5 h. Because of a lack of information about precipitation in the area before 2013, precipitation, temperature, and air humidity data were provided by the meteorological weather station which is operated by the German Meteorological Service (Deutscher Wetterdienst DWD). Wind velocity and incoming short-wave solar radiation data were provided from the DWD weather station near Hohenpeißenberg, 15 km to the southwest as they are not measured at the lysimeter area, where solar radiation was provided from the satellite observations of the Climate Monitoring Satellite Application Facility (Shajari et al., 2020).

The concentrations of the herbicide outflow have been measured using high-performance liquid chromatography (HPLC) using tandem mass spectrometric detection with direct injection (detection limit: 0.01 – 0.03 µg/l) in the period from April 2013 to November 2017. The frequency of sampling increases after application on a two-weekly basis depending on the amount of leachate. The solutes detected in the leachate are the applied herbicides which are metolachlor (MTLC) and its two metabolites, metolachlor ethane sulphonic acid (MESA) and metolachlor oxanilic acid (MOXA), terbuthylazine (TBA) and its four metabolites, desethyl-terbuthylazine (MT1), 2-hydroxy terbuthylazine (MT13), terbuthylazine 2 CGA 324007 (LM5), and terbuthylazine 1 SYN 545666, (LM6), as well as prosulfuron and nicosulfuron as studied by Strauß et al., (2017).

### 3.1.2 Soil characteristics

Regarding lysimeter 1, soil samples cannot be taken from the soil in the lysimeter as it should stay undisturbed. Therefore, the sample was picked from an area 1 kilometer from the original place of the soil on the lysimeter because that area was not accessible due to infrastructure and constructed buildings.

The soil type in lysimeter 1 is sandy gravel from the Munich gravel plain from a shooting area near Garching, Germany. The description of the soil is a calcareous regosol over calcareous sand, silt, and gravel that forms the A-horizon with a thickness of 50 cm. C-horizon consists of sandy gravel as described in Table 1 below:

**Table 1:** Soil characteristics of lysimeter 1 after Shajari et al., (2020)

Depth (m)	Horizon	description	<2 mm (%)	>2 mm (%)
0-20	A	Humic upper soil	51	49
20-30	A	Humic upper soil	49	51
30-40	A	Humic upper soil	67	33
40-50	A	Humic upper soil	34	66
50-100	C	Sandy gravel	19	81
100-200	C	Sandy gravel	21	79

### 3.1.3 Herbicide application

The application of herbicides to the lysimeters was once a year in late May or early June, 2014 to 2017. This corresponded to common agricultural practice. Metolachlor and terbuthylazine have been applied every year. Nicosulfuron was not applied in 2014 and 2015 as it is not allowed to apply it in the same area every year, and prosulfuron was applied in 2015, 2016, and 2017. The amounts of applied herbicides are shown in Table 2.

**Table 2:** Applied herbicides with their concentration between 2013 and 2017 after Strauß et al. (2017)

Product	Herbicide	Applied amount (mg/m <sup>2</sup> )				
		(Between brackets: the concentration of the applied solution (g/l))				
		28/05/2013	06/06/2014	03/06/2015	15/06/2016	01/06/2017
Gardo Gold	Metolachl or	46.1 (0.69)	117.3 (1.76)	96.0 (1.44)	81.0 (1.22)	70.0 (1.05)
	Terbuthyl azine	33.2 (0.50)	80.7 (1.21)	78.0 (1.17)	45.0 (0.68)	30.0 (0.45)
Milagro forte	Nicosulfur on	7.6 (0.11)	-	-	5.1 (0.08)	5.6 (0.08)
	Prosulfuro n	-	-	2.5 (0.04)	1.7 (0.03)	1.4 (0.02)

### 3.1.4 Sampling at the Study site

The collection of samples of precipitation and outflow at the study site is weekly which can be -in longer or shorter intervals- depending on the dry or wet conditions, respectively, as described in detail by Shajari et al. (2020). The precipitation was collected from a meteorological station at the study site which is operated by the German Meteorological Service (Deutscher Wetterdienst DWD). A heatable precipitation gauge (Pluvio, OTT Hydromet) was used for recording the precipitation amount automatically with a resolution of 0.5 h. Daily average air humidity and temperature data were collected from the station at the site. The daily average measurements of wind velocity and solar radiation were made at the DWD station located 15 km southwest of the lysimeter site in Hohenpeißenberg, Germany, as data were not available at the time of study at Wielenbach. Satellite observations for longwave radiation were collected from the Satellite Application Facility on Climate Monitoring (CM SAF, product CLARA-A2). The water seepage collection sampling period is from the end of May 2013 until the middle of October 2017.

## 3.2 Herbicides and their metabolites

### 3.2.1 Metolachlor

#### 3.2.1.1 Environmental fate

Metolachlor is an herbicide applied to control broadleaf and annual grassy weeds. It has been widely used in agriculture since 1978 as an herbicide on corn, soybeans, sorghum, cotton, peanuts, beans, potatoes, tomatoes, and other crops. It is usually applied to the surface of the soil before planting. Metolachlor requires rainfall or irrigation to move it into the soil to make it available for uptake by plant roots. Due to degradation, a fraction of the herbicide may not get to its target, and most will be degraded. Some of the metolachlor or its metabolites can be leached from the field and transported to groundwater, surface water, or the atmosphere. Studies showed that metolachlor and its metabolites were observed in many hydrologic bodies (McCarty et al., 2014).

The degradation half-life of metolachlor is between 7 and 14 days, as proved by Ismail & Quirinus, (2000), where the soil composition was (organic carbon 2%, clay 10%, silt

3.7%, sand 86.3%, pH 4.8). Metolachlor degradation was studied in an aqueous sediment environment using sandy loam for 112 days, the detected degradation rate of metolachlor was  $0.008 \text{ d}^{-1}$  and the half-life time was 34 days. The values were different in water where the degradation rate was  $0.012 \text{ d}^{-1}$  and the half-life time was 8 days. Although the degradation rate and half-life time in soil with and without switchgrass were found to be  $0.53 \text{ d}^{-1}$  6 days,  $0.52 \text{ d}^{-1}$ , and 9.6 days respectively (Mersie et al., 2004).

The dissemination of metolachlor in clay loam soil was studied by measuring the decline in residues, leachability, movement into drainage water, and contamination of groundwater by metolachlor. The studies show that the amounts of decrease in the metolachlor was in the first 15 cm for 332, 364, and 370 days respectively in 1987, 1988, and 1989, and the half-lives of 80, 99, 142 days were calculated. Metolachlor was found in groundwater between the fall of 1988 and the summer of 1989 at a depth of 1.2 to 4.6 m. It has been estimated that by the end of the fall the percentage of metolachlor is 0.06 and 0.19% for depths of 1.2 and 4.6 m, respectively (Frank et al., 1991).

### **3.2.1.2 Soil adsorption/mobility**

Metolachlor is dependent -in its mobility- inversely on soil organic matter and clay content. It tends mainly to be leached with preferential flow in clay soils rather than silty soils. Adsorption of metolachlor is higher in clay soils than in soils with low organic matter and clay content and adsorbs more readily to organic matter than to clay (Alhajjar et al., 1990; Weber et al., 2003). When soil organic matter is  $>2\%$ , leaching of metolachlor is not expected (Ahrens & Edwards, 1994). It has been found that the applied metolachlor is leached -after two precipitation periods with the intensity of 400 mm and 24 hours each step is 12 hours- with a concentration of  $0.2 \mu\text{g/L}$  after the first event to  $74.50 \mu\text{g/L}$  after the last 12 hours in a soil profile of 50 cm where clay content increasing in the base of sandy clay loam soil and sandy clay in the first 20 cm (Dores et al., 2013). Another study shows that metolachlor leaching was accompanied by an increase in the herbicide and its metabolites in the subsoil and leachate and depends on the half-life and the herbicide/soil binding factor ( $K_d$ ). Mobility also depends on the amount of input water (which can be described with the variable  $K_s$ ) and longevity ( $DT_{50}$ ) (Weber et al., 2006).

### **3.2.1.3 Environmental biodegradation**

Metolachlor degrades extensively by complex metabolic reactions in soil, plants, and animals (Ahrens & Edwards, 1994). Herbicide biodegradation occurs due to mineralization of such herbicides by microorganisms. The mineralization process is the ability of microorganisms to use the chemicals as a source of carbon and energy to grow (Zabaloy et al., 2011). By measuring  $^{14}\text{CO}_2$ , the study showed that the mineralization percentages of metolachlor after 35 days in anaerobic and aerobic conditions are 31 and 20 % respectively (Kanissery et al., 2018). The metolachlor half-life time of degradation ranges from 37.9 to 49.5 days in unsterilized soils. The rate of degradation increases directly with increasing the soil organic matter. Other soil properties affect the degradation rate like cation exchange capacity, pH, and clay content (Wu et al., 2011). The aerobic aquatic biodegradation of the half-life of metolachlor is 47 days. Metolachlor disappear in the groundwater free of aquifer material is so slow. It may take a lag period after which metolachlor starts to degrade in a half-life of 548-1074 days (Cavalier et al., 1991). It has

been found that the sterilization of the soil affects the degradation of the metolachlor. In the sterilized soils, the degradation process of metolachlor decreased in comparison with the unsterilized soils (Long et al., 2014). A study shows that the soil microbes decrease by many orders of magnitude with depth in the soil profile that is because the surface of the soils is richer in organic matter. Some of the microbiological populations can adapt and degrade metolachlor due to the repetitive application (Wu et al., 2011).

#### **3.2.1.4 Environmental abiotic degradation**

The half-life time of the aqueous photolysis is 70 days in case it was directly under sunlight and 0.17 days when the source is artificial. For example, for a mercury arc lamp with an intensity of 1600-2400 uW/sq cm, the half-life time will be 37 days. The photodegradation half-life of metolachlor in the sand soil is around 8 days with the natural light source. It is also one of the major reasons for the dissipation of metolachlor on the soil surface especially when there is a lack of rain (Ahrens & Edwards, 1994). Photolysis of metolachlor in water is impeded by humic substances. The half-life of metolachlor in distilled water, seawater, river water, and lake water were 8, 17, 24, and 29 days, respectively (Chesters et al., 1989; Dimou et al., 2005).

The increase in temperature during irradiation may volatilize an amount (5%) of the applied metolachlor. Photodegradation of metolachlor in the organic free, lake, in comparison to a 0.5 mg/L organic matter water is 8 to 11 and 22 days in the summer sunlight and 54, 77, and 231 days in winter natural light respectively (Kochany & Maguire, 1994). The major four transformation products of metolachlor due to photodegradation in water are [2-hydroxy-N(2-ethyl-6-methylphenyl)-N-(2-methoxy-1-methylethyl) acetamide]; [N-(2-ethyl-6-methylphenyl)-N-(2methoxy-1-methylethyl) acetamide]; [4-(2-ethyl-6-methylphenyl)-5-methyl-3-morpholinone]; [2-hydroxyN-(2-ethyl-6-methylphenyl) acetamide] (Kochany & Maguire, 1994).

#### **3.2.1.5 Volatilization from water/soil**

Volatilization was found to occur at high temperatures; however, it is not so effective in the fate process of metolachlor. Some losses can occur due to volatilisation by sunlight from the soil surface (Chesters et al., 1989). Metolachlor is supposed to be nonvolatile depending on the results of Henry's law constant ( $9.0 \times 10^{-9}$  atm-m<sup>3</sup>/mole) in soil with high water content and water surfaces (Chesters et al., 1989). However, volatilization may occur at high-temperature degrees 40 to 50 °C which is a good indication of the direct proportion of Henry's law constant with temperature (El-Nahhal et al., 1999). Metolachlor was applied to different soils with different moisture content, and it has been observed that the volatilization increases with increasing soil moisture content (Gish et al., 2009). Metolachlor is not likely to volatilize from the dry soil when the vapor pressure is  $3.1 \times 10^{-5}$  mm Hg (Wauchope et al., 1992). A study showed that the volatilization of metolachlor after application ranges from 5-20 % after application to soil (Prueger et al., 2017). In another study by Prueger et al., (2005) in which the volatilization of metolachlor was measured through the years from 1998 to 2002, it was clear that volatilization was high in the first 12-24 hours after application and then fades after 48-72 hours.

### 3.2.1.6 Transformation products of metolachlor

Metolachlor transforms into metabolites through abiotic and biotic processes (Zemolin et al., 2014). Two of these metabolites are biologically degraded, metolachlor ethane-sulfonic acid (MESA) (2-([2-ethyl-6 methylphenyl] [2- methoxy-1-methylethyl] amino) -2-oxoethanesulfonic acid) and metolachlor oxanilic acid (MOXA) (2-([2-ethyl-6-methylphenyl] [2- methoxy-1-methylethyl] amino)-2-oxoacetic acid) as in Table 4 and Figure 1 (Graham et al., 1999)

The water solubility of MESA is higher than that of MOXA and metolachlor, which are equal to 212,000 mg / L 967 mg / L., and 540 mg/L respectively (Rose et al., 2018). However, the two transformation products are persistent and can also accumulate in soil and water. Aerobic bacterial degradation is crucial in soil. The degradation opportunity of metolachlor depends on the flow direction of water in the soil, residence time, redox potential, microbiological activity, and aerobic and anaerobic conditions. The log exposure rate of metolachlor to micro-organisms results in a higher potential of degradation to MESA and MOXA (Graham et al., 1999). Around 10 percent of metolachlor applied in the soil are volatilized, 0.3% are from rainfall and less than 0.02% seep into groundwater, the remaining 90% of the applied metolachlor were taken up by plants or transformed (Rose et al., 2018). In Table 3, the properties of the two metabolites of metolachlor, MESA and MOXA.

**Table 3:** Degradation properties of metolachlor and its metabolites (MESA and MOXA) (Rose et al., 2018) NA: means not available

Compound	Koc ( mL/g OC)	Soil half-life at 25 °C (days)	Hydrolysis half-life (days, at 30 °C)	Avg. field dissipati on half-life (days)	Aerobic soil degradati on half-life (days)	Anaerobic soil degradati on half-life (days)
Metolachlor	180	10	> 200	114	26	37
MESA	13.5	70	NA	NA	NA	NA
MOXA	17	50	NA	NA	NA	NA

The high mobility of transformation products threatens the water resources such as groundwater, which renders delineation of the pathways of metabolites in the subsurface and usage of groundwater quality monitoring programmes (Farlin et al., 2018). Modelling studies of transport and fate performed under different agricultural conditions demonstrate the seepage of MESA into groundwater (Bayless et al., 2008). There is a successful simulation of the behavior of MESA in the groundwater aquifers, but other deep studies are still needed for different aquifers showing the variability of degradation rates of metolachlor as well as the sorption properties (Dubus et al., 2003).

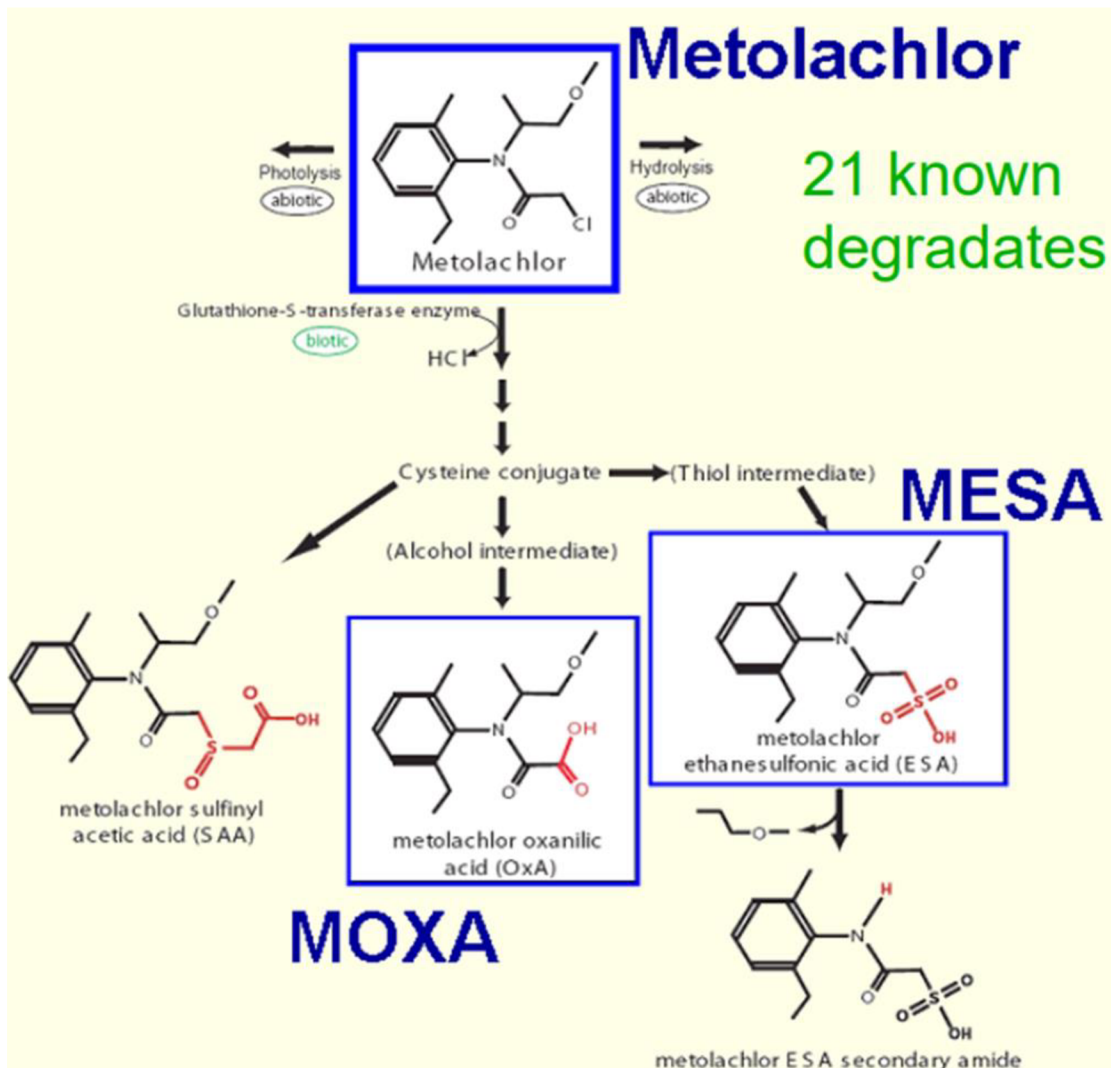


**Figure 1:** Biodegradation reactions of metolachlor herbicide and its major metabolite MESA and MOXA with a sum formula (Rose et al., 2012)

*Note.* From “A Holistic Assessment of the Occurrence of Metolachlor and 2 of its Degradates Across Environmental Settings Metolachlor Uses Pesticides in Surface Water and Groundwater Purpose of Study,” by C. E. Rose, H. L. Welch, R. H. Coupe, & P. D. Capel, 2012, In abstracts of papers of the American Chemical Society.

There are concentration differences of the metolachlor metabolites (MESA and MOXA) in groundwater and springs where MESA can reach tenfold the concentration of MOXA. The sorption strength can also control the predominance of MESA over MOXA in soil (Farlin et al., 2018).

### 3.2.2 Terbutylazine

Terbutylazine is one of the s-triazine herbicides used for selective weed control. But due to the high risk of using triazine in soil and its related metabolites, its use and production have been banned in European countries (Sass & Colangelo, 2006). That is



why terbuthylazine has been introduced instead as a substitute for triazine due to its favorable physicochemical properties like its lower solubility and higher adsorption. For such reasons, it poses a lower risk of groundwater contamination (EFSA, 2011a). However, the extensive use of this herbicide at levels exceeding the regulated limits is a source of contamination (Bottoni et al., 2013).

Terbuthylazine is weakly basic and in soil pH conditions is neutral and moderately hydrophobic ( $\log K_{ow} = 3.4$ , Table 5). The half-life in the soil is 167 days (Scherr et al., 2017). The transformation process of terbuthylazine is governed by two processes which are soil microbiology and chloro-hydrolysis abiotic degradation is of minor effect (Mandelbaum et al., 2008; Satsuma, 2010). The studies of atrazine were useful to the understanding of the biodegradation mechanisms of s-triazines. The two main pathways of degradation are oxidative N dealkylation and hydrolytic mineralization (Udiković-Kolić et al., 2012).

Transformation in soil and water through the biodegradation pathway (N-dealkylation) of terbuthylazine results in the formation of the metabolite desethyl-terbuthylazine (MT1) or detertbutyl-terbuthylazine, and the dichlorination pathway results in hydroxy terbuthylazine (MT13) (Karanasios et al., 2013). Hydroxy-dealkylated metabolites result in hydroxy-detertbutyl-terbuthylazine (Caracciolo et al., 2005).

Dealkylated metabolites are more soluble, therefore they are more mobile and more supposed to contaminate groundwater (Guzzella et al., 2003). The metabolites resulting from the hydroxylation process are less soluble and accordingly will be ready to be adsorbed to soil particles (EFSA, 2011a). The degradation rate of terbuthylazine is dependent on the treatment terbuthylazine history and soil self-remediation potential. Many factors can also affect the degradation of terbuthylazine like soil depth, soil pH, water content, temperature, organic matter, and soil texture (Kodešová et al., 2011).

### **3.2.2.1 Degradation and metabolism of terbuthylazine**

In a study carried out on sterilized and non-sterilized soils, terbuthylazine was applied to both. It was noticed that the half-life of terbuthylazine was much higher in the sterilized soil than in the non-sterilized soil because of the absence of bio-organisms that significantly affecting the degradation process. In the non-sterilized soils, it was found that the half-life of terbuthylazine of the soils amended by corn straw amended soils (55.5 days) is lower than that of the urban sewage sludge (73.7 days) and was generally higher than all other non-sterilized treatments. The lower degradation rate in the non-sterilized soils -amended by urban sewage sludge- could be due to the high amount of organic carbon in it and accordingly the high adsorption potential in it. The longest half-life was recorded in the sterilized soil samples. Those results give us an indication that using poultry compost and urban sewage sludge retards the degradation process of terbuthylazine in sterilized soils which indicates that they stimulate microbial activity, but they also increase the adsorption and reduce availability. The metabolism of terbuthylazine has been also observed, the parent compound degraded to desethyl-terbuthylazine which is the major product of metabolism (Dolaptsoglou et al., 2007). It has been proved that desethyl-terbuthylazine forms twice the amount of all other metabolites of terbuthylazine that have been found in the leachate together with desethyl-

terbuthylazine-2-hydroxy (MT14) after application of terbuthylazine in the soil which is considered potential pollution of groundwater (Guzzella et al., 2003).

#### **3.2.2.2 Bioavailability of terbuthylazine**

It has been found that the concentration of terbuthylazine in soils that are not amended is higher than soils amended by urban sewage sludge and a little higher than those amended by corn straw and poultry compost. This could be because of the high organic carbon and high sorption of terbuthylazine in urban sewage sludge-treated soil and the low availability of terbuthylazine (Dolaptsoglou et al., 2007; Guzzella et al., 2003).

#### **3.2.2.3 Mobility, leaching, and adsorption**

The leaching potential of terbuthylazine through the soil with water is high. But it has lower water solubility and tends to be absorbed by soil and organic matter particles (Kronvang et al., 2003). The metabolite desethyl-terbuthylazine shows more mobility than its parent compound (EFSA, 2011a). The ground ubiquity scores of the parent and its metabolite are 3.07 and 3.9 respectively, which means that they have high leaching ability. In a leaching test, it has been found that 70% of the applied terbuthylazine are in the leachate (Calderon et al., 2016). It was found in a study that terbuthylazine and its metabolites are not in the leachate of the 2 m deep lysimeter except for desethyl-terbuthylazine was found frequently in the leachate after the repeated application of terbuthylazine. The estimated half-lives of metolachlor -applied in the study with terbuthylazine- are 26 and 37 days, respectively, which indicates that terbuthylazine mineralizes faster than metolachlor (Schuhmann et al., 2019).

#### **3.2.2.4 Metabolites of terbuthylazine**

Terbuthylazine metabolism and transformation depend on soil microbes and chloro-hydrolysis. Its chlorine atom is influenced by the clay content and pH in the soil. This process forms the metabolite hydroxy terbuthylazine but the other process which depends on the biotic reaction and dealkylation of s-triazine forms the metabolite desethyl-terbuthylazine. Desethyl-terbuthylazine-2-hydroxy (MT14) results from the hydroxylation of desethyl-terbuthylazine (MT1) or the deethylation of hydroxy-terbuthylazine (MT13) (Guzzella et al., 2003).

The dealkylated metabolites like desethyl-terbuthylazine-2-hydroxy (MT14) and hydroxy-deterbytyl-terbuthylazine are found to be more water-soluble than terbuthylazine, hence, they have more potential to contaminate the aquatic environment. But on contrary, terbuthylazine tends to be retained and adsorbed to the soil due to the lower water solubility (EFSA, 2011a).

Results of the experiment on the terbuthylazine in a liquid medium under two different conditions. It was noticed that terbuthylazine was converted to triazine, which is a more soluble species, and they mix in the dissolved portion. LC-MS analysis showed that there are five intermediates of terbuthylazine during transformation. The study revealed that the M3-T bacterial culture is effective in the degradation of terbuthylazine (within 3 days). The first compound to be produced from this transformation by dichlorination is hydroxy-

terbuthylazine (MT13) as a dominant metabolite that will be transformed into LM5 which is subsequently transformed into LM6 (Jurina et al., 2014).

This study is interested in studying the transport and fate of four terbuthylazine metabolites that are desethylterbuthylazine (MT1), 2-hydroxy-terbuthylazine (MT13), 6-tert-butylamino-3-methyl-1H-[1,3,5]triazin-2,4-dione (terbuthylazine (LM6)), 6-tert-butylamino-[1,3,5]triazin-2,4-diol (terbuthylazine (LM5)) see Table 4. The metabolism reaction scheme is shown in Figure 2.

**Table 4:** Names, chemical SMILES, chemical formula and CAS identifier for the herbicides metolachlor, terbuthylazine, and their metabolites

Name	IUPAC Name	SMILES	Molecular Formula	CAS
<b>Metolachlor (MTLC)</b>	2-chloro-N-(2-ethyl-6-methylphenyl)-N-(1-methoxypropan-2-yl)acetamide <sup>[1a]</sup>	<chem>CCc1cccc(C)c1N(C(C)COC)C(=O)C</chem> <sup>[2a]</sup>	C <sub>15</sub> H <sub>22</sub> ClNO <sub>2</sub> <sup>[1a]</sup>	51218-45-2 <sup>[2a]</sup>
<b>Metolachlor ethanesulfonic acid (MESA)</b>	2-[2-ethyl-N-(1-methoxypropan-2-yl)-6-methylanilino]-2-oxoethanesulfonic acid <sup>[1b]</sup>	<chem>N(C(CS(=O)(=O)O)=O)(C(COC)C)C1=C(CC)C=CC=C1</chem> <sup>[2b]</sup>	C <sub>15</sub> H <sub>23</sub> NO <sub>5</sub> S <sup>[1b]</sup>	171118-09-5 <sup>[2b]</sup>
<b>Metolachlor oxanilic acid (MOXA)</b>	2-[2-ethyl-N-(1-methoxypropan-2-yl)-6-methylanilino]-2-oxoacetic acid <sup>[1c]</sup>	<chem>N(C(COC)C)(C(C(O)=O)=O)C1=C(C)C=CC=C1C</chem> <sup>[2c]</sup>	C <sub>15</sub> H <sub>21</sub> NO <sub>4</sub> <sup>[1c]</sup>	152019-73-3 <sup>[2c]</sup>
<b>Terbuthylazine (TBA)</b>	2-N-tert-butyl-6-chloro-4-N-ethyl-1,3,5-triazine-2,4-diamine <sup>[1d]</sup>	<chem>N(C(C)(C)C)C=1N=C(NCC)N=C(Cl)N1</chem> <sup>[2d]</sup>	C <sub>9</sub> H <sub>16</sub> ClN <sub>5</sub> <sup>[1d]</sup>	5915-41-3 <sup>[2d]</sup>
<b>Desethylterbuthylazine (MT1)</b>	2-N-tert-butyl-6-chloro-1,3,5-triazine-2,4-diamine <sup>[1e]</sup>	<chem>N(C(C)(C)C)C=1N=C(Cl)N=C(N)N1</chem> <sup>[2e]</sup>	C <sub>7</sub> H <sub>12</sub> ClN <sub>5</sub> <sup>[1e]</sup>	30125-63-4 <sup>[2e]</sup>
<b>2-hydroxy terbuthylazine (TBA-2-OH) (MT13)</b>	6-amino-4-(tert-butylamino)-1H-1,3,5-triazin-2-one <sup>[1f]</sup>	<chem>N(C(C)(C)C)C=1N=C(NCC)=NC(=O)N1</chem> <sup>[2f]</sup>	C <sub>7</sub> H <sub>13</sub> N <sub>5</sub> O <sup>[1f]</sup>	66753-06-8 <sup>[2f]</sup>
<b>terbuthylazine 2 CGA 324007 (LM5)</b>	6-(tert-butylamino)-3-methyl-1H-1,3,5-triazine-2,4-dione <sup>[1g]</sup>	<chem>OC1=NC(O)=NC(NC(C)(C)C)=N1</chem> <sup>[3]</sup>	C <sub>8</sub> H <sub>14</sub> N <sub>4</sub> O <sub>2</sub> <sup>[1g]</sup>	[-]
<b>terbuthylazine 1 SYN 545666 (LM6)</b>	6-(tert-butylamino)-1H-1,3,5-triazine-2,4-dione <sup>[1h]</sup>	<chem>O=C1N(C)C(O)=NC(NC(C)(C)C)=N1</chem> <sup>[3]</sup>	C <sub>7</sub> H <sub>12</sub> N <sub>4</sub> O <sub>2</sub> <sup>[1h]</sup>	[-]

**Table 5:** Physical and chemical properties of the herbicides terbuthylazine and metolachlor and their metabolites

Name	Molecular weight [g/mol]	log K <sub>ow</sub> [-]	Melting point [°C]	Vapor pressure [mm Hg]	Water solubility [mg/L] at 25 c	K <sub>aw</sub> (K <sub>h</sub> )	p <sub>ka</sub> [-]
<b>Metolachlor (MTLC)</b>	283.79 <sup>[1a]</sup>	3.13 <sup>[1a]</sup>	-62°C <sup>[2a]</sup>	3.13*10 <sup>-5</sup> <sup>[1a]</sup>	488 <sup>[1a]</sup>	9.0*10 <sup>-9</sup> <sup>[1a]</sup>	No dissociation <sup>[5a]</sup>
<b>Metolachlor ethanesulfonic acid (MESA)</b>	279.33 <sup>[1b]</sup>	1.3 <sup>[4]</sup>	[-]	1.99*10 <sup>-5</sup> <sup>[4]</sup>	238 <sup>[3]</sup>	1.06*10 <sup>-6</sup> <sup>[4]</sup>	3.21 <sup>[7]</sup>
<b>Metolachlor oxanilic acid (MOXA)</b>	329.4 <sup>[1c]</sup>	-1.24 <sup>[4]</sup>	[-]	1.99*10 <sup>-5</sup> <sup>[4]</sup>	212.461 <sup>[4]</sup>	1.13*10 <sup>-8</sup> <sup>[4]</sup>	[-]
<b>Terbuthylazine (TBA)</b>	229.71 <sup>[1d]</sup>	3.4 <sup>[1d]</sup>	177-179 °C <sup>[1d]</sup>	1.12*10 <sup>-6</sup> <sup>[1d]</sup>	9 <sup>[1d]</sup>	2.3*10 <sup>-8</sup> <sup>[1d]</sup>	2 <sup>[1d]</sup>
<b>Desethylterbuthylazine (MT1)</b>	201.66 <sup>[1e]</sup>	2.0*10 <sup>2</sup> <sup>[5b]</sup>	[-]	2.63*10 <sup>-6</sup> <sup>[5b]</sup>	327.1 <sup>[5b]</sup>	[-]	[-]
<b>2-hydroxy terbuthylazine (TBA-2-OH) (MT13)</b>	211.26 <sup>[1f]</sup>	1.82 <sup>[6]</sup>	[-]	[-]	7.19 <sup>[5c]</sup>	[-]	~5 <sup>[6]</sup>
<b>Terbuthylazine 2 CGA 324007 (LM5)</b>	198.22 <sup>[1g]</sup>	[-]	[-]	[-]	143 <sup>[8]</sup>	[-]	[-]
<b>Terbuthylazine 1 SYN 545666 (LM6)</b>	184.2 <sup>[1h]</sup>	[-]	[-]	[-]	398 <sup>[8]</sup>	[-]	[-]

[1a] (PubChem, 2022a), [1b] (PubChem, 2022b), [1c] (PubChem, 2022c), [1d] (PubChem, 2022d), [1e] (PubChem, 2022e), [1f] (PubChem, 2022f), [1g] (PubChem, 2022g), [1h] (PubChem, 2022h), [2a] (CAS, 2022a), [2b] (CAS, 2022b), [2c] (CAS, 2022c), [2d] (CAS, 2022d), [2e] (CAS, 2022e), [2f] (CAS, 2022f), [3] (EFSA, 2019), [4] (Bayless et al., 2008), [5a] (PPDB, 2022a), [5b] (PPDB, 2022b), [5c] (PPDB, 2022c), [6] (Schmitt et al., 1996), [7] (Gomis-berenguer et al., 2021), [8] (ECPR, 2015)

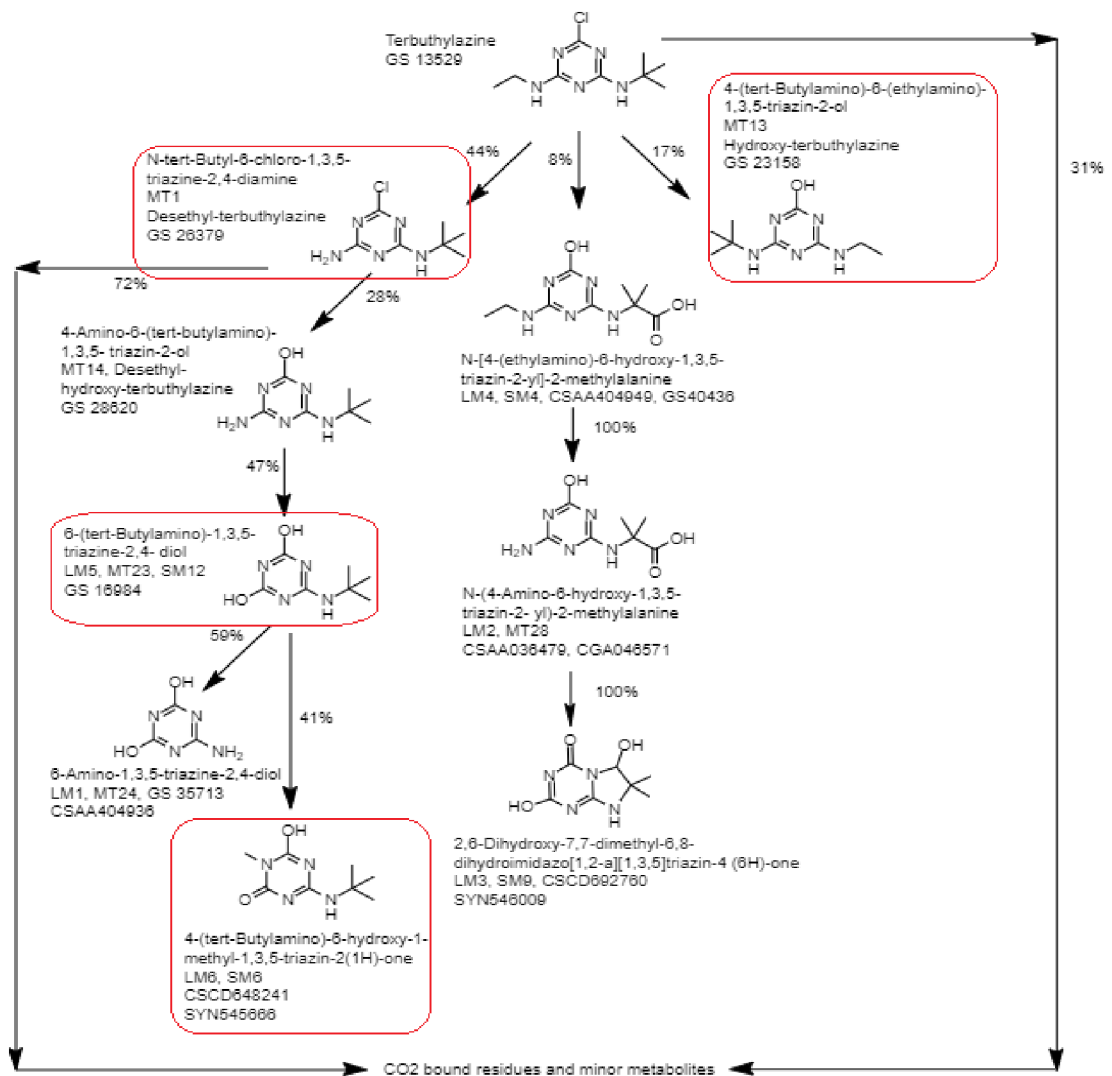


**Figure 2:** Schematic degradation reaction of terbuthylazine and its metabolites, metabolites marked in red are detected and measured in the leachate of the lysimeter and are compared with the modelled (ECPR, 2015)

## 4. Methodology

### 4.1 Numerical model setup

Determination of the transport and fate of metabolites of the concerned herbicides is the main idea behind this work. That was possible using the one-dimensional numerical model HYDRUS-1D (Šimůnek et al., 2018) for water and solute transport in a lysimeter vegetated with maize. The model describes the vertical motion of precipitation water carrying herbicides and related metabolites downward through the soil column. The software works to solve Richard's equation for the unsaturated water flow. The model domain is discretized into 201 nodes 1 cm distance each. Parameter estimation suit 17.2 (PEST) by Doherty, (2020b, 2020a) was used to calibrate the models and perform numerical automated optimization using the Jacobian matrix (Doherty, 2020b, 2020a).

#### 4.1.1 Water flow in the unsaturated zone

The HYDRUS-1D software package works to solve Richard's equation for variably saturated flow and advection-dispersion equations for solute and heat transport (Hopmans, 2011; Šimůnek et al., 2008, 2013, 2016, 2018):

$$\frac{\partial \theta}{\partial t} = \frac{\partial}{\partial z} \left[ k(h) \left( \frac{\partial h}{\partial z} + 1 \right) \right] - s(z, t) \quad (1)$$

where  $h$  is the water pressure head [L],  $\theta$  is the volumetric water content [ $L^3/L^3$ ],  $s$  is the sink term to account for root water uptake,  $Z$  is the spatial coordinate in the vertical direction and  $k$  is the unsaturated hydraulic conductivity [ $L/T^{-1}$ ] which can be calculated from the relationship:

$$K(h, x) = K_s(x)k_r(h, x) \quad (2)$$

where  $k_r$  is the relative hydraulic conductivity, and  $K_s$  is the saturated hydraulic conductivity. To determine the soil hydraulic parameters in the soil, the van Genuchten-Mualem approach has been used, where the soil hydraulic conductivity functions are used by van Genuchten (1980) together with the statistical pore-size distribution model of Mualem (1976) to formulate the equation of unsaturated hydraulic conductivity as shown below:

$$\theta(h) = \begin{cases} \theta_r + \frac{\theta_s - \theta_r}{[1 + |\alpha h|^n]^m} & h < 0 \\ \theta_s & h \geq 0 \end{cases} \quad (3)$$

$$K(\theta) = K_s S_e^{1/2} \left[ 1 - (1 - S_e^{1/m})^m \right]^2 \quad (4)$$

$$S_e = \frac{\theta - \theta_r}{\theta_s - \theta_r} \quad (5)$$

$$m = 1 - 1/n, \quad n > \quad (6)$$

where the parameters  $\theta_r$ , and  $\theta_s$  are the residual volumetric water content [ $L^3 L^{-3}$ ], saturated water content [ $L^3 L^{-3}$ ] respectively;  $\alpha$  and  $n$  are fitting parameters in soil water retention curve,  $K_s$  is the unsaturated hydraulic conductivity [ $LT^{-1}$ ],  $S_e$  is the effective saturation in the soil [-],  $l$  is the pore-connectivity parameter which has estimated value of 0.5 as an average in many soils (Mualem, 1976).

#### 4.1.2 Solute transport

The metabolite transport and fate model was set up using the HYDRUS-1D package. The model represents the variably saturated movement of water and solutes and the decay process of the herbicides applied in the soil under the effects of biodegradation. There are many orders of decay that can describe the fate of such compounds, such as zero-order, half-order, and first-order decay reactions. A simple assumption will be adopted in the case of solute transport and biodegradation in the soil, which is first-order kinetic biodegradation. Sequential first-order biodegradation for the herbicides to get the metabolites. The transformation rate is dependent on the amount of the chemicals present and the first-order biodegradation rate is calculated as follows:

$$\frac{\partial(\theta c)}{\partial t} = -\mu\theta c_t \quad (7)$$

where  $\mu$  is the first order biodegradation rate constant [ $d^{-1}$ ], multiplying  $c$  by  $\theta$  converts the concentration to a volume of soil. The unit of the equation is the mass loss rate per volume of soil [ $ML^{-3}T^{-1}$ ]. The equation shows the only solution phase of solute in soil undergoes decay. The half-life time of a chemical is  $T_{1/2}$  which is the time required for the chemical to decrease to half of its original concentration [T]. The half-life time of the chemical is also inversely proportional to the first-order biodegradation rate ( $\mu$ ) of the chemical which is shown in the relationship (David E. R. & Šimůnek, 2018):

$$\mu = \frac{\ln(2)}{T_{1/2}} \quad (8)$$

the advection and dispersion solute transport equations are generally formulated to include non-linear and non-equilibrium reactions between solid and liquid phases. Consider also zero-order production, first-order biodegradation, and first-order production to allow the modelling of solutes in a sequential first-order chain.

Instantaneous sorption is the most common way to figure out the relationship between the liquid and soil phase in the soil which can be expressed by different models of isotherms like the linear sorption isotherm represented by the linear equation (Šimůnek et al., 2013a):

$$s = K_d c \quad (9)$$

where  $s$  is sorption [ $M M^{-1}$ ],  $K_d$  is the sorption coefficient and  $c$  is the concentration in liquid pore space [ $M L^{-3}$ ]. Although sorption is in most cases non-linear which can be represented by the non-linear models like Freundlich and Langmuir isotherms which are used in HYDRUS-1D shown in the formula (Šimůnek et al., 2008; Šimůnek et al., 2013a):

$$s = \frac{k_f c^\beta}{1 + \eta c^\beta} \quad (10)$$

where  $k_f$  [ $L^{3\beta} M^{-\beta}$ ],  $\beta$  [-] and  $\eta$  [ $L^3 M^{-1}$ ] are isotherm coefficients. When  $\eta = 0$ , the equation will be for Freundlich isotherm and when  $\beta = 1$ , it will be for Langmuir isotherm. This work considers the solid phase of solutes and the products of biodegradation. The soil column in the lysimeter is composed of four layers which are considered in this work as a single homogeneous layer. Four different models are set up depending on the solute biodegradation chain scenarios and the percentage of production into metabolites and biodegradation into other products. As been shown before in the literature review chapter that the herbicide metolachlor has two main metabolites metolachlor ethano-sulphonic acid (MESA) and metolachlor Oxanilic acid (MOXA) which are formed in two chains with two degradation percentage. The same goes to terbuthylazine, where two chains are produced the first is hydroxy-2-terbuthylazine (MT13) and the second chain is desethyl-terbuthylazine (MT1), Desethyl-terbuthylazine-2-hydroxy (MT14), TBA 2 CGA 324007 (LM5), TBA 1 SYN 545666 (LM6).

To simulate the transport and fate of the multiple solutes of sequential first-order decay chain reaction some parameters need to be considered to get the concerned results. HYDRUS-1D code made it possible to consider this in the model via entering the values of biodegradation and production parameters together with sorption parameters as shown in Figure 3 below where the symbols  $c$ ,  $s$ , and  $g$  represent the concentration of the solute in the liquid, solid, and gas phases.  $\mu_w$ ,  $\mu_s$ , and  $\mu_g$  are the biodegradation constants of the parent in the gas, liquid, and solid phases respectively.  $\mu_{w,1}'$ ,  $\mu_{s,1}'$  and  $\mu_{g,1}'$  are the parameters responsible to produce daughters in a sequential first-order decay reaction where  $\mu_{g,1}'$  for the gas phase,  $\mu_{w,1}'$  for liquid phase, and  $\mu_{s,1}'$  for solid phase.  $K_d$  and  $K_g$  are the distribution coefficients between liquid and gaseous phases respectively. The symbols  $\gamma_{g,1}$ ,  $\gamma_{w,1}$ , and  $\gamma_{s,1}$  are representing the zero-order rate reaction for the gas, liquid, and solid phases respectively. The biodegradation process in Figure 3 shows the production of one solute (B), (C)... from the other (A) in a decay chain reaction developed codes in HYDRUS-1D was proven their efficiency to model the transport and fate of different solutes like pesticides, radionuclides, chlorinated aliphatic hydrocarbons, antibiotics, and explosives (Mallants et al., 2003).



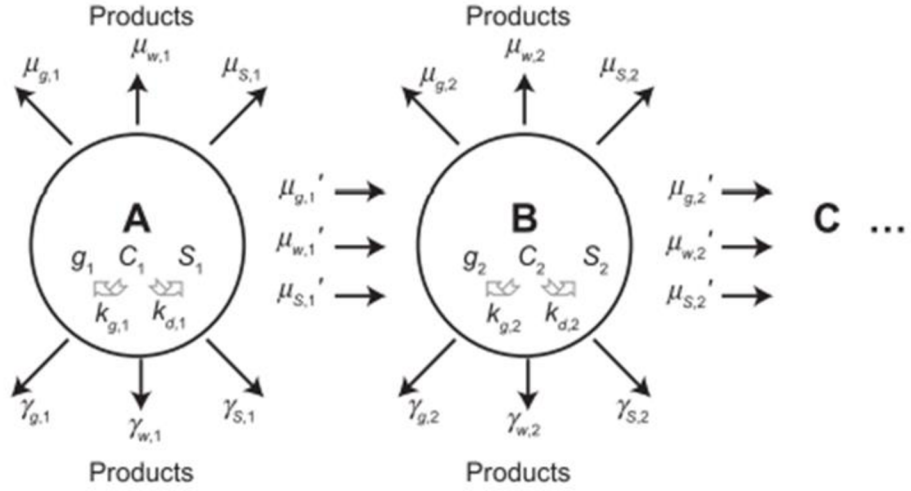


**Figure 3:** Biodegradation process of (solute A) and production of daughters (solute B, C ...) and the parameters governing the whole biodegradation process which are  $\mu_{w,1}$ ,  $\mu_{s,1}$ , and  $\mu_{g,1}$  and production parameters are  $\mu_{w,1}'$ ,  $\mu_{s,1}'$  and  $\mu_{g,1}'$  (Jacques et al., 2000; Šimůnek et al., 2013b; Šimůnek & van Genuchten, 1995)

The partial differential equations governing one-dimensional, non-equilibrium chemical transport of solutes in sequential first-order decay chain during transient water flow in a variably saturated porous medium are represented by the following equations:

$$\begin{aligned} \frac{\partial \theta c_1}{\partial t} + \frac{\partial \rho s_1}{\partial t} + \frac{\partial a_v g_1}{\partial t} & \quad (11) \\ & = \frac{\partial}{\partial x} \left( \theta D_1^w \frac{\partial C_1}{\partial x} \right) + \frac{\partial}{\partial x} \left( a_v D_1^g \frac{\partial g_1}{\partial x} \right) - \frac{\partial q C_1}{\partial x} - r_{a,1} \\ & - (\mu_{w,1} + \mu'_{w,1}) \theta c_1 - (\mu_{s,1} + \mu'_{s,1}) \rho s_1 \\ & - (\mu_{g,1} + \mu'_{g,1}) a_v g_1 + \gamma_{w,1} \theta + \gamma_{s,1} \rho + \gamma_{g,1} a_v \end{aligned}$$

$$\begin{aligned} \frac{\partial \theta c_k}{\partial t} + \frac{\partial \rho s_k}{\partial t} + \frac{\partial a_v g_k}{\partial t} & \quad (12) \\ & = \frac{\partial}{\partial x} \left( \theta D_k^w \frac{\partial C_k}{\partial x} \right) + \frac{\partial}{\partial x} \left( a_v D_k^g \frac{\partial g_k}{\partial x} \right) - \frac{\partial q C_k}{\partial x} \\ & - (\mu_{w,k} + \mu'_{w,k}) \theta c_k - (\mu_{s,k} + \mu'_{s,k}) \rho s_k \\ & - (\mu_{g,k} + \mu'_{g,k}) a_v g_k \\ & + \mu'_{g,k} \theta c_{k-1} + \mu'_{g,k} \rho s_{k-1} + \mu'_{g,k} a_v g_{k-1} + \gamma_{w,k} \theta \\ & + \gamma_{s,k} \rho + \gamma_{g,k} a_v - r_{a,k} \quad k \in (2, n_k) \end{aligned}$$

where the symbols  $c$ ,  $s$ , and  $g$  are the solute concentration in the liquid [ $\text{ML}^{-1}$ ], solid [ $\text{MM}^{-1}$ ], and gaseous [ $\text{ML}^{-3}$ ] phases respectively;  $q$  is the volumetric flux density [ $\text{LT}^{-1}$ ],  $\mu_w$ ,  $\mu_s$ ,

and  $\mu_g$  are the first order rate reaction constants for solutes in the liquid, solid and gas phases [ $T^{-1}$ ] respectively;  $\mu_w'$ ,  $\mu_s'$  and  $\mu_g'$  are the first order rate constant for production of the metabolites in the chain reaction in liquid, solid and gas phases respectively;  $\gamma_w$ ,  $\gamma_s$  and  $\gamma_g$  are the zero order rate constant for liquid [ $ML^{-3} T^{-1}$ ], solid [ $T^{-1}$ ] and gas [ $ML^{-3} T^{-1}$ ] phases respectively;  $\rho$  is the soil bulk density [ $M L^{-3}$ ],  $a_v$  is the air content [ $L^3 L^{-3}$ ],  $s$  is the sink term,  $r_a$  is the root nutrient uptake term [ $ML^{-3} T^{-1}$ ],  $D_w$ ,  $D_g$  is the dispersion coefficient [ $L^2 T^{-1}$ ] for the liquid and gas phases respectively; the subscripts  $w$ ,  $s$ , and  $g$  represent the liquid, solid and gas phases respectively;  $k$  subscript is the chain number,  $n$  is the number of solutes in the chain reaction. The nine zero- and first-order rate constants are used to show different reactions (biodegradation, volatilization, and precipitation).

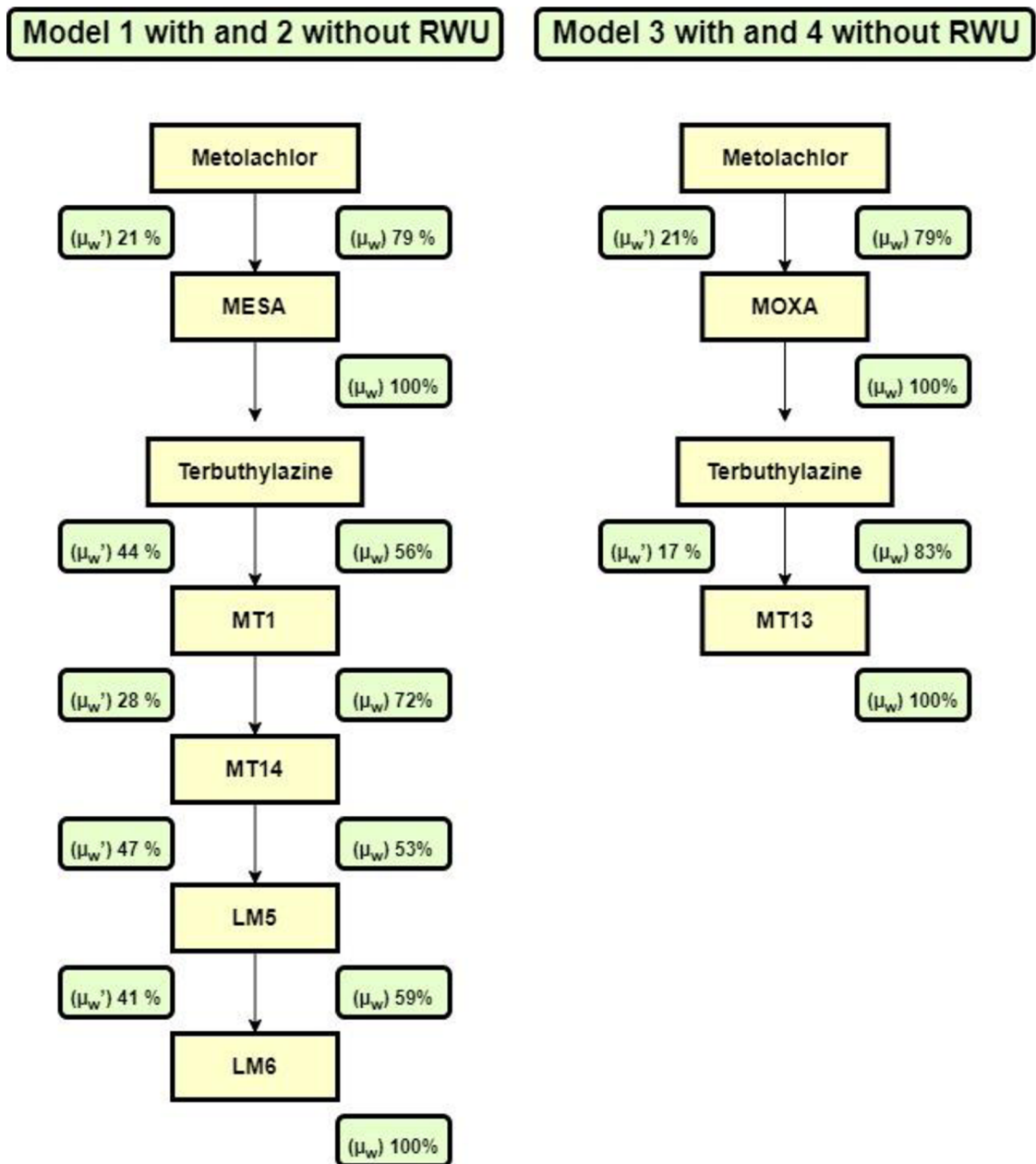


**Figure 4:** Biodegradation paths and production reaction of the metabolites from their parent herbicides with the percentage of biodegradation  $\mu_w$  and production  $\mu_w'$  with percentages of degradation and production after (ECPR, 2015)

The applied biodegradation chain of the herbicides is interrupted, where two independent reaction paths are considered. Since HYDRUS-1D does not consider the divergent and convergent reactants in the same path, the branching in the single path will be considered as a path by itself (Jacques et al., 2000). Four different models needed to be run to model the biodegradation. Two models are composed of a chain of terbutylazine metabolites (MT1, MT14, LM5, LM6) and a chain of metolachlor metabolite (MESA), with and

without root water uptake. Similarly, the other two models are composed of the second chain of terbuthylazine and its metabolite (MT13) together with the other metolachlor chain in which the metabolite (MOXA), with and without root water uptake. As discussed in the previous chapter, the reaction chains of both herbicides terbuthylazine and metolachlor are diverging forming branches that cannot be modelled in HYDRUS-1D in one model. The measured study results do not show the metabolite (MT14), but it was included in the model to complete the reaction chain to model the metabolites behind it (LM5 and LM6). The diagram in Figure 4 shows the arrangement of the scenarios followed to obtain the metabolites (daughters). In Table 6 and 7, the parameter values from the literature used to set up the four HYDRUS-1D models.

**Table 6:** Fitted parameters of biodegradation and production for model (1) before running PEST.

<b>Solutes</b>	<b><math>K_d</math></b> (Linear sorption isotherm rate) (cm <sup>3</sup> /mg)	<b><math>D_{50}</math></b> (Half-Life of biodegradation) (d)	<b><math>\mu_{total}</math></b> (Total biodegradation rate) (d <sup>-1</sup> )	<b><math>\mu_w</math></b> (Biodegradation rate for the solute in soil) (d <sup>-1</sup> )	<b><math>\mu_w'</math></b> (Biodegradation rate of the solute standing for chain reaction) (d <sup>-1</sup> )
(Metolachlor)	0.004 <sup>[1]</sup>	10 <sup>[2]</sup>	0.069 <sup>[2]</sup>	0.0416 <sup>[3]</sup>	0.015 <sup>[3]</sup>
(MESA)	0.00073 <sup>[1]</sup>	70 <sup>[2]</sup>	0.0099 <sup>[2]</sup>	0.0099 <sup>[2]</sup>	0
(Terbuthylazine)	0.00231 <sup>[4]</sup>	57.8 <sup>[4]</sup>	0.012 <sup>[4]</sup>	0.0067 <sup>[4]</sup>	0.0053 <sup>[4]</sup>
(MT1)	0.00285 <sup>[5]</sup>	61.8 <sup>[5]</sup>	0.0112 <sup>[5]</sup>	0.008 <sup>[5]</sup>	0.003 <sup>[5]</sup>
(MT14)	0.0044 <sup>[5]</sup>	115 <sup>[5]</sup>	0.006 <sup>[5]</sup>	0.003 <sup>[5]</sup>	0.003 <sup>[5]</sup>
(LM5)	0.000549 <sup>[5]</sup>	241 <sup>[5]</sup>	0.0029 <sup>[5]</sup>	0.0017 <sup>[5]</sup>	0.0012 <sup>[5]</sup>
(LM6)	0.000485 <sup>[5]</sup>	47 <sup>[5]</sup>	0.0147 <sup>[5]</sup>	0.0147 <sup>[5]</sup>	0

**Table 7:** Fitted parameters of degradation and production for model (2) before running PEST

<b>Solutes</b>	<b><math>K_d</math></b> (Linear sorption isotherm rate) (cm <sup>3</sup> /mg)	<b><math>D_{50}</math></b> (Half-Life of biodegradation) (d)	<b><math>\mu_{total}</math></b> (Total biodegradation rate) (d <sup>-1</sup> )	<b><math>\mu_w</math></b> (Biodegradation rate for the solute in soil) (d <sup>-1</sup> )	<b><math>\mu_w'</math></b> (Biodegradation rate of the solute standing for chain reaction) (d <sup>-1</sup> )
(Metolachlor)	0.004 <sup>[1]</sup>	10 <sup>[2]</sup>	0.069 <sup>[2]</sup>	0.0416 <sup>[3]</sup>	0.015 <sup>[3]</sup>
(MOXA)	0.00075 <sup>[1]</sup>	50 <sup>[2]</sup>	0.0138 <sup>[2]</sup>	0.0138 <sup>[2]</sup>	0
(Terbuthylazine)	0.00231 <sup>[4]</sup>	57.8 <sup>[4]</sup>	0.012 <sup>[4]</sup>	0.01 <sup>[4]</sup>	0.002 <sup>[4]</sup>
(MT13)	0.02 <sup>[5]</sup>	462 <sup>[5]</sup>	0.0015 <sup>[5]</sup>	0.0015 <sup>[5]</sup>	0

[1] (Sidoli et al., 2020), [2] (Rose et al., 2018), [3] (Baran & Gourcy, 2013; Maillard et al., 2016; P. J. Rice et al., 2002; Rose et al., 2018; SANCO, 2004), [4] (Alister et al., 2011; Dolaptsoglou et al., 2007; ECPR, 2015; EFSA., 2019; PPDB, 2022d), [5] (ECPR, 2015)

## 4.2 boundary conditions

The composition of the soil in lysimeter 1 is differentiated into four layers due to the grain size distribution. In this study, the consideration is one layer, as the differences are not big and to make it easier in modelling. The values of the fitted soil hydraulic parameters which are manually fitted by Imig et al., (2022b), from modeling stable water isotope transport are shown below in Table 8:

**Table 8:** Manually fitted soil hydraulic parameters by Imig et al. (2022b)

Depth [cm]	$\theta_r$ [cm <sup>3</sup> cm <sup>-3</sup> ]	$\theta_s$ [cm <sup>3</sup> cm <sup>-3</sup> ]	$\alpha$ [cm <sup>-1</sup> ]	$n$ [-]	$K_s$ [cm d <sup>-1</sup> ]	$I$ [-]	$D_L$ [cm]
<b>One-layer consideration</b>							
0-200	0.0176	0.23	0.30	1.25	6040	0.5	12
<b>Four-layers consideration</b>							
0-30	0.023	0.2	0.094	1.1	19148	0.5	15
30-40	0.023	0.21	0.163	1.12	24970	0.5	8
40-50	0.018	0.23	0.1	1.24	21845	0.5	6
50-200	0.01	0.214	0.069	1.2	38880	0.5	10

The adopted consideration is the single layer consideration due to the uncertainty in the soil hydraulic parameters of the four-layer consideration. The parameters used in this work are optimized using PEST to obtain the best fit between the measured and modelled values of the hydraulic parameters are shown in Table 9.

**Table 9:** Fitted transport parameters for lysimeter 1 without consideration of RWU used in the model after Imig et al. (submitted-b)

Depth [cm]	$\theta_r$ [cm <sup>3</sup> cm <sup>-3</sup> ]	$\theta_s$ [cm <sup>3</sup> cm <sup>-3</sup> ]	$\alpha$ [cm <sup>-1</sup> ]	$n$ [-]	$K_s$ [cm d <sup>-1</sup> ]	$I$ [-]	$D_L$ [cm]
0-200	0.007915636	0.302011	0.264269	1.43667	6040.20	1.5	18.0136

The initial conditions of the water flow were defined in pressure heads, in the range of 86 cm between -388 cm on the soil surface and -302 cm on the base. The upper boundary condition was the atmospheric boundary condition with a surface ponding ( $h = 5$  cm) where the water builds up on the surface of the soil when precipitation is greater than infiltration and evaporation. The equation (13) shows that the water layer thickness  $h$  increases or decreases depending on the increase of precipitation or infiltration and evaporation (Šimůnek et al., 2018).

$$-K = \left( \frac{\partial h}{\partial z} + \cos a \right) = q_0(t) - \frac{dh}{dt} \quad \text{at } x = L \quad (13)$$

The lower boundary conditions applied to the lysimeter system are the seepage face at the base of the lysimeter when the soil becomes saturated and the matric potential equals zero (no longer negative) at the bottom of the profile seepage face ( $h = 0$ ) for the lower boundary condition. The precipitation and actual evapotranspiration ( $ET$ ) were specified

at the upper flow boundary where actual evapotranspiration has been calculated from the water balance in the lysimeter as described in (Shajari et al., 2020). With respect to the boundary conditions for solute transport, the upper boundary is defined as a Cauchy-type condition. The flux concentration is controlled by the advective-dispersive fluxes which are active at the boundary, therefore, the concentrations of solutes are not fixed. Due to concentration gradient forming the fluxes, Dirichlet type is not the right boundary condition to be applied here where the lower boundary condition applied is the free drainage.

### 4.3 Plant uptake

The lysimeter is vegetated with maize plants during the soil in the period 2013 to 2017. The plant roots take water and solutes from the soil, which can be considered in the HYDRUS-1D model. There are processes accompanying the presence of plants which are water uptake, solutes uptake transpiration, and root growth.

#### 4.3.1 Transpiration

A model developed by Feddes et al. (1978) is to calculate the root water uptake depending on the potential transpiration  $T_p$  [ $L T^{-1}$ ] root density and pressure head. In our case, the amount of actual evapotranspiration is already calculated from the water balance as detailed by Shajari et al. (2020), so the amount of actual transpiration can be calculated with Beer's law:

$$T_p = ET_p(1 - e^{-k \cdot LAI}) = ET_p SCF = ET_p - E_p \quad (14)$$

where  $k$  is the radiation extension constant [-] which varies depending on the sun angle and distribution of plant and leaf,  $LAI$  is the leaf area index which is the projected area of leaves over the area of land [ $M^2 M^{-2}$ ], the average value of  $LAI$  is 1.2 as mentioned in Garcia et al. (2011). It also plays an essential role in generating input data to model the water balance of the vadose zone (Batsukh et al., 2021),  $ET_p$  is the evapotranspiration [MM], and  $SCF$  is the soil cover fraction [-]. Evaporation and precipitation are together representing the system-dependent boundary conditions of the model over the soil. HYDRUS-1D expects that the input values entered are for potential evapotranspiration to estimate the actual evapotranspiration using the value of the pressure head. To handle this issue with HYDRUS-1D, the minimum pressure head boundary condition was imposed at -1500000 cm (Groh et al., 2018; Imig et al., 2022b).

#### 4.3.2 Root uptake of dissolved compounds

It is an important process that can show efficient strategies for the production and irrigation of crops (Kuhlmann et al., 2012). Root water uptake is important to be able to know soil hydrology and crop growth. Some studies on the root water uptake modeling of maize in unsaturated soil revealed that irrigation water required for the plant increase with increasing the depth of water (Hou et al., 2016). From Richard's equation one can conclude that the sink term implies the amount of root water uptake which can be described by the following relationship:

$$S(h) = A(h)B(z)T_p \quad (15)$$

where  $A(h)$  is a dimensionless function,  $h$  ( $0 \leq h \leq 1$ ), and  $B(z)$  is the normalized water uptake distribution ( $\text{cm}^{-1}$ ).  $A(h)$  is the effect of water stress on root water uptake, and it has four different values depending on the pressure head values (Feddes et al., 1978; Feddes & Raats, 2004) described in the following equation:

$$A(h) = \begin{cases} h_{3 \text{ low}} & \text{if } T < T_{3 \text{ low}} \\ h_{3 \text{ high}} + \frac{h_{3 \text{ low}} - h_{3 \text{ high}}}{T_{\text{low}} - T_{3 \text{ low}}}, & \text{if } T_{3 \text{ low}} < T < T_{3 \text{ high}} \\ h_{3 \text{ high}} & \text{if } T > T_{3 \text{ high}} \end{cases} \quad (16)$$

where  $h_1$  is the point in the anaerobic conditions and  $h_4$  is the pressure head at the wilting point. Water uptake is at its optimal value between  $h_2$  and  $h_3$ . The adopted model for modeling the root water uptake in this work is the Feddes model (Feddes et al., 1978). Those parameters are needed to run the model which is already in the database of HYDRUS-1D for maize crop. The water uptake is considered optimal value between  $h_2$  and  $h_3$ . The methods of Feddes et al. (1978) aimed to calculate the amount of root water uptake from the soil depending on the potential transpiration.  $T_p$  is the potential transpiration rate ( $\text{mm d}^{-1}$ ) as shown in the equation below:

$$T_p = ET_p - E_p \quad (17)$$

where  $ET_p$  is estimated by the Penman-Monteith equation, while  $E_p$  is the potential evaporation, according to Beer's law (Ritchie, 1972):

$$E_p = ET_p e^{-kLAI} \quad (18)$$

where  $k$  is the plant canopy radiation attenuation coefficient which is a function of sun angle and distribution of plants and arrangement of leaves which has a default value of 0.463 for maize (Zhu et al., 2018).  $LAI$  is the Leaf Area Index.

The sink term can also be defined as the volume of water extracted from a unit volume of soil in a unit of time by the roots and can be calculated by the following relationship (Šimůnek & Hopmans, 2009):

$$S(h, x, t) = \alpha(h, x, t)S_p(x, t) \quad (19)$$

$$S_p(x, t) = b(x, t)T_p(t) \quad (20)$$

where  $\alpha(h, x, t)$  is a dimensionless coefficient of water stress ( $0 \leq \alpha \leq 1$ ), the soil pressure head can be used to calculate this parameter (Feddes et al., 1978),  $S_p$  is the potential root water uptake rate [ $\text{T}^{-1}$ ].  $T_p$  is the potential transpiration rate while  $b(x, t)$  is the normalized root distribution that helps regulate the potential transpiration within the soil profile.

$$b(x, t) = \begin{cases} \frac{1.667}{L_r} x > L - 0.2L_r & x > L - 0.2L_r \\ \frac{2.0833[1 - (L - x)/L_r]}{L_r} & x \in (L - L_r; L - 0.2L_r) \\ 0 & x < L - L_r \end{cases} \quad (21)$$

Where  $L_r$  [L] is the maximum depth that a root can reach with time, while  $L$  is the  $x$  coordinate from top to bottom of the soil profile.

The actual transpiration is calculated by the following equation where the sink term  $S(h, x, t)$  [ $T^{-1}$ ] is integrated over the zone of maximum root depth:

$$T_a = \int_{L_r} S(h, x, t) dx = T_p \int_{L_r} \alpha(h, x, t) b(x, t) dx \quad (22)$$

The stress function mentioned above in equation (16), is reducing the amount of potential root water uptake because of the water and solute stresses (Feddes & Raats, 2004) and the S-shape function used by van Genuchten, (1987) while a more complex function used by Feddes et al. (1978). Five different parameters are required for the stress response function used. As shown in Figure 5 the water uptake is dependent on the pressure head and the osmotic pressure, it is equal to zero at  $h_1$  and in the case of water stress (wilting point)  $h_4$ . The values of the parameters of the stress response function are included in the HYDRUS-1D database and can be determined from the GUI.

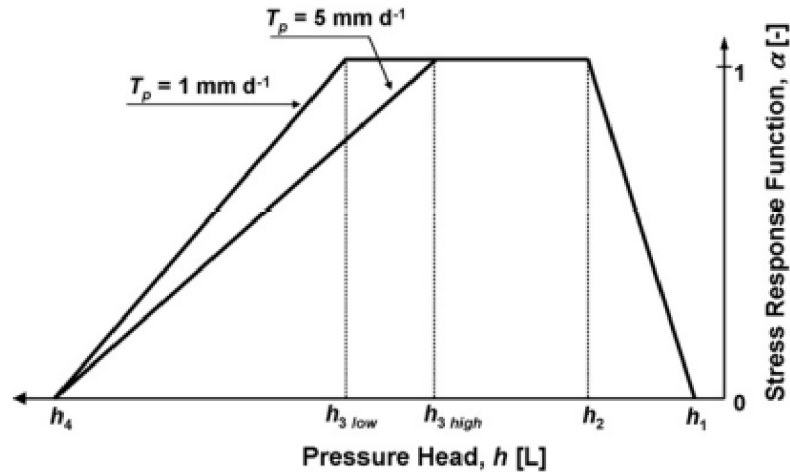


**Figure 5:** The parameters of the water uptake stress response function and the relationship between water uptake and the soil pressure head as described by Feddes et al. (1978) (Šimůnek & Hopmans, 2009)

The compensated root water uptake occurs in the soil where there is not enough water to be transpired by the roots. The ratio between the actual and potential root water uptake



from that uncompensated area is  $\omega_c$ , which is called the water stress index or root adaptability, it is a value (threshold) above which the root water uptake reduces in the more stressed parts of the root zone and increases in the less stressed parts in compensation. While the root water uptake is reduced when  $\omega_c$  is below the threshold but not yet equal to zero as shown in Figure 6.

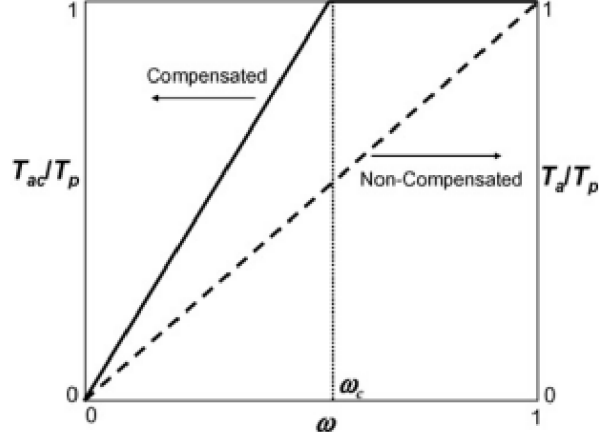


**Figure 6:** Relationship between the ratio of actual to potential transpiration and stress index ( $\omega$ ) (Šimůnek & Hopmans, 2009)

The uncompensated root water uptake is considered a special case of compensated root water uptake in the case of ( $\omega_c = 1$ ). Compensated actual transpiration ( $T_{ac}$ ) is the ratio between actual transpiration and stress index ( $T_a/\omega$ ), the ratio between the compensated actual transpiration to the potential transpiration where ( $\omega > \omega_c$ ) equals:

$$\frac{T_{ac}(t)}{T_p(t)} = \frac{T_a(t)}{T_p(t)\omega(t)} = \frac{\int_{\Omega_R} \alpha(h, h_\phi, x, z, t)b(x, z, t) d\Omega}{\omega(t)} = \frac{\omega(t)}{\omega(t)} \quad (23)$$

$$= 1,$$

$$S_c(h, h_\phi, x, z, t) = \alpha(h, h_\phi, x, z, t)b(x, z, t)L_t \frac{T_p(t)}{\omega(t)}$$

where the stress range is under the critical water stress ( $T_{ac} = T_a/\omega_c$ ) when ( $\omega < \omega_c$ ):

$$\frac{T_{ac}(t)}{T_p(t)} = \frac{T_a(t)}{T_p(t)\omega_c(t)} = \frac{\int_{\Omega_R} \alpha(h, h_\phi, x, z, t)b(x, z, t) d\Omega}{\omega_c} = \frac{\omega(t)}{\omega_c} \quad (24)$$

$$< 1,$$

$$S_c(h, h_\phi, x, z, t) = \alpha(h, h_\phi, x, z, t)b(x, z, t)L_t \frac{T_p(t)}{\omega_c}$$

It can be concluded that the water uptake compensation is proportional to water stress response function as the water uptake compensation is maximum with optimum root water

uptake, while it is equal to zero when the root water uptake is zero (in wilting or anaerobiosis point) (Šimůnek & Hopmans, 2009).

### 4.3.3 Root uptake of dissolved compounds

The roots of the plant work on providing the required nutrients for the plant to live and grow from the soil. This process can be either in an active or passive way. In other words, when the plant uptakes the nutrients that are already dissolved in the water this is the passive uptake, while the active uptake is any other possible mechanism for the roots that require energy against the electrochemical gradient. So, for the transpiration process to occur the plant needs to uptake water from the soil which is already carrying nutrients that is called passive process. The nutrient demand is  $R_p$  [ $\text{ML}^{-2}\text{T}^{-1}$ ] which is the amount of nutrients needed for the plant depending on the stage of growth and can be supplied by active or passive processes. As assumed by Šimůnek & Hopmans, (2009), the amount of nutrients is supplied first by the passive uptake then if it is not sufficient the active uptake takes place. The model can allow both passive and active nutrient uptake alone or both together. The active root nutrient uptake can be determined by the following equations:

$$r_a(x, z, t) = p_a(x, z, t) + a_a(x, z, t) \quad (25)$$

$$R_a(t) = P_a(t) + A_a(t) \quad (26)$$

where  $r_a$ ,  $p_a$ , and  $a_a$  are the total root nutrient uptake, passive and active nutrient uptake respectively, where the subscript  $a$  means actual. The lower case represents the root nutrient uptake from a certain point while the upper case represents the domain root nutrient uptake. Regarding passive nutrient uptake can be simulated by multiplying root water uptake carrying dissolved nutrients with the dissolved natural concentrations for concentrations below a defined maximum concentration ( $c_{max}$ ) (Šimůnek & Hopmans, 2009):

$$p_a(x, z, t) = s^*(x, z, t) \min[c(x, z, t), c_{max}] \quad (27)$$

where  $c$  is the dissolved nutrient concentration [ $\text{ML}^{-3}$ ],  $c_{max}$  is the maximum amount of nutrients dissolved in the solution [ $\text{ML}^{-3}$ ], when the  $c_{max}$  equals zero this means that there are no nutrients in the root water by passive nutrient uptake. The  $c_{max}$  parameter is a control parameter that does not have a physical meaning as it controls the amount of nutrients in passive uptake which is not real. The passive actual root nutrient uptake is  $p_a$  [ $\text{ML}^{-2}\text{T}^{-1}$ ] in the whole root zone and is calculated by integrating the passive root nutrient uptake locally over the whole root zone as shown below:

$$\begin{aligned} P_a(t) &= \frac{1}{L_t} \int_{\Omega_R} p_a(x, z, t) d\Omega = \frac{1}{L_t} \int_{\Omega_R} S^*(x, z, t) \min[c(x, z, t), c_{max}] d\Omega \\ &= \frac{T_p(t)}{\max[\omega(t), \omega_c]} \int_{\Omega_R} \alpha(h, h_\phi, x, z, t) b(x, z, t) \min[c(x, z, t), c_{max}] d\Omega \end{aligned} \quad (28)$$

where  $R_p$  [ $\text{ML}^{-2}\text{T}^{-1}$ ] is the potential nutrient demand and  $A_p$  [ $\text{ML}^{-2}\text{T}^{-1}$ ] is the active potential nutrient uptake.

$$A_p(t) = [R_p(t) - P_a(t), 0] \quad (29)$$

#### 4.3.4 Root growth

The root growth is described in HYDRUS-1D manuals (Šimůnek et al., 2018; Šimůnek et al., 2013b; Šimůnek & Hopmans, 2009):

$$L_R(t) = L_m f_r(t) \quad (30)$$

$$f_r(t) = \frac{L_0}{L_0 + (L_m - L_0)e^{-rt}} \quad (31)$$

where  $L_R$  [L] is the root depth at the time,  $L_0$  is the initial root depth [L],  $L_m$  is the maximum possible root depth [L],  $f_r(t)$  [-] is the root growth coefficient,  $t$  is time [T] and  $r$  is the root growth ratio [ $\text{T}^{-1}$ ], which equals 0.07 for maize. The maximum root depth for maize is 100 cm.

Two of the used approaches to calculating the root growth are the differential equation describing population is used to describe root depth (Hartmann et al., 2018):

$$\frac{dL_r}{dt} = rL_r \left(1 - \frac{L_r}{L_m}\right) \quad (32)$$

where  $L_r$  is the potential rooting depth [L] with no stress,  $r$  [ $\text{T}^{-1}$ ] is the root growth rate. The rooting depth can be calculated by the following equation where the stress factor is incorporated in the equation (32):

$$\frac{dL_a}{dt} = rS(t)L_a \left(1 - \frac{L_a}{L_m}\right) \quad (33)$$

where  $S(t)$  is environmental stress (dimensionless), and  $L_a$  is the actual rooting depth subjected to environmental stresses [L].  $L_a$  can be calculated as follows:

$$L_a(t_i) = L_a(t_{i-1}) + r \min[S_1(t_i), S_2(t_i)]L_a(t_{i-1}) * \left[1 - \frac{L_a(t_{i-1})}{L_m}\right] (t_i - t_{i-1}) \quad (34)$$

where  $S_1$  and  $S_2$  are stress factors affecting vertical penetration in the soil by plant roots as shown by Jones et al. (1991). From that approach, the considered root growth depends on the whole plant development, but the growth of roots does not necessarily affect the shoot growth. There is another approach built on Verhulst–Pearl logistic growth function, this function is applied in HYDRUS-1D and it is an analytical solution of the equation (32) (Šimůnek et al., 2016):

$$L_r(t_i) = \left(\frac{L_0}{L_0 + (L_m - L_0)e^{-rt}}\right) L_m \quad (35)$$

where  $L_0$  and  $L_r$  are the initial and potential root depths [L] respectively;  $L_m$  is the maximum rooting depth [L],  $r$  is the root growth rate [ $T^{-1}$ ] and  $t_i$  is the time step [T]. the other function describing the root growth rate [ $T^{-1}$ ] is a function based on the analysis of 48 crops in 135 fields proposed by Borg & Grimes, (1986), where  $t_m$  is the time required to reach the maximum root depth [T].

$$L_r(t_i) = L_m \left\{ 0.5 + 0.5 \sin \left[ 3.03 \left( \frac{t_i}{t_m} \right) - 1.47 \right] \right\} \quad (36)$$

#### 4.4 Model calibration

The applied model includes modeled data that needs to be optimized to fit well with the measured data. Some of the parameters are affecting the solute transport and fate in the soil as called the solute reaction parameters ( $K_d, \mu, \mu'$ ). The parameter estimation software used for that purpose is PEST.

##### 4.4.1 PEST

It is a software package that works on comparing the measured and modeled data, then it predicts the best values of the parameters of interest after finding the best fit for the modeled and measured data and this process is called (calibration). The distinct manner of PEST made it different from other algorithms, it works on the model input and output files directly to calibrate without programming. The good about using PEST is that it works on the model input and output files from the HYDRUS-1D model without the need to modify it. The method behind that tool is called inversion which works on the solution of inverse problems. The used version in this study is version 17.2 of the PEST suite (Doherty, 2020b, 2020a).

There are uncertainties in the estimated parameters with the model calibration process due to the nonunique status in the inversion process and due to the noise in the model data entered to be calibrated. Regularization is the process of simplification of the parameter to attain the uniqueness of finding a solution for the inverse problem. PEST suite includes many programs where the Bayes equation is the base of all of them.

PEST can interact with the model through the input and output files of the model. There are three types of files needed to be provided for PEST to work, the template file, the instructions file, and the control file. The template file is written to make PEST understand the model input file required to be changed before running the model which are the parameters of interest. The instructions file contains the method of how to read the output file and the numbers of the measurements of the model. While the control file contains the names of the template and instruction files also the model input and output files of the model, control variables, problem size, initial parameter value, measurements values...etc (Doherty, 2020b, 2020a).

PEST has four modes of operation which are estimation, predictive analysis, regularization, and pareto. The repetitive and iterative behavior of PEST is the calculations repeated many times using the Jacobian matrix to maintain the accuracy of the parameter's values determination. The Jacobian matrix has a column for each parameter and a row for

each observation. Once the Jacobian matrix is calculated after many model-runs, it can be used to calculate a set of parameters using different values called Marquardt lambdas.

Parallelization was used to run the model many times calculating the Jacobian matrix, where the manager PEST is using many agents to work in parallel. Parallel PEST and BEOPEST are being exploited for that purpose, they don't need files different from normal PEST but just one extra file to know where the agents' working directories will be, although it is optional for BEOPEST (Doherty, 2020b, 2020a).

#### 4.4.2 Model curve fit evaluation

To measure the predictive capability of the method used in the work above, five types of statistical performance indicators have been selected; root mean square error (*RMSE*), mean error (*ME*), coefficient of determination ( $R^2$ ), and Kling-Gupta efficiency (*KGE*).

The coefficient of determination is a term in the analysis of variance (ANOVA), it is the measure of the proportion of the explained variance in the data. So, the higher the value of  $R^2$ , the better the model as it could explain many of the variances in the data.

$$R^2 = 1 - \frac{\sum_{i=1}^n (y_i - \hat{y}_i)^2}{\sum_{i=1}^n (y_i - \bar{y})^2} \quad (37)$$

where  $y_1, \dots, y_n$  are the values of the data,  $\bar{y}$  is the average of observations,  $\hat{y}_i$  is the predicted part of  $y_i$  by the model fitting (di Buccianico, 2008).

The root mean square error is a statistical standard metric used to measure the model performance. The model prediction errors are calculated by subtracting the observations from the predictions  $e_i = P_i - O_i$  (Chai & Draxler, 2014; Willmott & Matsuura, 2005).

$$RMSE = \sqrt{\frac{1}{n} \sum_{i=1}^n e_i^2} \quad (38)$$

The mean error (*ME*) is an indicator of the overestimation of the modeled values when it is above zero ( $ME > 0$ ) or underestimation when it is below zero ( $ME < 0$ ) (Chai & Draxler, 2014; Stump et al., 2009a).

$$ME = \frac{1}{n} \sum_{i=1}^n e_i \quad (39)$$

The Kling-Gupta efficiency is a combination of three components of Nash-Sutcliffe efficiency (*NSE*) of the model errors bias, correlation, and ratio of variances. The *KGE* and its extension *KGE'* is dominating the recent hydrological model calibration literature (Kling et al., 2012; Liu, 2020).

$$KGE = 1 - \sqrt{(r - 1)^2 + (\alpha - 1)^2 + (\beta - 1)^2} \quad (40)$$

$$KGE' = 1 - \sqrt{(r - 1)^2 + (\beta - 1)^2 + (\gamma - 1)^2} \quad (41)$$

$$\beta = \frac{\mu_s}{\mu_o} \quad (42)$$

$$\gamma = \frac{\sigma_s/\mu_s}{\sigma_o/\mu_o} \quad (43)$$

where  $r$  is the correlation coefficient between simulated and observed data,  $\beta$  is the bias ratio,  $\gamma$  is the variability ratio,  $\mu_o$  is the mean value of the observed data,  $\mu_s$  is the mean value of the simulated data,  $\sigma$  is the standard deviation (Kling et al., 2012).

$$\tau = \frac{PQ}{\sqrt{(P + Q + T) * (P + Q + U)}} \quad (44)$$

Kendall's tau is the linear function of number of which are different pairs of items in two rankings. The function is 1 when the values are in the same order and equals -1 when they differ (Sanderson & Soboroff, 2007).

## 5. Results and discussion

### 5.1 Hydrus-1D application issues

Regarding the model run by HYDRUS-1D, there are some issues related to the flow model needed to be considered and solved. For instance, HYDRUS-1D does not consider the entered values of actual evapotranspiration and tends to reduce the amount entered because of water shortage in the system before dividing the evapotranspiration into evaporation and transpiration according to Beer's law mentioned in the previous chapter. Since actual evapotranspiration is considered an upper boundary condition, the value of  $h_{critA}$  which is the critical pressure head is set as a very low value (-1500000 cm) which prevents HYDRUS-1D from reducing its evapotranspiration. This value of the critical hydraulic head is so low and does not usually occur unless there is numerical instability due to water stress in the soil (Imig et al., 2022b).

The concentration of the solutes is calculated with the unit of mg/cm in the model because the Cauchy boundary condition is describing the solute flux which considers the amount of solute applied per square meter of soil surface. The amount of surface flux on the day of herbicide application is considered the solute flux which is calculated in mg/day. The evapotranspiration in the herbicide's application day is considered zero as the surface flux is considered solute flux and the amount of precipitation is assumed to be the applied herbicides, water flux is added to the day before and the day after application. While the root water uptake is calculated on the day of herbicides' application as well as interception of precipitation by plant leaves is considered.

### 5.2 Results of running HYDRUS-1D models

The models have been run in HYDRUS-1D are four. Those are because the software does not model the divergent and convergent branching in the chain reaction. The first two models are composed of one terbutylazine metabolites chain (MT1, MT14, LM5, LM6) and one metolachlor metabolite chain (MESA), with and without root water uptake. Similarly, the other two models are composed of the second chain of terbutylazine and its metabolite (MT13) together with the other metolachlor chain in which the metabolite (MOXA), with and without root water uptake.

#### 5.2.1 Results of the first model with and without RWU

The model calibration needed running of PEST software many times in the power shell, after many trials to fit the parameters affecting solute transport and biodegradation in the soil which are sorption coefficient  $K_d$ , the biodegradation rate in the liquid state  $\mu_w$  and the production rate of metabolites  $\mu_w'$ . Using different statistical indicators to identify the best herbicide-model parametrization. The model is run first using the values of the parameters collected from literature before calibration using PEST. The soil hydraulic parameters were entered depending on the fitted parameters inversely using PEST (Imig et al., submitted-b), those parameters are the Van Genuchten parameters ( $\theta_r, \theta_s, \alpha, n, K_s$ ) and longitudinal dispersity ( $D_L$ ) as mentioned in the methodology chapter. The parameters of solute reaction were also being used from literature and used as initial values to model the biodegradation and metabolites production in HYDRUS-1D.

In the previous studies on the site of Wielenbach, Germany, (Imig et al., 2022b) and (Shajari et al., 2020) worked on modeling the water flow using the data of two weighable lysimeters -one of those lysimeters is the interest of this study (Ly1)- using lumped-parameter model and HYDRUS-1D, where they used stable isotopes as natural tracers. In a continuation of that, Imig et al. (submitted-b) worked on the parametrization of the model previously done and fitting the water flow, isotope transport, and herbicides model parameters using PEST after running HYDRUS-1D. The results of modeling the herbicides together with biodegradation and production of metabolites in the soil are based on the results of fitted soil parameters by Imig et al. (submitted-b) and are being used in this work as a water flow model. The fitted solute transport and biodegradation parameters of the two model branches are mentioned in Table 10 and 11.

**Table 10:** Fitted parameters of biodegradation and production for model (1) after running PEST.

<b>Solutes</b>	<b><math>K_d</math></b> (Linear sorption isotherm rate) (cm <sup>3</sup> /mg)	<b><math>D_{50}</math></b> (Half-Life of biodegradation) (d)	<b><math>\mu_{total}</math></b> (Total biodegradation rate) (d <sup>-1</sup> )	<b><math>\mu_w</math></b> (Biodegradation rate of solute in soil) (d <sup>-1</sup> )	<b><math>\mu_w'</math></b> (Biodegradation rate of solute representing chain reaction) (d <sup>-1</sup> )
(MTLC)	0.008	7.7	0.0896	0.048	0.0416
(MESA)	0.00093	46.2	0.015	0.015	0
(TBA)	0.03	8	0.0853	0.08	0.0053
(MT1)	0.0055	15	0.046	0.0325	0.0135
(MT14)	0.1	15	0.045	0.03	0.015
(LM5)	0.055	7	0.095	0.045	0.05
(LM6)	0.0000005	4415	0.000157	0.000157	0

### 5.2.1.1 Metolachlor (MTLC)

The values of fitting of metolachlor biodegradation parameter is ( $k_d = 0.008$  cm<sup>3</sup>/mg) which is in the range mentioned in BAuA, (2021) between (0.001-0.0448 cm<sup>3</sup>/mg), biodegradation parameter ( $\mu_w = 0.048$  d<sup>-1</sup>) and first-order production rate ( $\mu_w' = 0.0416$  d<sup>-1</sup>), where the statistical evaluation of the modelled data with root water uptake (RWU) (ME (Mean error) = -0.005, KGE (Kling-Gupta Efficiency) = -0.082) and without RWU is (ME = -0.009, KGE = -0.172), where the total half lifetime simulated is calculated from the total biodegradation rate as used in (Stipičević et al., 2017):

$$\mu_{total} = \mu_w + \mu_w' \quad (45)$$

$$D_{50} = \ln(2) / \mu_{total} \quad (46)$$

From the earlier equation, it can conclude that the simulated half lifetime of MTLC  $D_{50} = 7.74$  d which is in good agreement with the literature (10 d) (Bayless et al., 2008; Capel



et al., 2008; Rose et al., 2018). The sorption coefficient of MTLC ( $k_d = 0.008 \text{ cm}^3/\text{mg}$ ) fitted in the model by PEST is in the range of the previous studies  $0.0013 - 0.0087 \text{ cm}^3/\text{mg}$  as in Alletto et al., (2013) and in agreement with the fitting results done by Imig et al. (submitted-a), where the fitted parameters of MTLC ( $k_d = 0.013 \text{ cm}^3/\text{mg}$  and  $\mu_{total} = 0.1 \text{ d}^{-1}$ ). The statistical evaluation is not satisfying as ( $R^2 = 0.001$ , with and without RWU), but (KGE with and without RWU =  $-0.172$  and  $-0.082$ , respectively) which can still be improved. The fitted production rate ( $\mu_w' = 0.0416 \text{ d}^{-1}$ ) is representing 40% of the biodegradation rate which agrees with previous studies (Baran & Gourcy, 2013; Maillard et al., 2016; SANCO, 2004).

From the simulation of the MTLC curves, it can be observed that there are five peaks of concentration representing the five applications of MTLC to the soil in the middle of every year from June 2013 to June 2017, it is apparent that there is overestimation of MTLC output in the modelled curve after first application (June 2013) as shown in Figure 7 in both with and without root water uptake where the measured concentration is ( $0.08 \text{ mg/cm}$ ) while the modelled ( $0.66 - 0.73 \text{ mg/cm}$  with and without RWU respectively), this can be due to the heavy rain as the precipitation was recorded to be the heaviest in 2013 ( $190 \text{ mm}$ ) in the time of application, while in measured data it is not noticed, which maybe because that was in the beginning of the application time where MTLC has not been adsorbed by soil particles which are yet to be saturated with herbicides. Regarding the low amount of measured MTLC, maybe because of the relatively short half-life time ( $7.7 \text{ d}^{-1}$ ) and fast biodegradation rate of MTLC as in (Vischetti et al., 1998).

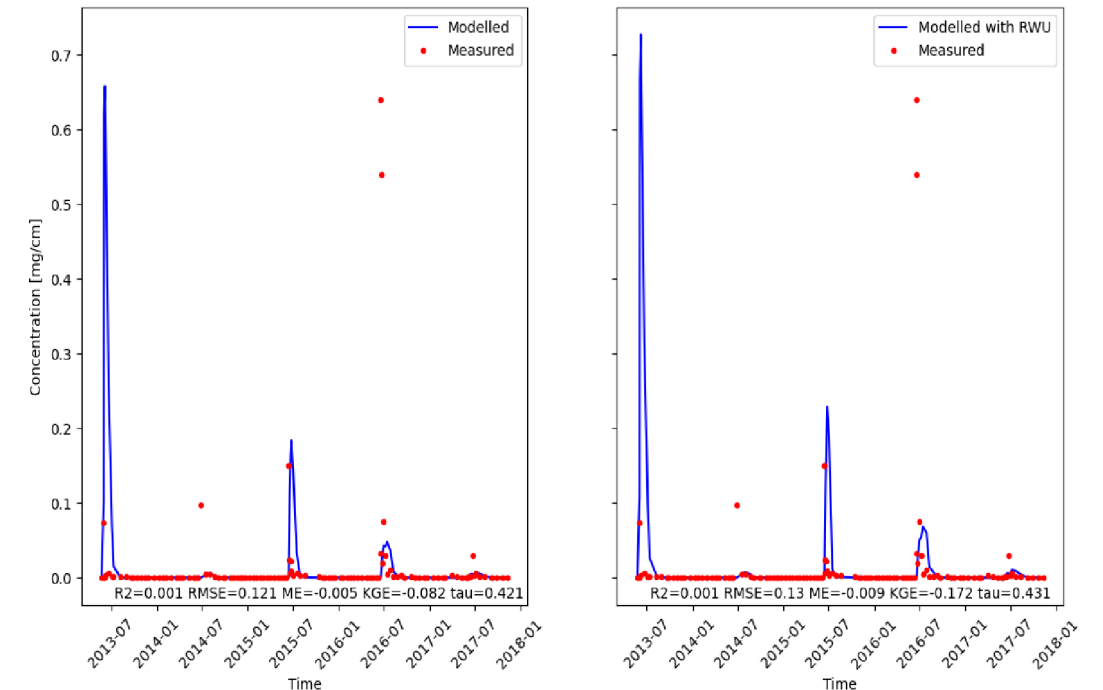


**Figure 7:** Metolachlor (MTLC) concentration in the first fitting model with and without root water uptake (in blue line) compared with the measured in the lysimeter drainage (in red dots),

through the whole simulation period where right diagram with root water uptake and the left diagram without, with statistical parameters in the base

In the second peak (June 2014) there is an underestimation in the modeled concentration (0.1 mg/cm) while modeled concentration is 0.01 and 0.012 mg/cm with and without RWU respectively), which can be due to the low precipitation rate (22 mm) in that year as it was the lowest year in precipitation rate. It can also be observed that there is no significant difference between the model with and without RWU for metolachlor, the small difference can be referred to as the simulation accuracy difference between both as shown by the statistical evaluation indicators.

The peak of July 2015 is almost equal to modeled (0.23 and 0.18 mg/cm with and without RWU respectively) and measured (0.15 mg/cm), the difference is assumed to be due to the accuracy of fitting, as it is more accurate in the modeled data without RWU, the difference is subtle, while it is bigger in RWU model as it is less accurate (KGE = -0.172), also the peak is relatively high as the rain was higher than the previous year 2014. It is worth noting that the measured values are peaking after application which is reasonable as it takes time through the soil profile to be leached, but it is interesting here that it appears earlier in high rain seasons as in 2013 and 2015 but it takes longer in 2014 as can be noticed in both models with and without RWU due to the low rain amount in that year.

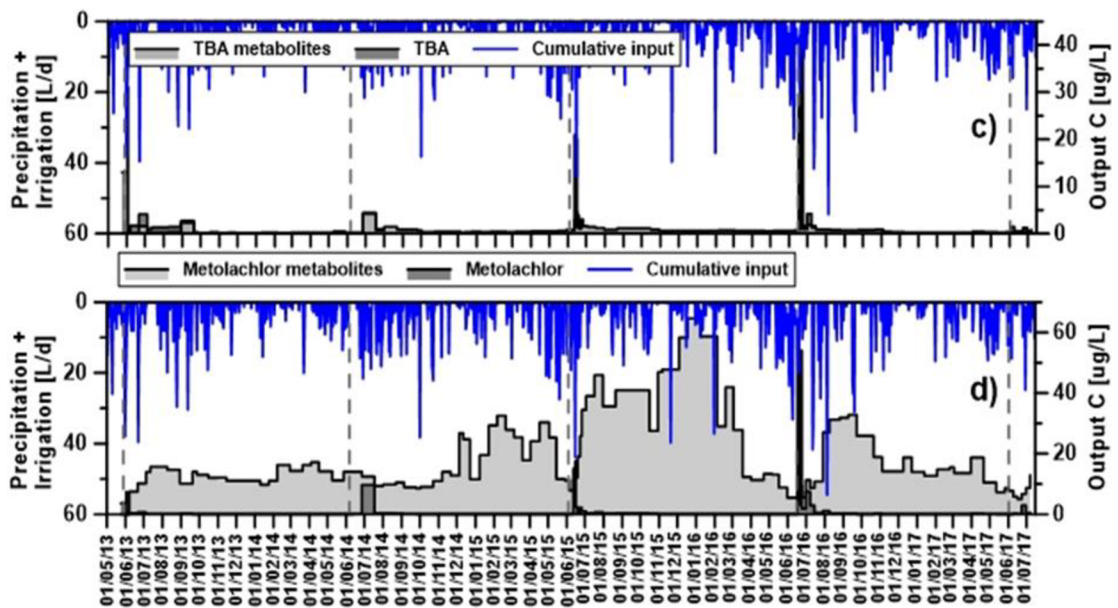


**Figure 8:** Measured concentrations of metolachlor, terbuthylazine, and their metabolites in the output leaching water and the amount of precipitation and irrigation water summed up in every season in lysimeter 1 by Imig et al. (submitted-a)

In the peak of June 2016, the modeled values are so underestimated (0.05 and 0.07 mg/cm with and without RWU respectively). The MTLC measured concentration is 0.64 mg/cm which is fivefold higher in concentration in comparison to other years, this could be due to the relatively high rain rate of 80 mm and the irrigation in 2016, it became the highest year of the amount of water in the soil as shown in Figure 8, together with the

remobilization of the previously adsorbed MTLC to soil particles from previous herbicide applications, another view can be due to preferential flow of the solute with water in the soil column. The first assumption is more powerful because, in comparison to the first year of application 2013 the peak was not so high although the rainfall was the highest recorded though the whole investigation period, there were no earlier applications that could be remobilized and appear in the outflow, plus the amount of herbicide applied was the lowest. In controversy in 2016, the amount of rain was half of the amount in 2013 but it affected the output MTLC because of the high amount of MTLC applied in the previous years and have been remobilized when the rain and irrigation together were high. Despite the high rain season in 2015, the output was two times lower than in 2016 because of the biodegradation of MTLC that dramatically increases after application and the sorption of an amount of metolachlor.

In 2017 after the application the rainfall was not high (50 mm) which is the second lowest rate after 2014 and it was preceded by a moderately rainy season, hence the outflow was low where the measured concentration was 0.04 mg/cm, while modeled concentration was (0.015 and 0.02 with and without RWU respectively).

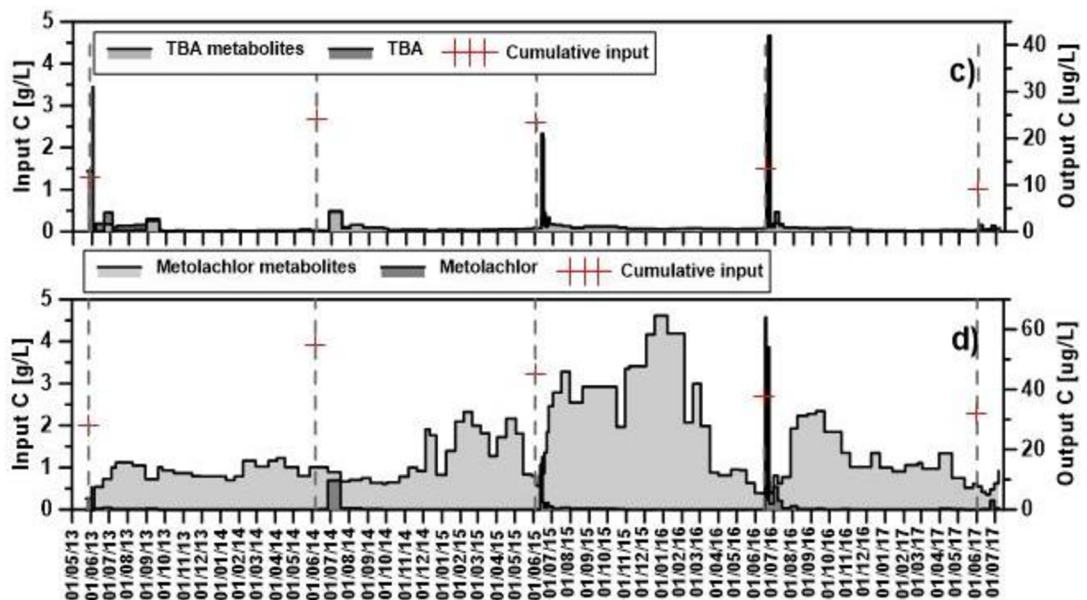


**Figure 9:** Measured concentrations of metolachlor, terbuthylazine, and their metabolites in the output leaching water as well as the concentration of applied "input" herbicides in lysimeter 1 by Imig et al. (submitted-a)

The metabolization of MTLC is higher and faster in comparison to TBA, as has been studied that the biodegradation rate of MTLC is high as the half-life is short as 7-10 days as mentioned (Capel et al., 2008; Rose et al., 2018), those parameters, as well as sorption coefficient, determine the leachability of the herbicide and the contamination risk of groundwater (Azcarate et al., 2015).

As mentioned in the earlier chapter that HYDRUS-1D models the biodegradation and production of metabolite branches but does not model the divergent and convergent

branches (Jacques et al., 2000). That was the reason there were two different models to model the two branches of the biodegradation chain of MTLC and TBA for the two approaches (with and without RWU).

### 5.2.1.2 Metolachlor ethane-sulfonic acid (MESA)

The modeled fitted value of the biodegradation rate is  $\mu_{total} = 0.015 \text{ d}^{-1}$  which is near to the rate ( $0.01 \text{ d}^{-1}$ ) (Bayless et al., 2008; Rose et al., 2018; Schuhmann et al., 2019), while the sorption coefficient ( $k_d = 0.00093 \text{ cm}^3/\text{mg}$ ) which is in agreement with the previous studies done by Krutz et al. (2004) on cultivated soil sorption estimation ( $0.00075 \text{ cm}^3/\text{mg}$ ) also agreeing with the study on a loamy to sandy soil in a weighable lysimeter where ( $K_d = 0.0002 \text{ cm}^3/\text{mg}$ ) (Kupfersberger et al., 2018), The metabolite of MTLC in the first model is MESA, is modeled as shown in Figure 10. The first peak of measured concentration in 2013 looks overestimated where it equals  $0.08 \text{ mg/cm}$  and the modeled equal ( $0.57$  and  $0.5 \text{ mg/cm}$ ) with and without RWU respectively, this can be because of the high rainfall that is maybe why the modeled concentration was higher as predicted by HYDRUS-1D. The low peak of measured MESA in 2013 can indicate that in the first application of the parent MTLC on the soil was more prone to be adsorbed especially in the upper parts of the soil and in soils with high organic carbon (Krutz et al., 2004), so the metabolites production is not high due to low biodegradation.

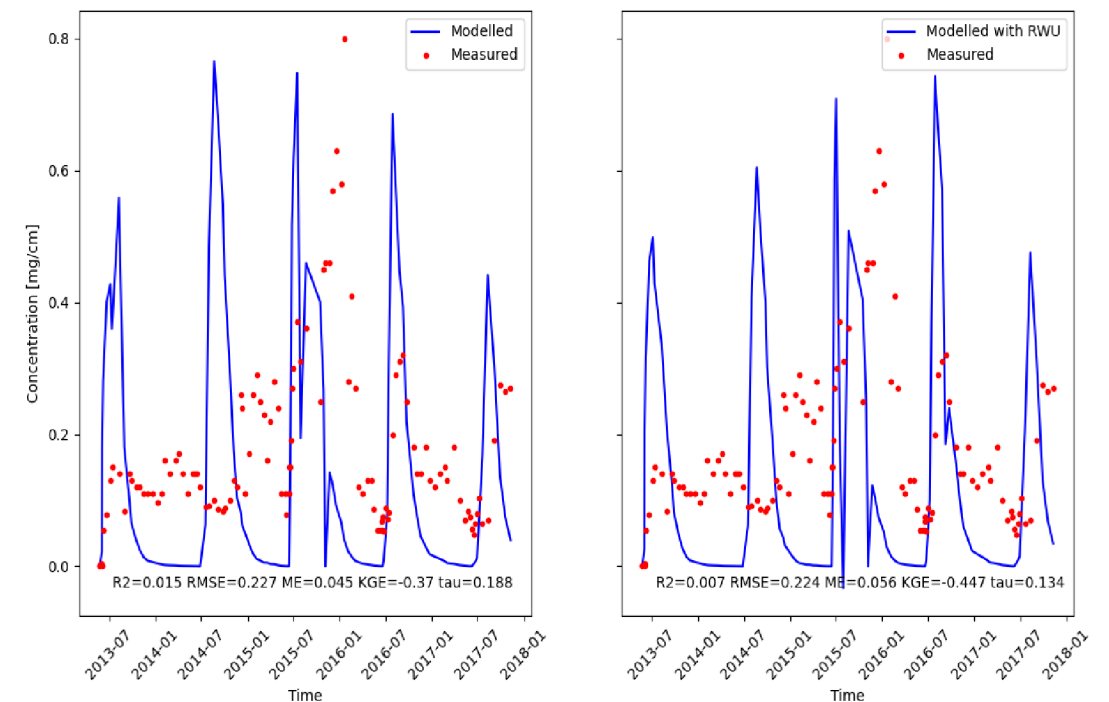


**Figure 10:** Metolachlor ethanesulfonic acid (MESA) concentration in the first fitting model with and without root water uptake (in blue line) compared with the measured in the lysimeter

drainage (in red dots), through the whole simulation period where right diagram with root water uptake and the left diagram without, with statistical parameters in the base

The conditions of sorption are assumed to be in equilibrium, so this assumption leads to uncertainties in the interpretation of the gap between the measured and modeled values. In the first two peaks of MESA in 2013 and 2014, the overestimation of measured data is noticeable, the second peak is highly overestimated where the concentration of 3.8 mg/cm for measured while 0.77 and 0.61 mg/cm for modeled with and without RWU respectively, although the amount of rain in that year was the lowest, this may be because of the adsorbed portion of the MTLC in the soil from the previous application so that amount was metabolized and remobilized. The third peak is in a rainy season when the MESA is leached and recorded the highest output in the investigation time. The measured concentration peaks the highest for MESA in the output recording at 0.8 mg/cm and the modeled concentrations are 0.75 and 0.72 mg/cm with and without RWU, respectively. From the whole investigation period in Figure 10, one can see that there is a lag in the measured peaks, they appear later than the modeled, and this lag is getting smaller with time through years until it is not noticed in the last two years, which supports the earlier assumption that MESA has been accumulating and being remobilized after every application. Another notice that supports the mobilization assumption, is that the values are peaking continuously in a scattered manner between the two applications which is rain-dependent throughout the year.

The 2016 measured peak is almost half the measured output of MESA in 2015, maybe because of the heavy rain in 2015. The three small different modeled peaks in the size after application in 2015 are showing the condition of combination between the moderate rainfall and the remobilized MESA from earlier applications. The last two peaks in 2016 and 2017 of modeled results are also overestimating the measured values. The measured values are not that high (0.32 – 0.29 mg/cm for 2016 and 2017 respectively) as in 2015 because the rain was not so high. The modeled concentrations in 2016 and 2017 are (0.69 and 0.76 mg/cm with and without RWU, respectively) and (0.44 and 0.47 mg/cm with and without RWU, respectively). It is worth noting that measured values are not returning to zero after application through the whole period, which may also be an indicator of the remobilization of the metabolite. The peaks of modeled data can be bifurcated in the years like 2013 without RWU, 2015 with and without RWU, and 2016 with RWU this may be because of the high amount of rainfall in those years as mentioned before where the highest is 2013 but it is more obvious in 2015 because this year had two of the conditions affected the peaks this way, one was the high rain and second is the remobilization of MESA from previous years 2013 and 2014. In comparison to MOXA, the mobility of MESA is almost eightfold higher which is in total agreement with Baran & Gourcy, (2013), Maillard et al. (2016), Rose et al. (2018) and White et al. (2010). White et al. (2010) also suggested that the formation of MOXA is not the preferred pathway of metolachlor.

### **5.2.1.3 Terbutylazine (TBA)**

The fitted parameter of biodegradation rate is  $0.0853 \text{ d}^{-1}$  which lies in the range of measured biodegradation value of TBA 0.006 and  $0.138 \text{ d}^{-1}$  as documented in (ECPR,

2015; PPDB, 2022d), biodegradation of the model done by Imig et al. (submitted-a) equals ( $0.08 \text{ d}^{-1}$ ) which supports the value here. The fitted linear sorption of TBA ( $k_d = 0.03 \text{ cm}^3/\text{mg}$ ) while the range of sorption is ((loamy sand) 0.0021 - (silty loam soil) 0.01  $\text{cm}^3/\text{mg}$ ) (ECPR, 2015; PPDB, 2022d), which is lower than the fitted value, this can be referred to the low output value of TBA in the modelled peak (underestimation of measured output from 2014 to 2017) combined with the relatively low estimated half-life (8 d). It has been studied also in dual porosity approach giving the value of ( $0.01 \text{ cm}^3/\text{mg}$ ) where it is also low in KGE value of TBA (0.06) (Imig et al., submitted-a). It also starts with overestimation of the measured concentration ( $0.31 \text{ mg}/\text{cm}$ ) but not so high after application in 2014, where the modelled concentrations after application in 2013 are 0.46-0.5  $\text{mg}/\text{cm}$  with and without RWU, respectively.

The herbicide terbuthylazine on contrary to MTLC is more persistent and does not degrade as fast. The second peak in 2014 is small like MTLC as the amount of rain was low. The measured concentration equals  $0.04 \text{ mg}/\text{cm}$ , and for the modelled ones are 0.02 and 0.12 with and without RWU. The third peak is higher as the amount of rain increased in 2015. The measured concentration is  $0.21 \text{ mg}/\text{cm}$ , it is also noticed that the peak of modelled value become sharper and nearer to application time when the precipitation increases. The modelled concentrations of the peak in 2015 are 0.18 and 0.22  $\text{mg}/\text{cm}$  with and without RWU, respectively. There is a little underestimation of the measured data in the TBA without RWU as in Figure 11, but this disappears in the data with RWU in 2015 which is more correct as showed by the ME and KGE values. In 2016, the measured values ( $0.42 \text{ mg}/\text{cm}$ ) are much higher due to the accumulation of TBA in the soil until the rainy season flushed it out same as what happened with metolachlor. There is big underestimation of the measured data in comparison to modelled due to the moderate rain amount. The values of the modelled concentrations are 0.04 and 0.05 with and without RWU, respectively. In the last year of application 2017, TBA was the lowest amount applied in all application period, also the rain was the second lowest rain in all investigation period, all that reduces the leached output of TBA. The measured concentration in 2017 is  $0.015 \text{ mg}/\text{cm}$ , while the modeled concentrations are 0.01 and 0.05 with and without RWU, respectively.

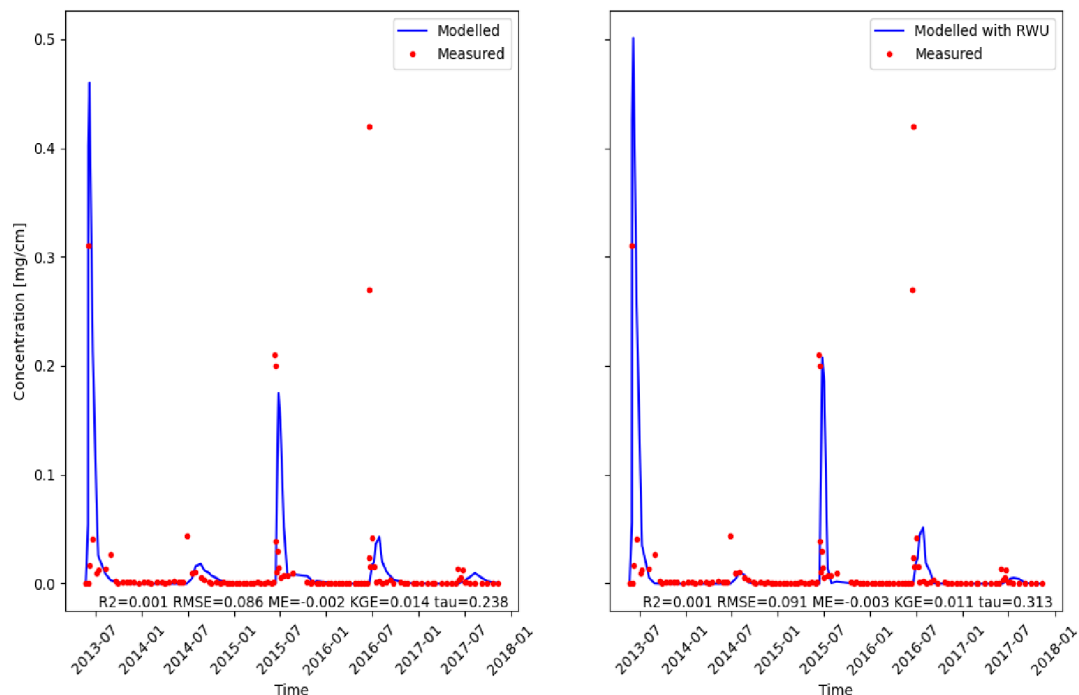


**Figure 11:** Terbutylazine (TBA) concentration in the first fitting model with and without root water uptake (in blue line) compared with the measured in the lysimeter drainage (in red dots), through the whole simulation period where right diagram with root water uptake and the left diagram without, with statistical parameters in the base

#### 5.2.1.4 Desethylterbutylazine (MT1)

The half-life and biodegradation rate of MT1 after fitting are (15 d,  $0.046 \text{ d}^{-1}$ ), which agree with the documented values range (69-15.5 d) ( $0.01\text{-}0.44 \text{ d}^{-1}$ ) normalized to the reference conditions ( $20^\circ\text{C}$ ) (ECPR, 2015). Sorption coefficient value ( $0.0055 \text{ cm}^3/\text{mg}$ ) is near to the values reported ( $0.00028 - 0.00329 \text{ cm}^3/\text{mg}$ ) (ECPR, 2015; PPDB, 2022a). The modelling process of the metabolites of one chain of terbutylazine starts with MT1 with the highest production percentage 44%. MT1 has also been discussed in chapter, it is the most popular metabolite of terbutylazine (ECPR, 2015). It is also known as the high mobility and low affinity to bind to the organic matter which poses a high risk to pollute groundwater (Loos et al., 2010; Tasca et al., 2018). MT1 starts with relatively high output -in comparison to other peaks of MT1-after first application of TBA. It is also apparent that the concentration of MT1 and other metabolites of TBA in the output is much lower than MTLC metabolites which indicate the lower biodegradation rate of TBA, and longer time needed for biodegradation in the soil (Schuhmann et al., 2019; Vischetti et al., 1998).

The first modelled peak after application in 2013 is representing the measured with a little overestimation. The measured concentration in 2013 is equal to  $0.018 \text{ mg/cm}$  which is relatively high because of the high rain season, but the beginning of the application as in previous solutes not so high in the output due to the sorption, while the modelled concentrations are  $0.026$  and  $0.031$  for with and without RWU, respectively.

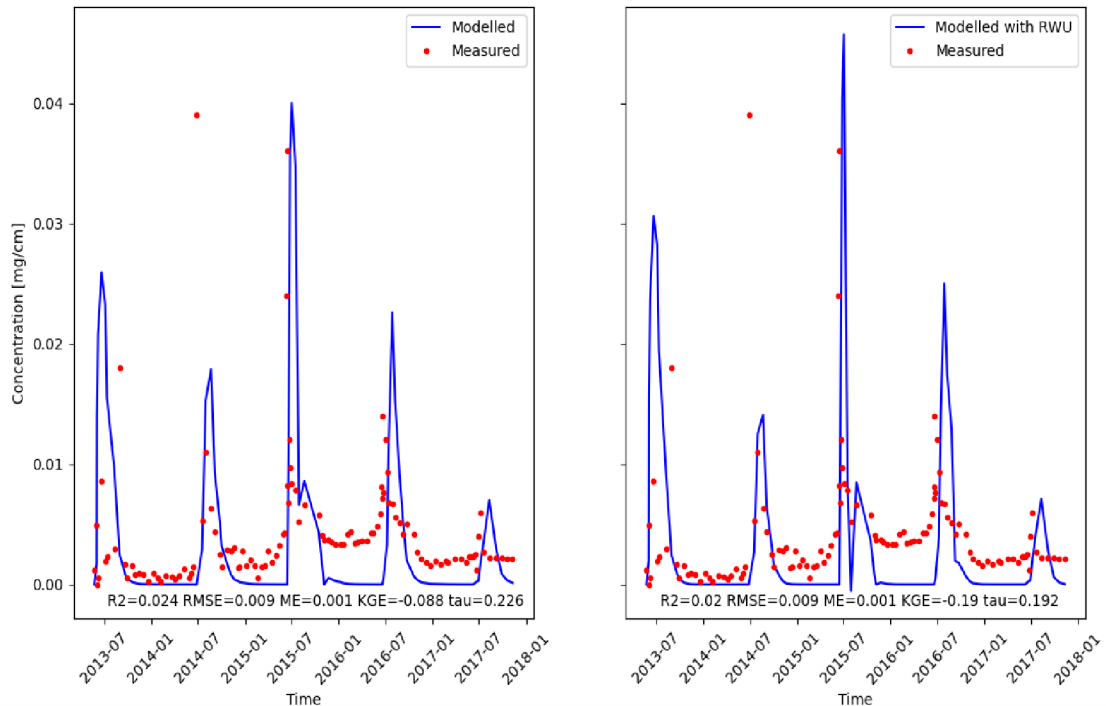


**Figure 12:** Desethetyl-terbutylazine (MT1) concentration in the first fitting model with and without root water uptake (in blue line) compared with the measured in the lysimeter drainage (in red dots), through the whole simulation period where right diagram with root water uptake and the left diagram without, with statistical parameters in the base

The second peak of modeled data in 2014 after the application is moderately high, while the measured peak is the highest in the investigation period (0.039 mg/cm) which is controversial with TBA in the same year, precipitation and irrigation were not enough for the TBA to appear high in the output but was good for biodegradation and forming MT1 as the amount of rain in that year were the lowest, moreover, this can be referred to remobilization of MT1 from previous year, while the modeled peaks of concentration are recorded as 0.013 and 0.014 mg/cm with and without RWU, respectively. The modeled concentrations are underestimating the measured data because of maybe the low amount of rainfall, the model could not expect the higher leaching behavior of MT1 than TBA as described by Guzzella et al. (2003), where the sorption of MT1 was studied by Ronka & Bodylska, (2021) and proved to be 5 times lower than other TBA metabolites and TBA itself, which indicates the higher mobility of that compound.

The measured data in the third peak in 2015 (0.036 mg/cm) is almost equal to the modeled data (0.04 and 0.046 mg/cm with and without RWU, respectively), this time the model could simulate the measured output well because the high amount of rainfall. The modeled concentration with RWU is higher because of the difference in accuracy between modeled with and without RWU as shown in the statistical evaluation parameters values in Figure 12. The peak of 2016 of the measured concentration was not that high because of the high leaching of TBA in that year due to the high amount of rainfall which affected the concentration of MT1 because of the lack of biodegradation. The measured concentration



in 2016 is 0.014 mg/cm and the modeled concentrations are 0.0225 and 0.025 mg/cm with and without RWU, respectively. The modeled concentration is higher than the measured described as a small overestimation as it was supposed to have a moderate amount of rain, and this should have increased the leached MT1. The last peak of 2017 is the lowest measured concentration in the investigation period. This is because the low rainfall affected the leaching of the applied TBA. Moreover, the applied TBA in 2017 was the lowest amount, and that year has been preceded by two high rainy seasons in 2015 and 2016 that removed most of the accumulated metabolite MT1 from the soil. The measured concentration of MT1 in 2017 is 0.006 mg/cm while the modeled concentrations are 0.007 with RWU and without RWU also the same value. The measured points appear in Figure 12 are getting higher and the data points never come back to zero after application from 2013 until 2016 in between the application peaks. This indicates the accumulation of the MT1 particles every year after application.

#### **5.2.1.5 Terbutylazine 2 CGA 324007 (LM5)**

The fitted biodegradation rate ( $0.095 \text{ d}^{-1}$ ) and the half-life of LM5 (7 d) are not in the range of the studies (36.5-70 d) (ECPR, 2015). The sorption rate is the biodegradation chain of TBA that continues after MT1 there are other metabolites in the chain which is MT13 but it is not of interest to this study and has not been detected in the outflow. The next metabolite in the chain is LM5 as shown in Figure 13, the first peak of measured concentration in 2013 is not so high (0.0013 mg/cm), despite the heavy rain in that year as calculated by Imig et al. (submitted-a). The modeled concentrations are 0.00175 and 0.0008 with and without RWU, respectively, where the difference between them is referred to as the accuracy of model calibration. In the measured data, the increase of the concentration can be noticed between the first application in 2013 and the second one in 2014, it is not represented in the modeled data, referring to Figure 13, the amount of precipitation and irrigation is decreasing after the application at 09/2013, in meanwhile, the biodegradation started to increase and the LM5 became mobile but less than MT1 as discussed by (EFSA, 2019; ECPR, 2015).

The second peak of the measured concentration in 2014 equals 0.0014 mg/cm, which is almost the same as in 2013. The rainfall was the lowest in 2014 which decreases the leachability of TBA which be more active for biodegradation and increases MT1 which will also increase the production of LM5 in the chain. The modeled concentrations in 2014 are 0.0021 and 0.0013 mg/cm with and without RWU, respectively, the difference between them both is in the accuracy of the statistical evaluation. The third and the highest peak of measured concentration is in 2015 when the rainfall was high which led to mobilizing of LM5 produced in 2015 and relics of previous years. The measured concentration is recorded to be 0.0035 mg/cm, while the modeled concentrations underestimate the measured, they are recorded as 0.0019 and 0.0012 with and without RWU, respectively. The underestimation of the measured concentrations comes from the model fitting accuracy as shown in Figure 13, the KGE = -0.265 and -0.348 with and without RWU, respectively, where the model without RWU is nearer to accuracy it can be noticed that the modeled peak is getting higher. In 2015, there are two modeled peaks, those peaks are reflecting the heavy rain events after the application of the parent TBA. The measured peak of LM5 after application in 2016 is lower than the previous year at

0.0018 mg/cm because of the moderate rainfall, where the modeled concentrations are also underestimating the measured values (0.0014 and 0.0012 with and without RWU, respectively) which can be due to the model fitting accuracy as discussed before. Regarding the 2017 modeled peak, it has been recorded as 0.0013 mg/cm, which is compatible to a good extent with the modeled concentrations recorded as 0.0008 and 0.0006 with and without RWU, respectively.

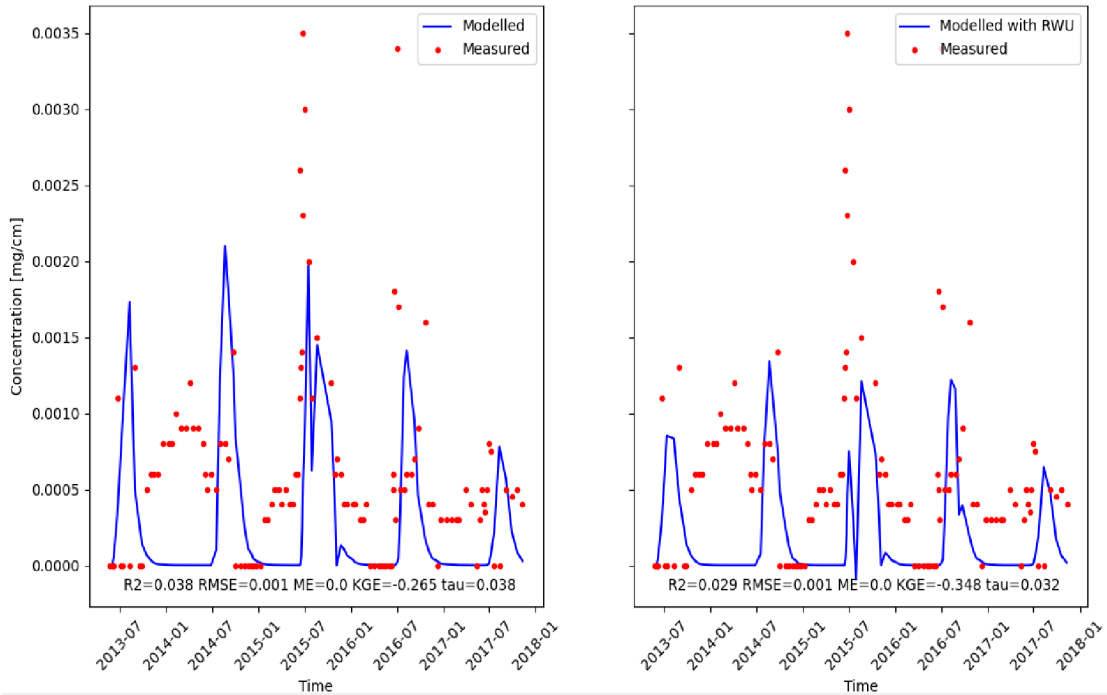


**Figure 13:** Terbutylazine 2 CGA 324007 (LM5) concentration in the first fitting model with and without root water uptake (in blue line) compared with the measured in the lysimeter drainage (in red dots), through the whole simulation period where right diagram with root water uptake and the left diagram without, with statistical parameters in the base

### 5.2.1.6 Terbutylazine 1 SYN 545666 (LM6)

As a continuation of the biodegradation chain of the metabolites detected in the output of the lysimeter 1, the metabolite LM6 is included in the model and compared to the measured points. LM6 is peaking the highest directly after the first application of the parent TBA in 2013. The concentration peak of the measured data is recorded as 0.0055 mg/cm. The relatively high peak of LM6 in 2013 is referred to the high amount of rainfall in 2013. The modeled concentration peaks are recorded as 0.0049 and 0.0025 mg/cm with and without RWU, respectively. The modeled peaks without RWU are describing the measured values well with a little underestimation. From the values of KGE in Figure 14, (-0.388 and -0.212 with and without RWU) are getting more correct with lowering the magnitude of the modeled peak indicating the real underestimation of the measured data, the high measured peak can be attributed to the high mobility of the LM6 - as discussed in EFSA, (2019) - in the soil after being produced as represented by the measured data. The second measured concentration peak in 2014 appears in Figure 14 saw to be 0.0029

mg/cm, where the modeled concentrations are 0.0073 and 0.006 with and without RWU, respectively, where the accuracy of fitting increases as KGE decreases in the model with RWU as shown in the Figure 14. The amount of rain falls in 2014 was low but the leaching of MT1 was high as in Figure 12 before it degrades in the chain forming LM5 and LM6. The amount of leached LM6 started to increase the entire year after application in June 2013 which supports the assumption that the accumulation of LM6 in the soil until the beginning of 2017.

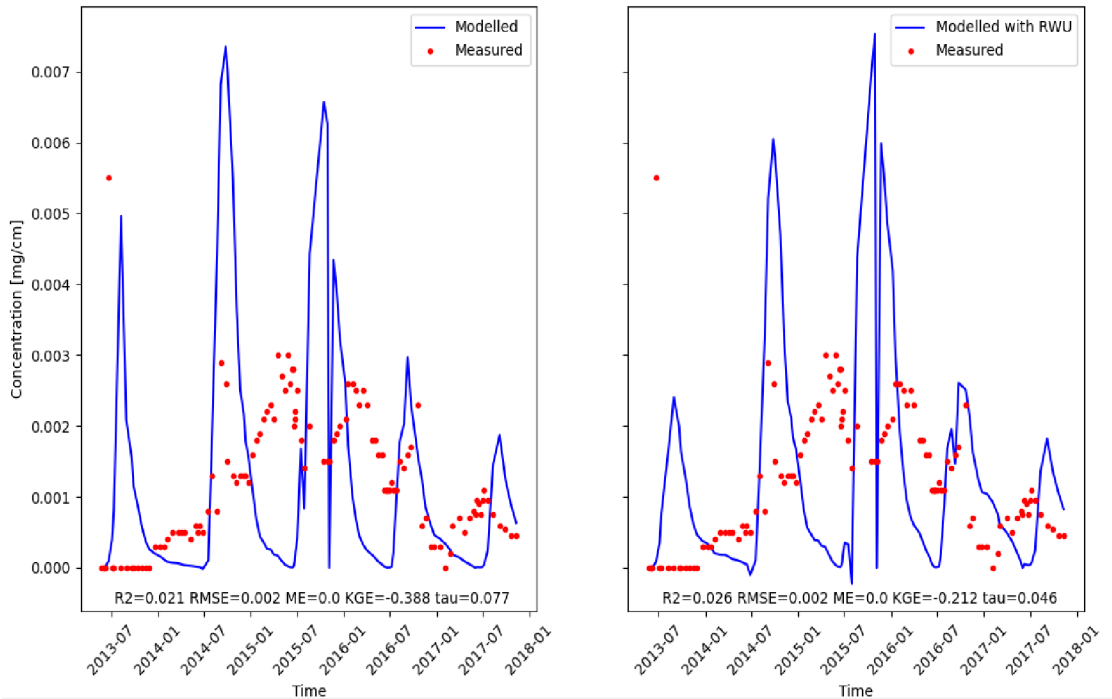


**Figure 14:** Terbutylazine 1 SYN 545666 (LM6) concentration in the first fitting model with and without root water uptake (in blue line) compared with the measured in the lysimeter drainage (in red dots), through the whole simulation period where right diagram with root water uptake and the left diagram without, with statistical parameters in the base

The measured concentration of LM5 in 2015 is divided into two peaks which are the same in all earlier metabolites of MTLA (MESA and MOXA) and terbutylazine (MT1, LM5, LM6, and MT13). The reason behind that might be the heavy rain after different applications which worked on remobilization of the metabolites in the soil. The highest peak of measured concentrations is 0.003 mg/cm while the highest modeled concentration peaks are 0.0065 and 0.0075 mg/cm with and without RWU, respectively. The modeled peaks are getting higher with increasing the accuracy of the fitting and having the right KGE values, which shows that the peaks are overestimating the measured data. The lower measured values compared to the modeled can be due to the high leaching amount of the later metabolite in the chain (LM5) which produced LM6. The measured peak concentration of 2016 is low (0.0022 mg/cm) compared to the amount leached in 2015 in the two peaks, where the modeled concentrations are 0.003 and 0.0026 mg/cm with and without RWU, respectively where the modeled and measured values are compatible. The

measured concentration peak in 2017 is 0.001 mg/cm, which is low due to the low amount of rainfall. While the modeled concentration peaks are 0.0018 for both values with and without RWU. The values of modeled and measured data are not too distinct.

### 5.2.2 Results of the second model with and without RWU

The second model was applied in HYDRUS-1D as mentioned in the methodology chapter because HYDRUS-1D does not consider the divergence and convergence of the biodegradation chain. Hence, the second model was done to model the other branches of MTLC and TBA. As shown in Table 11, the fitted parameters using PEST.

**Table 11:** Fitted parameters of biodegradation and production for model (2) after running PEST

Solutes	$K_d$ (Linear sorption isotherm rate) (cm <sup>3</sup> /mg)	$D_{50}$ (Half-Life of biodegradation) (d)	$\mu_{total}$ (Total biodegradation rate) (d <sup>-1</sup> )	$\mu_w$ (Biodegradation rate for the solute in soil) (d <sup>-1</sup> )	$\mu_w'$ (Biodegradation rate of solute representing chain reaction) (d <sup>-1</sup> )
(Metolachlor) (MTLC)	0.00401	8.7	0.0796	0.0416	0.038
(MOXA)	0.00093	43.8	0.0158	0.0158	0
(Terbutylazine) (TBA)	0.03	8	0.0853	0.08	0.0053
(MT13)	0.1	23.1	0.03	0.03	0

#### 5.2.2.1 Metolachlor (MTLC)

The concentrations of the modeled MTLC in the second model are lower than in the first model as shown in Figure 15. Although it looks like the magnitude of the first model peaks, the first peak in 2013 of the modeled concentration (0.33 and 0.26 mg/cm with and without RWU, respectively) is overestimating the measured peak, where also the same interpretation of high rainfall can be the reason why it looks higher. The second modeled peak (0.005 and 0.001 mg/cm with and without RWU respectively) is underestimating the measured values which can be referred to as the low rainfall in 2014. The modeled peak of 2015 is (0.08 and 0.03 mg/cm with and without RWU, respectively) underestimating the measured data while the rainfall was the highest in 2015, this can be attributed to the biodegradation of MTLC which affected the output concentration which is apparent in all the peaks. The modeled peak in 2016 is underestimating the measured where the modeled data is (0.03 mg/cm for both with and without RWU), this can be attributed to the moderate rainfall. The modeled peaks of 2017 are so low due to low rainfall, the values of concentrations are 0.005 and 0.003 with and without RWU respectively.

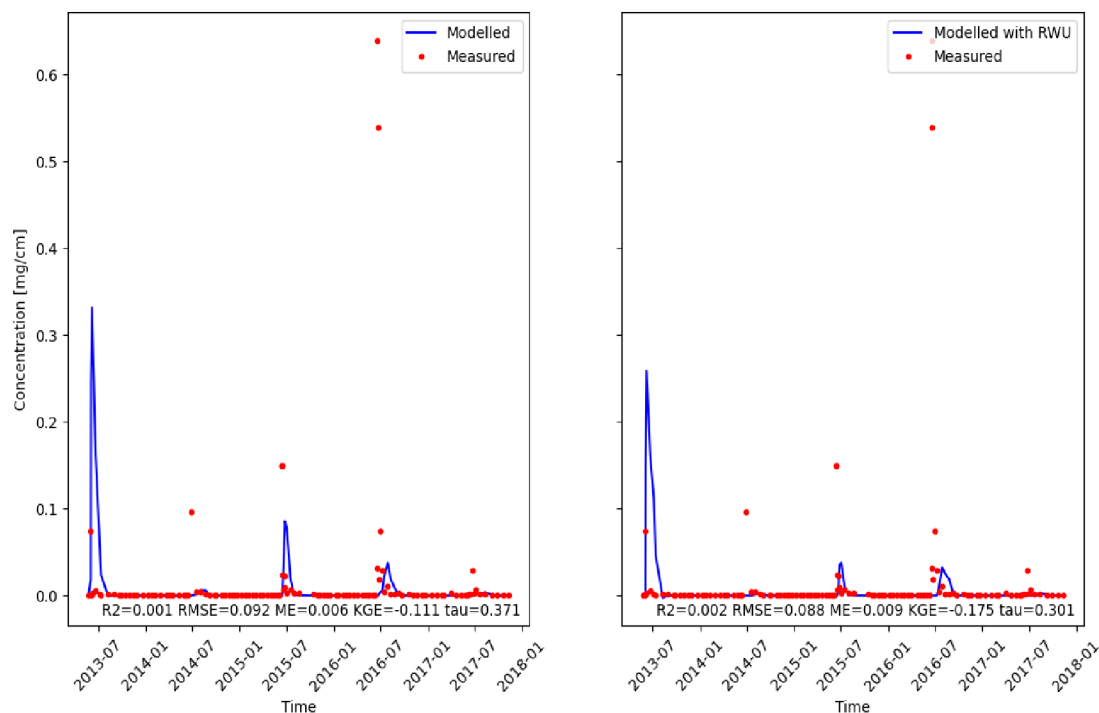


**Figure 15:** Metolachlor (MTLC) concentration in the second fitting model with and without root water uptake (in blue line) compared with the measured in the lysimeter drainage (in red dots), through the whole simulation period where right diagram with root water uptake and the left diagram without, with statistical parameters in the base

### 5.2.2.2 Metolachlor oxanilic acid (MOXA)

The fitted biodegradation rate and half-life of MOXA are ( $0.0158 \text{ d}^{-1}$ , 43.8 d) which are still near to the values in Rose et al. (2018). The sorption coefficient ( $0.00093 \text{ cm}^3/\text{mg}$ ) is also near to the value mentioned in (Sidoli et al., 2020) ( $0.00075 \text{ cm}^3/\text{mg}$ ). The second branch of biodegradation of metolachlor is MOXA which is lower in amount and mobility than MESA. The measured concentration peak in 2013 ( $0.025 \text{ mg/cm}$ ) is underestimated by the modeled peaks ( $0.122$  and  $0.155$  with and without RWU, respectively). The reason behind the overestimation is the high rainfall in 2013, while the measured concentration is not so high because of the sorption of MOXA as it was the first year of application. The second measured peak in 2014 is low  $0.01 \text{ mg/cm}$  but it gets higher with time through the year and is peaking again high at the beginning of 2015 ( $0.035 \text{ mg/cm}$ ) which can be attributed to the remobilization of MOXA from the last year also maybe because of the increase of precipitation at the beginning of 2015. The modeled concentration peaks of MOXA in 2014 are  $0.1$  and  $0.06$  with and without RWU, respectively, the peaks of the modeled values are overestimating the measured peak due to the remobilization from the previous year and the statistical evaluation values are less accurate than the other one with RWU, that made the model without RWU have a higher peak.

The measured concentration in 2015 is high at  $0.087 \text{ mg/cm}$  which is due to the high rainfall. The modeled concentration peaks of MOXA ( $0.165$  and  $0.085 \text{ mg/cm}$  with and

without RWU respectively) are overestimating the measured values in the model without RWU and there is almost no difference in the model with RWU in which the statistical parameters are more accurate. The two peaks in the model in 2015 are showing always through the metabolites the effect of heavy rain and remobilization. The measured concentration peak in 2016 is 0.067 mg/cm, where the peak is moderate because of the moderate rainfall in 2016. The modeled concentration peaks are (0.145 and 0.140 with and without RWU respectively), which are overestimating the measured values due to the relatively high rain and the remobilization from previous years which is not apparent in the measured data. There is no big difference between the effect of statistical accuracy with and without RWU. The measured concentration peak is 0.025 mg/cm is low because of the low precipitation, the modeled concentrations numerically determined are (0.055 and 0.45 mg/cm with and without RWU, respectively) slightly overestimating the measured values especially in the model without RWU.

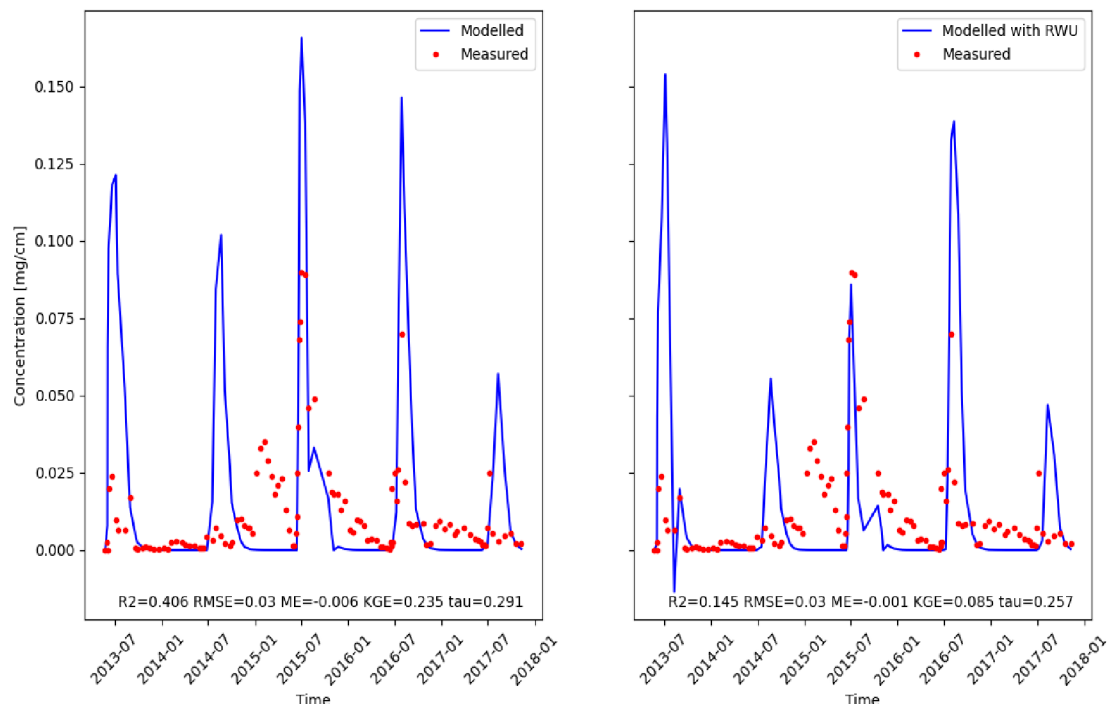


**Figure 16:** Metolachlor oxanilic acid (MOXA) concentration in the second fitting model with and without root water uptake (in blue line) compared with the measured in the lysimeter drainage (in red dots), through the whole simulation period where right diagram with root water uptake and the left diagram without, with statistical parameters in the base

### 5.2.2.3 Terbutylazine (TBA)

The amount of the TBA concentration after application in the second model is noticed to be lower in comparison to the TBA modeled before in the first model. As shown in Figure 17, The modeled concentration peaks in 2013 after application are 0.255 and 0.195 mg/cm with and without RWU, respectively, the modeled peaks are not overestimated like the first model as can be seen in the values of statistical evaluation parameters, the more it becomes more accurate the more it becomes near to the measured

values. The values of the modeled concentrations are low in 2014 (0.005 mg/cm for both with and without RWU), because of the low rainfall. The values of modeled concentrations in 2015 are lower than the measured peaks (0.07 and 0.04 mg/cm with and without RWU, respectively) when the rainfall was high which was supposed to be higher, but this can be attributed to the fitting statistical accuracy.

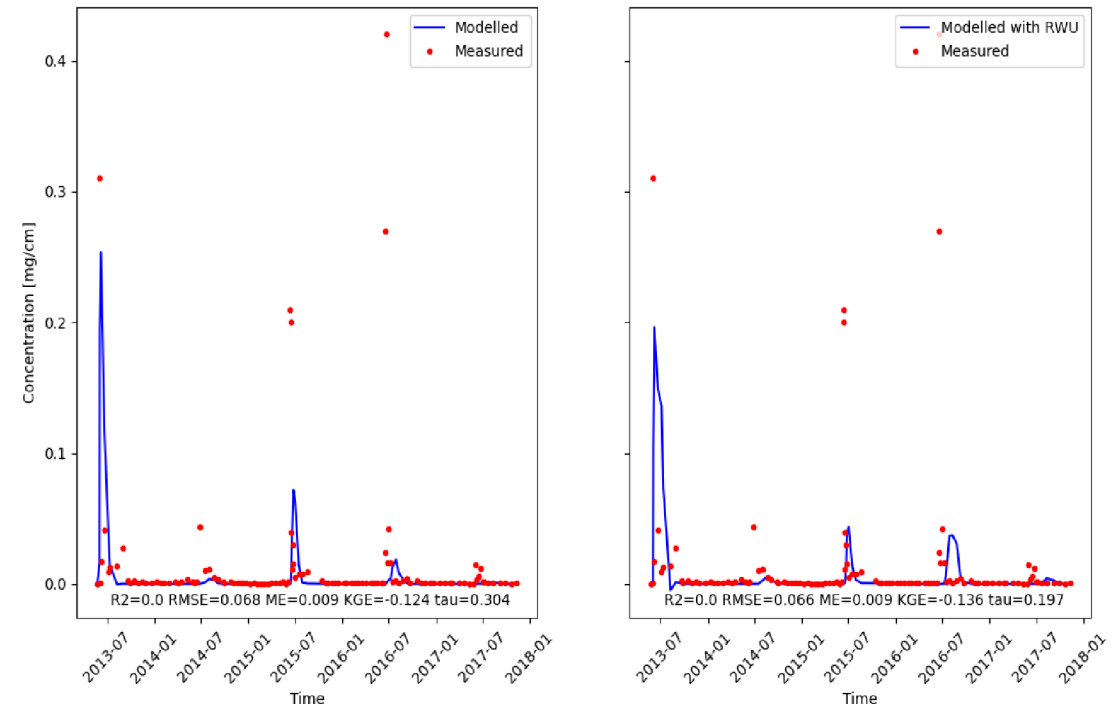


**Figure 17:** Terbutylazine (TBA) concentration in the second fitting model with and without root water uptake (in blue line) compared with the measured in the lysimeter drainage (in red dots), through the whole simulation period where right diagram with root water uptake and the left diagram without, with statistical parameters in the base

The modeled peaks in 2016 (0.02 and 0.035 with and without RWU, respectively) are so underestimating the measured peaks, where the measured peaks are so high maybe because of the remobilization of the TBA previously applied to the soil. The modeled values in 2017 are low and are like the measured because of the low rain.

#### 5.2.2.4 2-hydroxy-terbutylazine (MT13)

The modeled and fitted parameters of biodegradation rate and sorption for MT13 are (0.03 d<sup>-1</sup>, 0.1 cm<sup>3</sup>/mg) respectively, which are low in comparison to values mentioned in ECPR, (2015) for sandy loam soil (0.008 d<sup>-1</sup>, 0.0084 cm<sup>3</sup>/mg) where those values can be the second branch of TBA biodegradation is represented by MT13, which is detected in the outflow of the lysimeter. The measured concentration in 2013 is high (0.004 mg/cm) in comparison to the other years Figure 18. But is low if compared to the MT1 because of the percentage of biodegradation (ECPR, 2015). The modeled concentrations are high (0.005 and 0.0052 mg/cm with and without RWU, respectively) and in agreement with the measured values, this high value is interpreted in the light of the high biodegradation

of the parent TBA and the high rainfall in 2013. The second measured peak in 2014 is moderate (0.0026 mg/cm) as the parent is not so high in the output which affected the biodegradation of part of the TBA sorbed, the modeled concentration with RWU (0.0005 mg/cm) is near to the measured data which is near to the accuracy, while the modeled concentration without RWU is underestimating the measured data which may be due to the low precipitation or the lower accuracy of model fitting as indicated by the statistical parameters. The measured concentrations of 2015 are the highest (0.0045 mg/cm) due to the high precipitation, where the modeled concentrations are slightly underestimating the measured data which can be because of the difference in the model to describe the slight anomalies because of the equilibrium assumption in the sorption. The modeled peak values are 0.0032 and 0.003 mg/cm with and without RWU, respectively. The measured concentration peak in 2016 is almost the same as in 2015 (0.0028 mg/cm) because the effect of rain in 2016 made the concentration modeled higher in the model with RWU (0.004 mg/cm). On contrary, the modeled value without RWU is not high (0.0018 mg/cm) which can be referred to the decrease of accuracy in comparison to the model with RWU. The measured concentration peak in 2017 is (0.0006 mg/cm) which is not high because of low rain. The modeled concentrations are 0.0002 and 0.001 with and without RWU, respectively, where modeled values without RWU are underestimating measured ones because of the lower accuracy of model fitting.

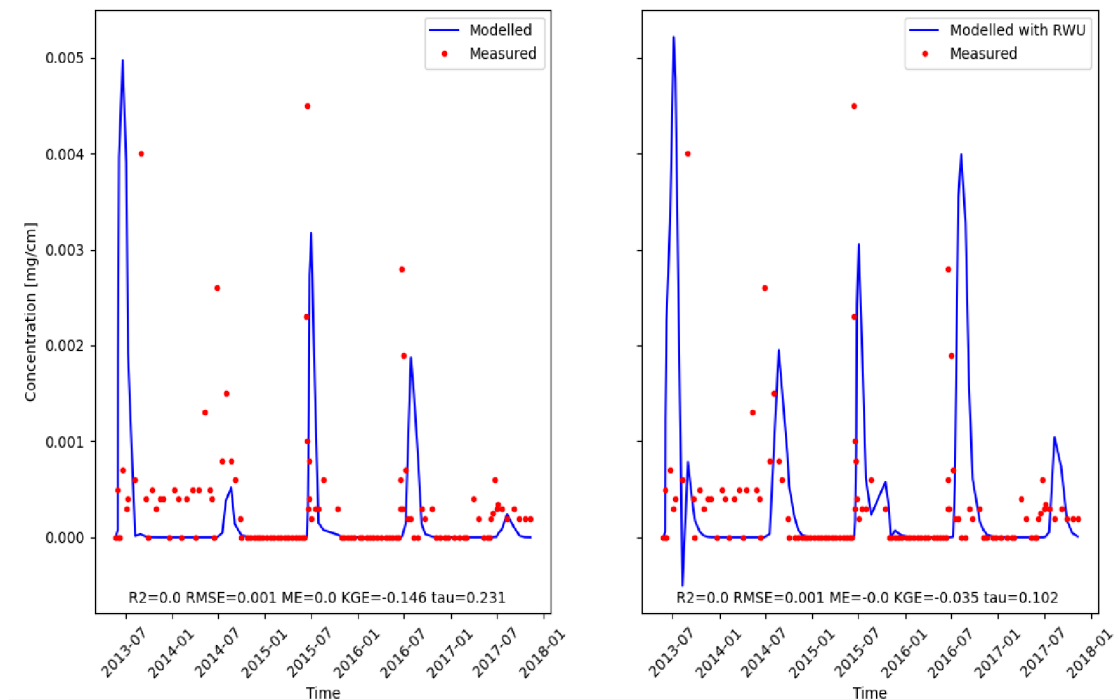


**Figure 18:** 2-hydroxy terbuthylazine (MT13) concentration in the second fitting model with and without root water uptake (in blue line) compared with the measured in the lysimeter drainage



(in red dots), through the whole simulation period where right diagram with root water uptake and the left diagram without, with statistical parameters in the base

### **5.3 Discussion of root water uptake**

The model with RWU in the modeled data can be noticed that it is not so significantly different than the model without RWU. The modelled solutes with RWU which are getting better value of KGE and higher peak values due to overestimation are TBA of first model (KGE with RWU = 0.01, without = 0.01), LM6 (KGE with RWU = -0.21, without = -0.38) and MT13 (KGE with RWU = -0.19, without = -0.08), also lower due underestimation is MOXA (KGE with RWU = 0.085, without = 0.23). While the other solutes with RWU are getting worse values of KGE with higher peaks due to overestimation are MTLC first model (KGE with RWU = -0.17, without = -0.08) and MT1 (KGE with RWU = -0.19, without = -0.08), and with lower peaks due to underestimation as in TBA second model (KGE with RWU = -0.13, without = -0.12), MTLC second model (KGE with RWU = -0.17, without = -0.11), MESA (KGE with RWU = -0.44, without = -0.37) and LM5 (KGE with RWU = -0.34, without = -0.26).

The values of statistical evaluation parameters are low in the model which shows a shortcoming in the efficiency of the model, but we can still rely on one parameter (KGE) in the evaluation of modeled data in this work. However, the values of KGE also need improvement which can be done using dual-porosity approaches.

## 6. Summary and conclusion

This study contributes to process understanding concerning the behavior of the four herbicides metolachlor, terbutylazine, nicosulfuron, and porosulfuron applied to a lysimeter filled with sandy to loamy gravel soil (Ly1) in four successive years from 2013 to 2017. The applied herbicides have been applied yearly in late May or June, according to common agricultural practice. Throughout the whole investigation period, the weighable lysimeter drainage has been monitored and samples have been taken for analysis and concentration determination for each solute. Two numerical reactive transport models have been set up to track the transport and fate of the herbicides and their metabolites using HYDRUS-1D software. The fitted parameters are the linear sorption coefficient ( $K_d$ ), the first order biodegradation rate ( $\mu_w$ ), and the first order metabolite production rate ( $\mu_w'$ ). The models were used to determine the important processes of biodegradation, sorption to the soil and plant uptake of water and solute. The parameter  $\mu_w'$  is particularly important in the present study, as it is responsible for producing the metabolites and modeling them with the entered percentage in the chain reaction.

Modelled results have been compared to the measured values to evaluate the goodness of fit. A parameter estimation software (PEST) has been used to fit the parameters of interest. A python code has been used to modify the code of HYDRUS-1D to add the parameters of interest and to write the template, instructions, and control files to run PEST. Fitted parameters have been compared to the values mentioned in the literature to make sure of their plausibility.

The contribution of biodegradation and sorption can be concluded from the peaks when comparing the curve characteristics of metabolites with their parent compounds. Some observations are over- or underestimated by the simulations, however the estimate contributions and rates of biodegradation and sorption appear plausible in comparison to literature findings. The modeled concentrations of the parent herbicides metolachlor and TBA are mostly underestimating the observations except for 2013 where peaks are overestimated because of the high rain rates. The remobilization and accumulation were not clear in the modelled data as in the measured data, but still, the values of the peaks are in the reasonable range of three- to fivefold over- or underestimating the observations.

The model approach can be improved for future studies, e.g., by considering dual-porosity and dual-permeability approaches that can describe the presence of different flow domains and preferential flow paths. This might be able to better describe observed rapid concentration changes and quick appearances of chemicals in lysimeter discharge. This would require more frequent data measurements of the outflow - e.g., to be every two days instead of weekly- to reduce uncertainties. Simulations considering root water uptake did not show a significant difference to those without. This could be studied in more detail with different assumptions concerning water and chemical uptake into plants. In future studies, biodegradation and sorption should be distinguished in the macropores (preferential flow paths) and the subsurface matrix. Moreover, physical, and chemical nonequilibrium should be investigated and compared to the equilibrium approach applied in the present study. The model should be improved against model errors which can be possible by the identification of herbicides and metabolites concentrations and

information about sorption and biodegradation in the soil as well as the conditions of the unsaturated matrix.

In general, pesticide leaching models studying fate and transport have been improving over the last years. They should be developed further to support protecting the environment against contaminants and to identify risks to soil ecosystems and groundwater (where pesticide application should be reduced or replaced by crops grown organically).

## 7. References

- Ahrens, W. H., & Edwards, M. T. (1994). *Weed Science Society of America Herbicide Handbook*.
- Alhajjar, B. J., Simsiman, G. v., & Chesters, G. (1990). Fate and transport of alachlor, metolachlor and atrazine in large columns. *Water Science and Technology*, 22(6), 87–94. <https://doi.org/10.2166/wst.1990.0055>
- Alister, C., Araya, M., & Kogan, M. (2011). Relación entre la adsorción y la lixiviación de herbicidas en el suelo. *Ciencia e Investigacion Agraria*, 38(2), 243–251. <https://doi.org/10.4067/S0718-16202011000200010>
- Alletto, L., Benoit, P., Bolognesi, B., Couffignal, M., Bergheaud, V., Dumény, V., Longueval, C., & Barriuso, E. (2013). Sorption and mineralisation of S-metolachlor in soils from fields cultivated with different conservation tillage systems. *Soil and Tillage Research*, 128, 97–103. <https://doi.org/10.1016/j.still.2012.11.005>
- American Chemical Society (CAS) Common Chemistry. (2022a). *Desethylterbuthylazine, a division of the American Chemical Society, n.d. (CAS RN: 30125-63-4). Licensed under the Attribution-Noncommercial 4.0 International License (CC BY-NC 4.0)*. [https://commonchemistry.cas.org/detail?cas\\_rn=30125-63-4](https://commonchemistry.cas.org/detail?cas_rn=30125-63-4)
- American Chemical Society (CAS) Common Chemistry. (2022b). *Hydroxyterbuthylazine, a division of the American Chemical Society, n.d. (CAS RN: 66753-07-9). Licensed under the Attribution-Noncommercial 4.0 International License (CC BY-NC 4.0)*. [https://commonchemistry.cas.org/detail?cas\\_rn=66753-07-9](https://commonchemistry.cas.org/detail?cas_rn=66753-07-9)
- American Chemical Society (CAS) Common Chemistry. (2022c). *Metolachlor., a division of the American Chemical Society, n.d. (CAS RN: 51218-45-2). Licensed under the Attribution-Noncommercial 4.0 International License (CC BY-NC 4.0)*. [https://commonchemistry.cas.org/detail?cas\\_rn=51218-45-2&search=metolachlor](https://commonchemistry.cas.org/detail?cas_rn=51218-45-2&search=metolachlor)

- American Chemical Society (CAS) Common Chemistry. (2022d). *Metolachlor ESA. a division of the American Chemical Society, n.d. (CAS RN: 171118-09-5). Licensed under the Attribution-Noncommercial 4.0 International License (CC BY-NC 4.0).* [https://commonchemistry.cas.org/detail?cas\\_rn=171118-09-5](https://commonchemistry.cas.org/detail?cas_rn=171118-09-5)
- American Chemical Society (CAS) Common Chemistry. (2022e). *Metolachlor oxanilic acid. a division of the American Chemical Society, n.d. (CAS RN: 152019-73-3). Licensed under the Attribution-Noncommercial 4.0 International License (CC BY-NC 4.0).* [https://commonchemistry.cas.org/detail?cas\\_rn=152019-73-3](https://commonchemistry.cas.org/detail?cas_rn=152019-73-3)
- American Chemical Society (CAS) Common Chemistry. (2022f). *Terbutylazine, a division of the American Chemical Society, n.d. (CAS RN: 5915-41-3). Licensed under the Attribution-Noncommercial 4.0 International License (CC BY-NC 4.0).* [https://commonchemistry.cas.org/detail?cas\\_rn=5915-41-3](https://commonchemistry.cas.org/detail?cas_rn=5915-41-3)
- An, Q., Wu, Y., Li, D., Hao, X., Pan, C., & Rein, A. (2022). Development and application of a numerical dynamic model for pesticide residues in apple orchards. *Pest Manag. Sci.*
- Andert, S. (2021). The method and timing of weed control affect the productivity of intercropped maize (*Zea mays* L.) and bean (*Phaseolus vulgaris* L.). *Agriculture (Switzerland)*, *11*(5). <https://doi.org/10.3390/agriculture11050380>
- Anlauf, R., Schaefer, J., & Kajitvichyanukul, P. (2018). Coupling HYDRUS-1D with ArcGIS to estimate pesticide accumulation and leaching risk on a regional basis. *Journal of Environmental Management*, *217*, 980–990. <https://doi.org/10.1016/j.jenvman.2018.03.099>
- Arias-Estévez, M., López-Periago, E., Martínez-Carballo, E., Simal-Gándara, J., Mejuto, J. C., & García-Río, L. (2008). The mobility and degradation of pesticides in soils and the pollution of groundwater resources. In *Agriculture, Ecosystems and Environment* (Vol. 123, Issue 4, pp. 247–260). <https://doi.org/10.1016/j.agee.2007.07.011>

- Azcarate, M. P., Montoya, J. C., & Koskinen, W. C. (2015). Sorption, desorption and leaching potential of sulfonylurea herbicides in Argentinean soils. *Journal of Environmental Science and Health - Part B Pesticides, Food Contaminants, and Agricultural Wastes*, 50(4), 229–237.  
<https://doi.org/10.1080/03601234.2015.999583>
- Baran, N., & Gourcy, L. (2013). Sorption and mineralization of S-metolachlor and its ionic metabolites in soils and vadose zone solids: Consequences on groundwater quality in an alluvial aquifer (Ain Plain, France). *Journal of Contaminant Hydrology*, 154, 20–28. <https://doi.org/10.1016/j.jconhyd.2013.07.009>
- Baran, N., Mouvet, C., Dagnac, T., & Jeannot, R. (2004). *Infiltration of Acetochlor and Two of Its Metabolites in Two Contrasting Soils*.
- Batsukh, K., Zlotnik, V. A., Suyker, A., & Nasta, P. (2021). Prediction of biome-specific potential evapotranspiration in mongolia under a scarcity of weather data. *Water (Switzerland)*, 13(18). <https://doi.org/10.3390/w13182470>
- BAuA. (2021). Proposal for Harmonised Classification and Labelling, Based on Regulation (EC) No 1272/2008 (CLP Regulation), Annex VI, Part 2, International Chemical Identification: S-metolachlor (ISO). *Federal Institute for Occupational Safety and Health, Dortmund, Germany*.  
<https://echa.europa.eu/documents/10162/e826d559-4fea-917f-c1d5-69009cf79c8f>
- Bayless, E. R., Capel, P. D., Barbash, J. E., Webb, R. M. T., Hancock, T. L. C., & Lampe, D. C. (2008). Simulated Fate and Transport of Metolachlor in the Unsaturated Zone, Maryland, USA. *Journal of Environmental Quality*, 37(3), 1064–1072. <https://doi.org/10.2134/jeq2006.0562>
- BMG, (Bundesministerium für Gesundheit). (2014). *Aktionswerte bezüglich nicht relevanter Metaboliten von Pflanzenschutzmittel-Wirkstoffen in Wasser für den menschlichen Gebrauch*.

- Boivin, A., Šimůnek, J., Schiavon, M., & van Genuchten, M. Th. (2006). Comparison of Pesticide Transport Processes in Three Tile-Drained Field Soils Using HYDRUS-2D. *Vadose Zone Journal*, 5(3), 838–849. <https://doi.org/10.2136/vzj2005.0089>
- Borg, H., & Grimes, D. W. (1986). *Depth Development of Roots with Time: An Empirical Description*.
- Bottoni, P., Grenni, P., Lucentini, L., & Caracciolo, A. B. (2013). Terbutylazine and other triazines in Italian water resources. *Microchemical Journal*, 107, 136–142. <https://doi.org/10.1016/J.MICROC.2012.06.011>
- Brumovský, M., Bečanová, J., Kohoutek, J., Borghini, M., & Nizzetto, L. (2017). Contaminants of emerging concern in the open sea waters of the Western Mediterranean. *Environmental Pollution*, 229, 976–983. <https://doi.org/10.1016/j.envpol.2017.07.082>
- Brunetti, G., Šimůnek, J., Kodešova, R., & Šejna, M. (2022). *The Dynamic Plant Uptake Module for HYDRUS Simulating the Translocation and Transformation of Neutral Compounds in the Soil-Plant Continuum*.
- Calderon, M. J., de Luna, E., Gomez, J. A., & Hermosin, M. C. (2016). Herbicide monitoring in soil, runoff waters and sediments in an olive orchard. *Science of the Total Environment*, 569–570, 416–422. <https://doi.org/10.1016/j.scitotenv.2016.06.126>
- Capel, P. D., McCarthy, K. A., & Barbash, J. E. (2008). National, Holistic, Watershed-Scale Approach to Understand the Sources, Transport, and Fate of Agricultural Chemicals. *Journal of Environmental Quality*, 37(3), 983–993. <https://doi.org/10.2134/jeq2007.0226>
- Caracciolo, A. B., Giuliano, G., Grenni, P., Cremisini, C., Ciccoli, R., & Ubaldi, C. (2005). Effect of urea on degradation of terbutylazine in soil. *Environmental Toxicology and Chemistry*, 24(5), 1035–1040. <https://doi.org/10.1897/04-253R.1>
- Cavalier, T. C., Lavy, T. J., & Mattice, J. D. (1991). *Persistence of Selected Pesticides in Ground-Water Samples* (Vol. 29, pp. 225–231).

- Chai, T., & Draxler, R. R. (2014). Root mean square error (RMSE) or mean absolute error (MAE)? *Geosci. Model Dev. Discuss*, 7, 1525–1534.  
<https://doi.org/10.5194/gmdd-7-1525-2014>
- Chen, Z., Chen, Y., Vymazal, J., Kule, L., & Koželuh, M. (2017). Dynamics of chloroacetanilide herbicides in various types of mesocosm wetlands. *Science of the Total Environment*, 577, 386–394. <https://doi.org/10.1016/j.scitotenv.2016.10.216>
- Chesters, G., Simsiman, G. v., Levy, J., Alhajjar, B. J., Fathulla, R. N., & Harkin, J. M. (1989). Environmental fate of alachlor and metolachlor. *Reviews of Environmental Contamination and Toxicology*, 110, 1–74. [https://doi.org/10.1007/978-1-4684-7092-5\\_1](https://doi.org/10.1007/978-1-4684-7092-5_1)
- Cheviron, B., & Coquet, Y. (2009). Sensitivity Analysis of Transient-MIM HYDRUS-1D: Case Study Related to Pesticide Fate in Soils. *Vadose Zone Journal*, 8(4), 1064–1079. <https://doi.org/10.2136/vzj2009.0023>
- Cheyns, K., Mertens, J., Diels, J., Smolders, E., & Springael, D. (2010). Monod kinetics rather than a first-order degradation model explains atrazine fate in soil mini-columns: Implications for pesticide fate modelling. *Environmental Pollution*, 158(5), 1405–1411. <https://doi.org/10.1016/j.envpol.2009.12.041>
- Crisanto, T., Sgnchez-Camazano, M., Arienzo', M., & S&chez-Martin, M. J. (1995). Adsorption and mobility of metolachlor in surface horizons of soils with low organic matter content. In *the Science of the Total Jhnonment The Science of the Total Environment* (Vol. 166).
- David E. R., & Šimůnek, J. (2018). *David Radcliffe\_ Jiri Simunek - Soil Physics with Hydrus\_ Modeling and Applications-CRC Press*.
- Deutsches Maiskomitee e.V. (DMK). (2022). *Gesamtfl ächenentwicklung Maisanbau*, [http://www.maiskomitee.de/web/public/Fakten.aspx/Statistik/Deutschland/Gesamtfl\\_ächenentwicklung](http://www.maiskomitee.de/web/public/Fakten.aspx/Statistik/Deutschland/Gesamtfl_ächenentwicklung).
- di Buccianico, A. (2008). Coefficient of determination (R<sup>2</sup>). *Encyclopedia of Statistics in Quality and Reliability*, 1.



- Dimou, A. D., Sakkas, V. A., & Albanis, T. A. (2005). Metolachlor photodegradation study in aqueous media under natural and simulated solar irradiation. *Journal of Agricultural and Food Chemistry*, 53(3), 694–701.  
<https://doi.org/10.1021/jf048766w>
- Doherty, J. (2020a). *Model-Independent Parameter Estimation User Manual Part I: PEST, SENSAN and Global Optimisers*. (7th ed.).
- Doherty, J. (2020b). *Model-Independent Parameter Estimation User Manual Part II: PEST Utility Support Software Watermark Numerical Computing*.
- Dolaptsoglou, C., Karpouzas, D. G., Menkissoglu-Spiroudi, U., Eleftherohorinos, I., & Voudrias, E. A. (2007). Influence of Different Organic Amendments on the Degradation, Metabolism, and Adsorption of Terbutylazine. *Journal of Environmental Quality*, 36(6), 1793–1802. <https://doi.org/10.2134/jeq2006.0388>
- Domagalski, J. L., Ator, S., Coupe, R., McCarthy, K., Lampe, D., Sandstrom, M., & Baker, N. (2008). Comparative Study of Transport Processes of Nitrogen, Phosphorus, and Herbicides to Streams in Five Agricultural Basins, USA. *Journal of Environmental Quality*, 37(3), 1158–1169. <https://doi.org/10.2134/jeq2007.0408>
- Dores, E. F. G. C., de Souza, L., Villa, R. D., & Pinto, A. A. (2013). Assessment of metolachlor and diuron leaching in a tropical soil using undisturbed soil columns under laboratory conditions. *Journal of Environmental Science and Health - Part B Pesticides, Food Contaminants, and Agricultural Wastes*, 48(2), 114–121.  
<https://doi.org/10.1080/03601234.2013.726900>
- Dubus, I. G., Brown, C. D., & Beulke, S. (2003). Sources of uncertainty in pesticide fate modelling. *Science of the Total Environment*, 317(1–3), 53–72.  
[https://doi.org/10.1016/S0048-9697\(03\)00362-0](https://doi.org/10.1016/S0048-9697(03)00362-0)
- EC, (European Commission). (1998). Directive 98/83/EC of the Council of 3 November 1998 on the quality of water intended for human consumption. *Official Journal of the European Communities*, 330, 32–45.

- Eckhardt, D. A., Kappel, W. M., Coon, W. F., & Phillips, P. J. (1999). Herbicides and their metabolites in Cayuga Lake and its tributaries, New York. *US Geological Survey Toxic Substances Hydrology Program—Proceedings of the Technical Meeting*, 2, 395–403.
- EFSA. (2011a). Use of the EFSA Comprehensive European Food Consumption Database in Exposure Assessment. *EFSA Journal*, 9(3), 1–34.  
<https://doi.org/10.2903/j.efsa.2011.2097>
- EFSA. (2011b). Conclusion on the peer review of the pesticide risk assessment of the active substance terbuthylazine. *EFSA Journal*, 9(1).  
<https://doi.org/10.2903/j.efsa.2011.1969>
- EFSA. (2012). Review of the existing maximum residue levels (MRLs) for S-metolachlor according to Article 12 of Regulation (EC) No 396/2005. *EFSA Journal*, 10(2). <https://doi.org/10.2903/j.efsa.2012.2586>
- EFSA, Abdourahime, H., Anastassiadou, M., Arena, M., Auteri, D., Barmaz, S., Brancato, A., Bura, L., Carrasco Cabrera, L., Chaideftou, E., Chiusolo, A., Court Marques, D., Crivellente, F., de Lentdecker, C., Egsmose, M., Fait, G., Ferreira, L., Gatto, V., Greco, L., ... Villamar-Bouza, L. (2019). Updated peer review of the pesticide risk assessment for the active substance terbuthylazine in light of confirmatory data submitted. In *EFSA Journal* (Vol. 17, Issue 9). Wiley-Blackwell Publishing Ltd. <https://doi.org/10.2903/j.efsa.2019.5817>
- El-Nahhal, Y., Nir, S., Margulies, L., & Rubin, B. (1999). Reduction of photodegradation and volatilization of herbicides in organo-clay formulations. *Applied Clay Science*, 14(1–3), 105–119. [https://doi.org/10.1016/S0169-1317\(98\)00053-2](https://doi.org/10.1016/S0169-1317(98)00053-2)
- European Council and Parliament Regulation (ECPR). (2015). *Addendum to the assessment report on terbuthylazine prepared by the rapporteur Member State the United Kingdom in light of confirmatory data, November 2015*.  
<https://doi.org/10.1145/3132847.3132886>

- European Union. (2009). Directive 2009/28/EC of the European Parliament and of the Council of 23 April 2009 on the promotion of the use of energy from renewable sources and amending and subsequently repealing Directives 2001/77/EC and 2003/30/EC. *Official Journal of the European Union*, 5.
- Eurostat. (2022). *Grain maize and corn-cob-mix by area, production and humidity [WWW Document]*. <https://ec.europa.eu/eurostat/web/products-datasets/-/tag00093>
- Farlin, J., Gallé, T., Bayerle, M., Pittois, D., Köppchen, S., Krause, M., & Hofmann, D. (2018). Breakthrough dynamics of s-metolachlor metabolites in drinking water wells: Transport pathways and time to trend reversal. *Journal of Contaminant Hydrology*, 213, 62–72. <https://doi.org/10.1016/J.JCONHYD.2018.05.002>
- Feddes, R. A., Kowalik, P. J., & Zaradny, H. (1978). *Simulation of field water use and crop yield*. Wageningen: Centre for agricultural publishing and documentation.
- Feddes, R. A., & Raats, P. A. C. (2004). *Parameterizing the soil-water-plant root system*. In *Unsaturated-zone modeling*. 6, 95–141.
- Fenoll, J., Garrido, I., Hellín, P., Flores, P., Vela, N., & Navarro, S. (2015). Use of different organic wastes as strategy to mitigate the leaching potential of phenylurea herbicides through the soil. *Environmental Science and Pollution Research*, 22(6), 4336–4349. <https://doi.org/10.1007/s11356-014-3652-7>
- Frank, R., Logan, L., & Clegg, B. S. (1991). Pesticide and Polychlorinated Biphenyl Residues in Waters at the Mouth of the Grand, Saugeen, and Thames Rivers, Ontario, Canada, 1986-1990. In *Arch. Environ. Contam. Toxicol* (Vol. 21).
- Garcia, C. A., Andraski, B. J., Stonestrom, D. A., Cooper, C. A., Šimůnek, J., & Wheatcraft, S. W. (2011). Interacting Vegetative and Thermal Contributions to Water Movement in Desert Soil. *Vadose Zone Journal*, 10(2), 552–564. <https://doi.org/10.2136/vzj2010.0023>
- Ghosh, R. K., Singh, N., & Singh, S. B. (2016). Effect of fly ash amendment on metolachlor and atrazine degradation and microbial activity in two soils.

*Environmental Monitoring and Assessment*, 188(8). <https://doi.org/10.1007/s10661-016-5486-x>

Gilliom, R. J., Barbash, J. E., Crawford, C. G., Hamilton, P. A., Martin, J. D., Nakagaki, N., Nowell, L. H., Scott, J. C., Stackelberg, P. E., Thelin, G. P., & Wolock, D. M. (2006). *The Quality of Our Nation's Waters—Pesticides in the Nation's Streams and Ground Water, 1992-2001*.

Gish, T. J., Prueger, J. H., Kustas, W. P., Daughtry, C. S. T., McKee, L. G., Russ, A., & Hatfield, J. L. (2009). Soil moisture and metolachlor volatilization observations over three years. *J Environ Qual*, 38(5):1. <https://doi.org/10.2134/jeq2008.0276>.

Gomis-berenguer, A., Sidoli, P., & Cagnon, B. (2021). Adsorption of metolachlor and its transformation products, ESA and OXA, on activated carbons. *Applied Sciences (Switzerland)*, 11(16). <https://doi.org/10.3390/app11167342>

Graham, W. H., Graham, D. W., Denoyelles, F., Smith, V. H., Larive, C. K., & Thurman, E. M. (1999). Metolachlor and alachlor breakdown product formation patterns in aquatic field mesocosms. *Environmental Science and Technology*, 33(24), 4471–4476. <https://doi.org/10.1021/es990686z>

Groh, J., Diamantopoulos, E., Duan, X., Ewert, F., Heinlein, F., Herbst, M., Holbak, M., Kamali, B., Kersebaum, K., Kuhnert, M., Nendel, C., Priesack, E., Steidl, J., Sommer, M., Pütz, T., Vanderborght, J., Vereecken, H., Wallor, E., Weber, T. K. D., ... Gerke, H. H. (2022). Same soil, different climate: Crop model intercomparison on translocated lysimeters. *Vadose Zone Journal*. <https://doi.org/10.1002/vzj2.20202>

Groh, J., Stumpp, C., Lücke, A., Pütz, T., Vanderborght, J., & Vereecken, H. (2018). Inverse Estimation of Soil Hydraulic and Transport Parameters of Layered Soils from Water Stable Isotope and Lysimeter Data. *Vadose Zone Journal*, 17(1), 170168. <https://doi.org/10.2136/vzj2017.09.0168>

- Guzzella, L., Pozzoni, F., & Giuliano, G. (2006). Herbicide contamination of surficial groundwater in Northern Italy. *Environmental Pollution*, 142(2), 344–353.  
<https://doi.org/10.1016/j.envpol.2005.10.037>
- Guzzella, L., Rullo, S., Pozzoni, F., & Giuliano, G. (2003). Studies on Mobility and Degradation Pathways of Terbutylazine Using Lysimeters on a Field Scale. *Journal of Environmental Quality*, 32(3), 1089–1098.  
<https://doi.org/10.2134/jeq2003.1089>
- Hartmann, A., Šimůnek, J., Aidoo, M. K., Seidel, S. J., & Lazarovitch, N. (2018). Implementation and Application of a Root Growth Module in HYDRUS. *Vadose Zone Journal*, 17(1), 170040. <https://doi.org/10.2136/vzj2017.02.0040>
- Herrmann, A. (2013). Biogas Production from Maize: Current State, Challenges and Prospects. 2. Agronomic and Environmental Aspects. In *Bioenergy Research* (Vol. 6, Issue 1, pp. 372–387). Springer Science and Business Media, LLC.  
<https://doi.org/10.1007/s12155-012-9227-x>
- Hopmans, J. W. (2011). Infiltration and Unsaturated Zone. In *Treatise on Water Science* (pp. 103–114). Elsevier. <https://doi.org/10.1016/B978-0-444-53199-5.00031-2>
- Hou, L., Zhou, Y., Bao, H., & Wenninger, J. (2016). Simulation of maize (*Zea mays* L.) water use with the HYDRUS-1D model in the semi-arid Hailiutu River catchment, Northwest China. *Hydrological Sciences Journal*, 1–11.  
<https://doi.org/10.1080/02626667.2016.1170130>
- Imig, A., Augustin, L., Groh, J., Pütz, T., Elsner, M., Einsiedl, F., & Rein, A. (submitted-a). *Fate of herbicides in cropped lysimeters: 2. Leaching of four maize herbicides considering different model setups.*
- Imig, A., Augustin, L., Groh, J., Pütz, T., & Rein, A. (2022). Inverse modelling of herbicide transport during transient flow in vegetated weighable lysimeters. *EGU General Assembly*. <https://doi.org/10.5194/egusphere-egu22-5664>

- Imig, A., Augustin, L., Groh, J., Pütz, T., Zhou, T., Einsiedl, F., & Rein, A. (submitted-b). *Fate of herbicides in cropped lysimeters: 1. Influence of different processes on unsaturated flow.*
- Imig, A., Shajari, F., Augustin, L., Einsiedl, F., & Rein, A. (2022). Improved lumped-parameter and numerical modeling of unsaturated water flow and stable water isotopes. *Groundwater*. <https://doi.org/10.1111/gwat.13244>
- Ismail, B. S., & Quirinus, L. (2000). Mobility and persistence of metolachlor in two common Malaysian agricultural soils. *Bulletin of Environmental Contamination and Toxicology*, 65(4), 530–536. <https://doi.org/10.1007/s001280000156>
- Jacques, D., Šimůnek, J., & van Genuchten, M. Th. (2000). *Tutorial 4 I. Water Flow and Solute Transport in a Layered Soil Profile*. 1–11.
- Jones, C. A., Bland, W. L., Ritchie, J. T., & Williams, J. R. (1991). *Simulation of Root Growth*.
- Jurina, T., Terzić, S., Ahel, M., Stipičević, S., Kontrec, D., Kurtanjek, Ž., & Udiković-Kolić, N. (2014). Catabolism of terbuthylazine by mixed bacterial culture originating from s-triazine-contaminated soil. *Applied Microbiology and Biotechnology*, 98(16), 7223–7232. <https://doi.org/10.1007/s00253-014-5774-8>
- Kanissery, R. G., Welsh, A., Gomez, A., Connor, L., & Sims, G. K. (2018). Identification of metolachlor mineralizing bacteria in aerobic and anaerobic soils using DNA-stable isotope probing. *Biodegradation*, 29, 117–128. <https://doi.org/10.1007/s10532-017-9817-6>
- Karanasios, E. C., Tsiropoulos, N. G., & Karpouzias, D. G. (2013). Quantitative and qualitative differences in the metabolism of pesticides in biobed substrates and soil. *Chemosphere*, 93(1), 20–28. <https://doi.org/10.1016/j.chemosphere.2013.04.049>
- Kling, H., Fuchs, M., & Paulin, M. (2012). Runoff conditions in the upper Danube basin under an ensemble of climate change scenarios. *Journal of Hydrology*, 424–425, 264–277. <https://doi.org/10.1016/j.jhydrol.2012.01.011>

- Kochany, J., & Maguire, R. J. (1994). Sunlight Photodegradation of Metolachlor in Water. *Journal of Agricultural and Food Chemistry*, 42(2), 406–412.  
<https://doi.org/10.1021/jf00038a032>
- Kodešová, R., Kočárek, M., Kodeš, V., Drábek, O., Kozák, J., & Hejtmánková, K. (2011). Pesticide adsorption in relation to soil properties and soil type distribution in regional scale. *Journal of Hazardous Materials*, 186(1), 540–550.  
<https://doi.org/10.1016/j.jhazmat.2010.11.040>
- Köhne, J. M., Köhne, S., Mohanty, B. P., & Šimůnek, J. (2004). *Inverse Mobile-Immobile Modeling of Transport During Transient Flow: Effects of Between-Domain Transfer and Initial Water Content*. [www.vadosezonejournal.org](http://www.vadosezonejournal.org)
- Köhne, J. M., Köhne, S., & Šimůnek, J. (2009). A review of model applications for structured soils: b) Pesticide transport. *Journal of Contaminant Hydrology*, 104(1–4), 36–60. <https://doi.org/10.1016/j.jconhyd.2008.10.003>
- Konstantinou, I. K., Hela, D. G., & Albanis, T. A. (2006). The status of pesticide pollution in surface waters (rivers and lakes) of Greece. Part I. Review on occurrence and levels. *Environmental Pollution*, 141(3), 555–570.  
<https://doi.org/10.1016/j.envpol.2005.07.024>
- Kronvang, B., Iversen, H. L., Løkke, H., Vejrup, K., Mogensen, B. B., Hansen, A., Hansen, L. B., & Agency, D. E. P. (2003). Pesticides in streams and subsurface drainage water within two arable catchments in Denmark: Pesticide application, concentration, transport and fate. *Pesticide Research*, 69, 141.
- Krutz, L. J., Gentry, T. J., Senseman, S. A., Pepper, I. L., & Tierney, D. P. (2006). Mineralisation of atrazine, metolachlor and their respective metabolites in vegetated filter strip and cultivated soil. *Pest Management Science*, 62(6), 505–514.  
<https://doi.org/10.1002/ps.1193>
- Krutz, L. J., Senseman, S. A., McInnes, K. J., Hoffman, D. W., & Tierney, D. P. (2004). Adsorption and Desorption of Metolachlor and Metolachlor Metabolites in Vegetated Filter Strip and Cultivated Soil. *Environ. Qual.*, 33, 939–9445.

- Kuhlmann, A., Neuweiler, I., van der Zee, S. E. A. T. M., & Helmig, R. (2012). Influence of soil structure and root water uptake strategy on unsaturated flow in heterogeneous media. *Water Resources Research*, 48(2).  
<https://doi.org/10.1029/2011WR010651>
- Kupfersberger, H., Klammler, G., Schumann, A., Brückner, L., & Kah, M. (2018). Modeling Subsurface Fate of S -Metolachlor and Metolachlor Ethane Sulfonic Acid in the Westliches Leibnitzer Feld Aquifer . *Vadose Zone Journal*, 17(1), 170030.  
<https://doi.org/10.2136/vzj2017.01.0030>
- Ladu, J. L. C., & Zhang, D. R. (2011). Modeling atrazine transport in soil columns with HYDRUS-1D. *Water Science and Engineering*, 4(3), 258–269.  
<https://doi.org/10.3882/j.issn.1674-2370.2011.03.003>
- Liu, D. (2020). A rational performance criterion for hydrological model. *Journal of Hydrology*, 590. <https://doi.org/10.1016/j.jhydrol.2020.125488>
- Long, Y. H., Li, R. Y., & Wu, X. M. (2014). Degradation of S-metolachlor in soil as affected by environmental factors. *Journal of Soil Science and Plant Nutrition*, 14(1), 189–198. <https://doi.org/10.4067/S0718-95162014005000015>
- Loos, R., Locoro, G., Comero, S., Contini, S., Schwesig, D., Werres, F., Balsaa, P., Gans, O., Weiss, S., Blaha, L., Bolchi, M., & Gawlik, B. M. (2010). Pan-European survey on the occurrence of selected polar organic persistent pollutants in ground water. *Water Research*, 44(14), 4115–4126.  
<https://doi.org/10.1016/j.watres.2010.05.032>
- López-Piñeiro, A., Peña, D., Albarrán, Á., Sánchez-Llerena, J., & Becerra, D. (2014). Long-term effects of olive mill waste amendment on the leaching of herbicides through undisturbed soil columns and mobility under field conditions. *Soil and Tillage Research*, 144, 195–204. <https://doi.org/10.1016/j.still.2014.08.001>
- Maillard, E., Lange, J., Schreiber, S., Dollinger, J., Herbstritt, B., Millet, M., & Imfeld, G. (2016). Dissipation of hydrological tracers and the herbicide S-metolachlor in



- batch and continuous-flow wetlands. *Chemosphere*, *144*, 2489–2496.  
<https://doi.org/10.1016/j.chemosphere.2015.11.027>
- Mallants, D., Jacques, D., & Zeevaert, T. (2003). Modelling <sup>226</sup>Ra, <sup>222</sup>Rn, and <sup>210</sup>Pb migration in a proposed surface repository of very low-level long-lived radioactive waste. *Proceedings of the International Conference on Radioactive Waste Management and Environmental Remediation, ICEM*, *2*, 823–830.  
<https://doi.org/10.1115/ICEM2003-4632>
- Mandelbaum, R. T., Sadowsky, M. J., & Wackett, L. P. (2008). Microbial Degradation of s-Triazine Herbicides. *The Triazine Herbicides*, 301–328.  
<https://doi.org/10.1016/B978-044451167-6.50025-8>
- McCarty, G. W., Hapeman, C. J., Rice, C. P., Hively, W. D., McConnell, L. L., Sadeghi, A. M., Lang, M. W., Whittall, D. R., Bialek, K., & Downey, P. (2014). Metolachlor metabolite (MESA) reveals agricultural nitrate-N fate and transport in Choptank River watershed. *Science of the Total Environment*, *473–474*, 473–482.  
<https://doi.org/10.1016/j.scitotenv.2013.12.017>
- Mersie, W., McNamee, C., Seybold, C., Wu, J., & Tierney, D. (2004). Degradation of metolachlor in bare and vegetated soils and in simulated water-sediment systems. *Environmental Toxicology and Chemistry*, *23*(11), 2627–2632.  
<https://doi.org/10.1897/04-60>
- Mualem, Y. (1976). A new model for predicting the hydraulic conduc. *Water Resources Research*, *12*(3), 513–522.
- National Center for Biotechnology Information. (2022a). *PubChem Compound Summary for CID 4169, Metolachlor*.  
<https://pubchem.ncbi.nlm.nih.gov/compound/4169>
- National Center for Biotechnology Information. (2022b). *PubChem Compound Summary for CID 22206, Terbutylazine*.  
<https://pubchem.ncbi.nlm.nih.gov/compound/22206>

- National Center for Biotechnology Information. (2022c). *PubChem Compound Summary for CID 582098, 6-(tert-Butylamino)-1,3,5-triazine-2,4-diol*.  
<https://pubchem.ncbi.nlm.nih.gov/compound/582098>
- National Center for Biotechnology Information. (2022d). *PubChem Compound Summary for CID 6426849, Metolachlor ethanesulfonic acid*.  
<https://pubchem.ncbi.nlm.nih.gov/compound/6426849>
- National Center for Biotechnology Information. (2022e). *PubChem Compound Summary for CID 15842092, Metolachlor OA*.  
<https://pubchem.ncbi.nlm.nih.gov/compound/15842092>
- National Center for Biotechnology Information. (2022f). *PubChem Compound Summary for CID 129318140, Desethyl Terbutylazine-d9*.  
<https://pubchem.ncbi.nlm.nih.gov/compound/129318140>
- National Center for Biotechnology Information. (2022g). *PubChem Compound Summary for CID 135495928, Terbutylazine-2-hydroxy*.  
<https://pubchem.ncbi.nlm.nih.gov/compound/135495928>
- National Center for Biotechnology Information. (2022h). *PubChem Compound Summary for CID 139597106*.  
<https://pubchem.ncbi.nlm.nih.gov/compound/139597106>
- Navarro, S., Vela, N., & Navarro, G. (2007). Review. An overview on the environmental behaviour of pesticideresidues in soils. *Spanish Journal of Agricultural Research*, 5(3), 357–375.
- Papiernik, S. K., Koskinen, W. C., Cox, L., Rice, P. J., Clay, S. A., Werdin-Pfisterer, N. R., & Norberg, K. A. (2006). Sorption-desorption of imidacloprid and its metabolites in soil and vadose zone materials. *Journal of Agricultural and Food Chemistry*, 54(21), 8163–8170. <https://doi.org/10.1021/jf061670c>
- Pesticide Properties Data Base (PPDB). (2022a). *Desethyl-terbutylazine (Ref: GS26379)*. <https://sitem.herts.ac.uk/aeru/ppdb/en/Reports/1494.htm>

- Pesticide Properties Data Base (PPDB). (2022b). *Hydroxy-terbuthylazine (Ref: GS 23158)*. <https://sitem.herts.ac.uk/aeru/ppdb/en/Reports/1495.htm>
- Pesticide Properties Data Base (PPDB). (2022c). *Metolachlor (Ref: CGA 24705)*. <https://sitem.herts.ac.uk/aeru/ppdb/en/Reports/465.htm>
- Pesticide Properties Data Base (PPDB). (2022d). *Terbuthylazine. Vadose Zone Journal*, 3, 1309–1321. <https://sitem.herts.ac.uk/aeru/ppdb/en/Reports/623.htm>
- Postigo, C., & Barceló, D. (2015). Synthetic organic compounds and their transformation products in groundwater: Occurrence, fate and mitigation. *Science of the Total Environment*, 503–504, 32–47. <https://doi.org/10.1016/j.scitotenv.2014.06.019>
- Prueger, J. H., Alfieri, J., Gish, T. J., Kustas, W. P., Daughtry, C. S. T., Hatfield, J. L., & McKee, L. G. (2017). Multi-Year Measurements of Field-Scale Metolachlor Volatilization. *Water, Air, and Soil Pollution*, 228(2). <https://doi.org/10.1007/s11270-017-3258-z>
- Prueger, J. H., Gish, T. J., McConnell, L. L., McKee, L. G., Hatfield, J. L., & Kustas, W. P. (2005). Solar radiation, relative humidity, and soil water effects on metolachlor volatilization. *Environmental Science and Technology*, 39(14), 5219–5226. <https://doi.org/10.1021/es048341q>
- Rein, A., Legind, C. N., & Trapp, S. (2011). New concepts for dynamic plant uptake models. *SAR and QSAR in Environmental Research*, 22(1–2), 191–215. <https://doi.org/10.1080/1062936X.2010.548829>
- Rice, C. P., McCarty, G. W., Bialek-Kalinski, K., Zabetakis, K., Torrents, A., & Hapeman, C. J. (2016). Analysis of metolachlor ethane sulfonic acid (MESA) chirality in groundwater: A tool for dating groundwater movement in agricultural settings. *Science of the Total Environment*, 560–561, 36–43. <https://doi.org/10.1016/j.scitotenv.2016.04.007>
- Rice, P. J., Anderson, T. A., & Coats, J. R. (2002). Degradation and persistence of metolachlor in soil: Effects of concentration, soil moisture, soil depth, and

- sterilization. *Environmental Toxicology and Chemistry*, 21(12), 2640–2648.  
<https://doi.org/10.1002/etc.5620211216>
- Ritchie, J. T. (1972). Model for Predicting Evaporation from a Row Crop with Incomplete Cover. *Water Resour. Res.*, 8, 1204–1213.
- Ronka, S., & Bodylska, W. (2021). Sorption properties of specific polymeric microspheres towards desethyl-terbuthylazine and 2-hydroxy-terbuthylazine: Batch and column studies. *Materials*, 14(11). <https://doi.org/10.3390/ma14112734>
- Rose, C. E., Coupe, R. H., Capel, P. D., & Webb, R. M. T. (2018). Holistic assessment of occurrence and fate of metolachlor within environmental compartments of agricultural watersheds. *Science of The Total Environment*, 612, 708–719.  
<https://doi.org/10.1016/J.SCITOTENV.2017.08.154>
- Rose, C. E., Welch, H. L., Coupe, R. H., & Capel, P. D. (2012). A Holistic Assessment of the Occurrence of Metolachlor and 2 of its Degradates Across Environmental Settings Metolachlor Uses Pesticides in Surface Water and Groundwater Purpose of Study. [Conference Presentation Abstract] In *ABSTRACTS OF PAPERS OF THE AMERICAN CHEMICAL SOCIETY*, 244(1155 16TH ST, NW, WASHINGTON, DC 20036 USA: AMER CHEMICAL SOC.).
- Sánchez-Martín, M. J., Crisanto, T., Lorenzo, L. F., Arienzo, M., & Sanchez-Camazano, M. (1995). Influence of Leaching Rates on <sup>14</sup>C-Metolachlor Mobility. In *Bull. Environ. Contam. Toxicol* (Vol. 54). Springer-Verlag New York Inc. |~1~1 r.
- SANCO. (2004). *Review Report for the Active Substance S-metolachlor SANCO/1426/2001 — Rev. 3, 4 October 2004 Document of the European Commission (25 pp.)*.
- Sanderson, M., & Soboroff, I. (2007). *Problems with Kendall's Tau*. 928.
- Sarmah, A. K., Close, M. E., Pang, L., Lee, R., & Green, S. R. (2005). Field study of pesticide leaching in a Himatangi sand (Manawatu) and a Kiripaka bouldery clay loam (Northland). 2. Simulation using LEACHM, HYDRUS-1D, GLEAMS, and

- SPASMO models. *Australian Journal of Soil Research*, 43(4), 471–489.  
<https://doi.org/10.1071/SR04040>
- Sass, J. B., & Colangelo, A. (2006). European Union bans atrazine, while the United States negotiates continued use. *International Journal of Occupational and Environmental Health*, 12(3), 260–267. <https://doi.org/10.1179/oeh.2006.12.3.260>
- Satsuma, K. (2010). Mineralization of s-triazine herbicides by a newly isolated *Nocardioides* species strain DN36. *Applied Microbiology and Biotechnology*, 86(5), 1585–1592. <https://doi.org/10.1007/s00253-010-2460-3>
- Schaerlaekens, J., Mallants, D., Šimůnek, J., van Genuchten, M. Th., & Feyen, J. (1999). Numerical simulation of transport and sequential biodegradation of chlorinated aliphatic hydrocarbons using CHAIN\_2D. *Hydrological Processes*, 13(17), 2847–2859. [https://doi.org/10.1002/\(SICI\)1099-1085\(19991215\)13:17<2847::AID-HYP903>3.0.CO;2-M](https://doi.org/10.1002/(SICI)1099-1085(19991215)13:17<2847::AID-HYP903>3.0.CO;2-M)
- Scherr, K. E., Bielská, L., Kosubová, P., Dinisová, P., Hvězdová, M., Šimek, Z., & Hofman, J. (2017). Occurrence of Chlorotriazine herbicides and their transformation products in arable soils. *Environmental Pollution*, 222, 283–293. <https://doi.org/10.1016/j.envpol.2016.12.043>
- Schmitt, P., Garrison, A. W., Freitag, D., & Kettrup, A. (1996). Separation of s-triazine herbicides and their metabolites by capillary zone electrophoresis as a function of pH. *Journal of Chromatography A*, 723(1), 169–177. [https://doi.org/10.1016/0021-9673\(95\)00805-5](https://doi.org/10.1016/0021-9673(95)00805-5)
- Schuhmann, A., Klammler, G., Weiss, S., Gans, O., Fank, J., Haberhauer, G., & Gerzabek, M. H. (2019). Degradation and leaching of bentazone, terbuthylazine and S-metolachlor and some of their metabolites: A long-term lysimeter experiment. *Plant, Soil and Environment*, 65(5), 273–281. <https://doi.org/10.17221/803/2018-PSE>
- Scuri, S., Torrisci, M., Cocchioni, M., & Dell'Uomo, A. (2006). The European Water Framework Directive 2000/60/EC in the evaluation of the ecological status of

- watercourses. Case study: The river Chienti (central Apennines, Italy). *Acta Hydrochimica et Hydrobiologica*, 34(5), 498–505.  
<https://doi.org/10.1002/aheh.200600646>
- Shajari, F., Einsiedl, F., & Rein, A. (2020). Characterizing Water Flow in Vegetated Lysimeters with Stable Water Isotopes and Modeling. *Groundwater*, 58(5), 759–770. <https://doi.org/10.1111/gwat.12970>
- Sidoli, P., Devau, N., Jaramillo, R. A., & Baran, N. (2020). Reactivity of vadose-zone solids to S-metolachlor and its two main metabolites: case of a glaciofluvial aquifer. *Environmental Science and Pollution Research*, 27(18), 22865–22877. <https://doi.org/10.1007/s11356-020-08579-6>
- Sidoli, P., Lassabatere, L., Angulo-Jaramillo, R., & Baran, N. (2016). Experimental and modeling of the unsaturated transports of S-metolachlor and its metabolites in glaciofluvial vadose zone solids. *Journal of Contaminant Hydrology*, 190, 1–14. <https://doi.org/10.1016/j.jconhyd.2016.04.001>
- Šimůnek, J., & Hopmans, J. W. (2009). Modeling compensated root water and nutrient uptake. *Ecological Modelling*, 220(4), 505–521. <https://doi.org/10.1016/j.ecolmodel.2008.11.004>
- Šimůnek, J., Jacques, D., Langergraber, G., Bradford, S. A., Šejna, M., & van Genuchten, M. Th. (2013a). Numerical modeling of contaminant transport using HYDRUS and its specialized modules. *Journal of the Indian Institute of Science*, 93(2), 265–284.
- Šimůnek, J., Šejna, M., Saito, H., Sakai, M., & van Genuchten, M. Th. (2013b). *The HYDRUS-1D Software Package for Simulating the One-Dimensional Movement of Water, Heat, and Multiple Solutes in Variably-Saturated Media* (Issue June).
- Šimůnek, J., Šejna, M., & van Genuchten, M. Th. (2018). *Hydrus-1d. code for simulating the one-dimensional movement of water, heat, and multiple solutes in variably saturated porous media.*

- Šimůnek, J., & van Genuchten, M. Th. (1995). Numerical model for simulating multiple solute transport in variably- saturated soils. *Water Pollution III: Modelling, Measuring and Prediction*, 21–30.
- Šimůnek, J., van Genuchten, M. Th., & Šejna, M. (2008). Development and Applications of the HYDRUS and STANMOD Software Packages and Related Codes. *Vadose Zone Journal*, 7(2), 587–600. <https://doi.org/10.2136/vzj2007.0077>
- Šimůnek, J., van Genuchten, M. Th., & Šejna, M. (2016). Recent Developments and Applications of the HYDRUS Computer Software Packages. *Vadose Zone Journal*, 15(7), 1–25. <https://doi.org/10.2136/vzj2016.04.0033>
- Stipičević, S., Mendaš, G., Dvorščak, M., Fingler, S., Galzina, N., & Barić, K. (2017). Dissipation dynamics of terbuthylazine in soil during the maize growing season. *Arhiv Za Higijenu Rada i Toksikologiju*, 68(4), 336–342. <https://doi.org/10.1515/aiht-2017-68-3063>
- Strauß, C., Bayer, A., & Obernolte, M. (2017). Lysimeteruntersuchungen zum Austragsverhalten von im Maisanbau eingesetzten Herbiziden unter Freilandbedingungen (Standort Wielenbach). *17. Gumpensteiner Lysimetertagung 2017*, 27–32.
- Stumpp, C., Maloszewski, P., Stichler, W., & Fank, J. (2009). Environmental isotope ( $\delta^{18}\text{O}$ ) and hydrological data to assess water flow in unsaturated soils planted with different crops: Case study lysimeter station “Wagna” (Austria). *Journal of Hydrology*, 369(1–2), 198–208. <https://doi.org/10.1016/j.jhydrol.2009.02.047>
- Stumpp, C., Nützmann, G., Maciejewski, S., & Maloszewski, P. (2009). A comparative modeling study of a dual tracer experiment in a large lysimeter under atmospheric conditions. *Journal of Hydrology*, 375(3–4), 566–577. <https://doi.org/10.1016/j.jhydrol.2009.07.010>
- Sur, R., Kley, C., & Sittig, S. (2022). Field leaching study - Inverse estimation of degradation and sorption parameters for a mobile soil metabolite and its pesticide

- parent. *Environmental Pollution*, 310, 119794.  
<https://doi.org/10.1016/j.envpol.2022.119794>
- Tasca, A. L., Puccini, M., & Fletcher, A. (2018). Terbutylazine and desethylterbutylazine: Recent occurrence, mobility and removal techniques. *Chemosphere*, 202, 94–104. <https://doi.org/10.1016/j.chemosphere.2018.03.091>
- Toccalino, P. L., Gilliom, R. J., Lindsey, B. D., & Rupert, M. G. (2014). Pesticides in groundwater of the United States: decadal-scale changes, 1993-2011. *Ground Water*, 52, 112–125. <https://doi.org/10.1111/gwat.12176>
- Trakal, L., Kodešová, R., & Komárek, M. (2013). Modelling of Cd, Cu, Pb and Zn transport in metal contaminated soil and their uptake by willow (*Salix × smithiana*) using HYDRUS-2D program. *Plant and Soil*, 366(1–2), 433–451.  
<https://doi.org/10.1007/s11104-012-1426-x>
- Udiković-Kolić, N., Scott, C., & Martin-Laurent, F. (2012). Evolution of atrazine-degrading capabilities in the environment. *Applied Microbiology and Biotechnology*, 96(5), 1175–1189. <https://doi.org/10.1007/s00253-012-4495-0>
- Ulrich, U., Pfannerstill, M., Ostendorp, G., & Fohrer, N. (2021). Omnipresent distribution of herbicides and their transformation products in all water body types of an agricultural landscape in the North German Lowland. *Environmental Science and Pollution Research*, 28, 44183–44199. <https://doi.org/10.1007/s11356-021-13626-x>/Published
- Umwelt Bundesamt. (2022, August 3). *Groundwater is named water body type 2022*.  
<https://www.umweltbundesamt.de/en>
- Umweltbundesamt. (2015). *Gesundheitliche Orientierungswerte (GOW) für nicht relevante Metaboliten (nrM) von Wirkstoffen aus Pflanzenschutzmitteln (PSM)*. :  
[https://www.umweltbundesamt.de/sites/default/files/medien/374/dokumente/tabelle\\_gow\\_nrm2.pdf](https://www.umweltbundesamt.de/sites/default/files/medien/374/dokumente/tabelle_gow_nrm2.pdf)



- van Genuchten, M. Th. (1980). A closed-form equation for predicting the hydraulic conductivity of unsaturated soils. *Soil Science Society of America Journal*, 44(5), 892–898.
- van Genuchten, M. Th. (1987). *A numerical model for water and solute movement in and below the root zone*. Research Report No 121, U.S. Salinity Laboratory, USDA, ARS, Riverside, CA.
- Vischetti, C., Leita, L., Marucchini, C., Porzi, G., & Vischetti Liviana Leita Cesare Marucchini Gianni Porzi, C. (1998). Degradation and mobility of metolachlor and terbuthylazine in a sandy clay loam soil. In *Agronomie, EDP Sciences* (Vol. 18, Issue 2). <https://hal.archives-ouvertes.fr/hal-00885875>
- Wauchope, R. D., Buttler, T. M., Hornsby, A. G., Augustijn-Beckers, P. W. M., & Burt, J. P. (1992). The SCS/ARS/CES pesticide properties database for environmental decision-making. *Reviews of Environmental Contamination and Toxicology*, 123, 1–156. [https://doi.org/10.1007/978-1-4612-2862-2\\_1](https://doi.org/10.1007/978-1-4612-2862-2_1)
- Weber, J. B., McKinnon, E. J., & Swain, L. R. (2003). Sorption and mobility of <sup>14</sup>C-labeled imazaquin and metolachlor in four soils as influenced by soil properties. *Journal of Agricultural and Food Chemistry*, 51(19), 5752–5759. <https://doi.org/10.1021/jf021210t>
- Weber, J. B., Taylor, K. A., & Wilkerson, G. G. (2006). Soil and herbicide properties influenced mobility of atrazine, metolachlor, and primisulfuron-methyl in field lysimeters. *Agronomy Journal*, 98(1), 8–18. <https://doi.org/10.2134/agronj2004.0221>
- White, P. M., Potter, T. L., & Culbreath, A. K. (2010). Fungicide dissipation and impact on metolachlor aerobic soil degradation and soil microbial dynamics. *Science of the Total Environment*, 408(6), 1393–1402. <https://doi.org/10.1016/j.scitotenv.2009.11.012>

- Willmott, C. J., & Matsuura, K. (2005). Advantages of the mean absolute error (MAE) over the root mean square error (RMSE) in assessing average model performance. *Climate Research*, 30, 79–82. [www.int-res.com](http://www.int-res.com)
- Wołejko, E., Jabłońska-Trypuć, A., Wydro, U., Butarewicz, A., & Łozowicka, B. (2020). Soil biological activity as an indicator of soil pollution with pesticides – A review. In *Applied Soil Ecology* (Vol. 147). Elsevier B.V. <https://doi.org/10.1016/j.apsoil.2019.09.006>
- Wu, X. M., Li, M., Long, Y. H., Liu, R. X., Yu, Y. L., Fang, H., & Li, S. N. (2011). Effects of adsorption on degradation and bioavailability of metolachlor in soil. *Journal of Soil Science and Plant Nutrition*, 11(3), 83–97. <https://doi.org/10.4067/S0718-95162011000300007>
- Zabaloy, M. C., Zanini, G. P., Bianchinotti, V., Gomez, M. A., & Garland, J. L. (2011). Herbicides in the Soil Environment: Linkage between Bioavailability and Microbial Ecology. *Herbicides, Theory and Applications*. <https://doi.org/10.5772/12880>
- Zeitbild Wissen. (2013). *Bioenergie*, 55. Jahrgang, April 2013, herausgegeben von der Zeitbild Verlag und Agentur für Kommunikation GmbH, Kaiserdamm 20, 14057 Berlin, in Zusammenarbeit mit der Fachagentur Nachwachsende Rohstoffe e. V.
- Zemolin, C. R., Avalia, L. A., Cassol, G. V., Massey, J. H., & Camargo, E. R. (2014). Environmental fate of S-metolachlor-a review ENVIRONMENTAL FATE OF S-METOLACHLOR-A REVIEW-Dinâmica Ambiental do Herbicida S-metolachlor-Revisão. 32(3), 655–664.
- Zhu, W., Li, H., Qu, H., Wang, Y., Misselbrook, T., Li, X., & Jiang, R. (2018). Water Stress in Maize Production in the Drylands of the Loess Plateau. *Vadose Zone Journal*, 17(1), 180117. <https://doi.org/10.2136/vzj2018.06.0117>